Mutagenesis and recombinant expression of active site variants of the *Arabidopsis* CC-type glutaredoxin GRX480 reveal an altered protein expression profile in *E.coli* and changes in structural integrity of the GRX480 protein and its associated complex formation.

Colleen Murphy, B. Sc

A Thesis submitted to the Center for Biotechnology

in partial fulfillment of the requirements for the degree of

Master of Science

Brock University

St. Catharines, ON

Abstract

Stress conditions such as high temperature, drought, high salinity, metal stress, and pathogenic infection significantly increase production of reactive oxygen species (ROS) in the cell. Glutaredoxins (GRXs) are small redox proteins that possess conserved cysteine (C or Cys) residues in their active site and exhibit oxidoreductase activity to protect vital proteins from oxidative damage. CPYC and CGFS type GRXs can be found in humans, yeast, *E.coli*, and both lower and higher plants. The CC-type class is entirely plant-specific and is thought to have emerged with the evolution of intricate signalling mechanisms involved in plant disease resistance and floral complexity. The *Arabidopsis* CC-type glutaredoxin, GRX480, possesses a Cys-Cys-Met-Cys (CCMC) active site and is thought to participate in the salicylic acid (SA) mediated pathways involved in plant Systemic Acquired Resistance (SAR) to confer immediate and long term resistance to biotrophic pathogens. The structural and stoichiometric properties of the GRX480 protein remain uncharacterized and the mystery surrounding the role of the conserved cysteine residue (C**C**MC) in CC-type glutaredoxins make this protein a prime candidate for mutagenesis studies. The *AtGRX480* genetic sequence was codon optimized to allow for improved recombinant expression in *E.coli* cell cultures. Single (SCMC, CSMC, CCMS), double (SSMC, CSMS, SCMS), and triple (SSMS) GRX480 active site variants were created by site directed mutagenesis and a *Strep II* tag was added to the C-terminal end of the protein for isolation purposes. Recombinant expression of these proteins in *E.coli* DE3 cells caused a drastic decrease in total protein concentration when compared to untransformed cultures. Wildtype GRX480 exhibited a 6.5 fold decrease while the active site variants exhibited fold reductions within a range of 1.9 to 12.7, the CSMS and CSMC variants being the lowest and highest fold

reductions respectively. All recombinant protein expression caused a decrease in protein bands within the 36-32, 20, 16, and 12 kDa range of the native protein expression profile of *E.coli* cultures. When isolating the GRX480 proteins on the FPLC adapted *Strep*-column, a single injection of crude protein solution was ineffective in isolating sufficient amounts of protein to be examined by SDS-PAGE and immunoblot analysis. The utilization of a multiple injection method drastically improved GRX480 protein isolate yield from the column, however the majority of the protein remained bound to the column as desthiobiotin was demonstrated to be a poor eluting substrate. Examination of this isolate by gel filtration chromatography, SDS-PAGE, and immunoblot revealed that wildtype GRX480 (CCMC) and the SCMC, CSMS, SSMC, and SSMS variants form a tetrameric complex *in vitro.* The SCMS, CSMS, and CCMS variants exhibited formation of an extremely large complex, a trimeric complex, or were not observable as an intact protein during gel filtration respectively. The SCMC, CCMS, CSMC, and CSMS variants displayed a distinct degradation pattern in the N-terminal region of the protein with the CSMC and CSMS variants possessing an additional distinct degradation band. Submission of the GRX480 amino acid sequence to the I-TASSER (Iterative Threading ASSEmbly Refinement) server revealed alternative GSH binding amino residues other than the N-terminal active site cysteine. High sequence homology and predicted structural similarities of GRX480 to monothiol and dithiol glutaredoxins known to be involved in iron-sulfur [FeS]-cluster biosynthesis or [Fe-S] mediated redox sensing were also identified by I-TASSER. These results together offer novel and previously unreported features of the GRX480 protein in terms of complex formation, the roles of the active site cysteine residues, and the observed changes in native *E.coli* protein concentrations with recombinant expression of the GRX480 protein.

Acknowledgments

Firstly, I would like to thank Dr. Charles Després for giving me the opportunity to pursue this research project and for his guidance throughout. I have learned a number of new techniques and have gained a deeper understanding and appreciation of the intricate molecular signalling mechanisms that exist and are shared between diverse species. I would also like to thank the members of my supervisory committee, Dr. Vincenzo De Luca and Dr. Tony Yan, for their suggestions and perspectives during my research progress. The guidance and support of the many past and present members of the Després and De Luca labs is very much appreciated. I would like also like to extend my thanks to the staff members at Brock University who provided support and the opportunity to be a part of the pursuit of knowledge during my time as a student and teaching assistant. I would like to thank my friends, family, and my significant other for their unwavering support and love during this entire process. Lastly, I would like to dedicate this work to my grandparents who always stressed the importance of education and came to this country to build a better life for our family. I know they would be proud to see my efforts come to full fruition.

TABLE OF CONTENTS

ABSTRACT 1

ACKNOWLEDGEMENTS 3

TABLE OF CONTENTS 4

LIST OF TABLES 8

LIST OF FIGURES 8

CHAPTER 1 - INTRODUCTION AND LITERATURE REVIEW

1.1 Reactive Oxygen Species and the Cellular Redox State.....12

1.2 Glutaredoxins.....13

1.3 The Glutaredoxin Reaction Mechanism.....14

1.4 Glutaredoxin Classes.....15

1.5 Glutaredoxins in Abiotic Stress Responses.....17

1.6 Glutaredoxins in Floral Development.....18

1.7 Glutaredoxins in Plant Disease Resistance and Iron Homeostasis.....20

1.8 The Structure and Expression of Glutaredoxins.....23

1.9 Glutaredoxins and related proteins in *Escherichia coli*.....25

CHAPTER 2 - EXPERIMENTAL OBJECTIVES.....28

CHAPTER 3 - MATERIALS AND METHODS

3.1 *AtGRX480* Codon Optimization, Active Site Mutation, and Plasmid Construction.....29

3.2 Bacterial Transformation.....31

3.3 Bacterial Culture and Recombinant Protein Expression.....31

3.4 FPLC-adapted *Strep*-Column Protein Purification.....33

3.5 Bradford Protein Assays.....34

3.6 FPLC-adapted Gel Filtration.....35

3.7 SDS-PAGE, Immunoblot, and Protein Visualization.....36

3.8 Protein Structure Prediction.....37

CHAPTER 4 – RESULTS

4.1 Recombinant expression of *Strep*-tagged wildtype and active site variants of the *Arabidopsis* GRX480 protein causes an alteration in the expression profile of native *E.coli* proteins.....38

4.2 A multiple injection method is needed to isolate GRX480 from a *Strep*-tag purification column.....40

4.3 The active site variants of the GRX480 protein require differing volumes of crude protein extract for *Strep*-column isolation and successful use in gel filtration.....44

4.4 Mean total protein concentrations from crude recombinant *E.coli* expression and *Strep*-column protein isolates differ for GRX480 active site variants.....44

4.5 The GRX480 SCMC, CCMS, CSMC, and CSMS active site variants exhibit a distinct degradation pattern and the highest concentration of the GRX480 protein when purified from the *Strep*-column.....49

4.6 The wildtype GRX480 protein and active site variants display atypical behaviour when analyzed by gel filtration.....50

4.7 Wildtype GRX480 and the SCMC, CSMS, SSMC, and SSMS variants form a tetrameric complex *in vitro*.....61

4.8 The CSMC and SCMS variants of GRX480 exhibit differences in complex formation *in vitro*.....62

4.9 The CSMC and CSMS variants exhibit the same distinct degradation pattern after elution from the gel filtration column as observed after *Strep*-column isolation.....62

4.11 I-TASSER results suggest that *Arabidopsis* GRX480 has high sequence homology and predicted structural similarities to glutaredoxins involved in iron-sulfur [Fe-S] cluster assembly and may bind GSH through amino acid residues other than the N-terminal active site cysteine.....64

CHAPTER 5 – DISCUSSION AND FUTURE DIRECTIONS

5.1 Tetrameric complex formation is normally associated with monothiol glutaredoxins involved in iron-sulfur [Fe-S] cluster assembly.....69

5.2 The SSMS active site variant can form a tetrameric complex *in vitro* despite complete absence of the active cite Cys residues, suggesting alternate modes of binding GSH.....74

5.3 The CSMC and CSMS variants reveal an increase in specific regions of the N-terminal domain of the protein that are prone to degradation when the conserved Cys and the C-terminal Cys are absent.....75

5.4 The incomplete and/or unstable formation of a tetrameric complex in CSMS, the fragility of the CCMS protein, and the unexplainably large complex formed by the SCMS variant during gel filtration suggests an interplay between the Cys residues of the active site sequence.....78

5.5 The changes observed in the expression profile of native *E.coli* proteins may be the result of similarities in activity or interaction between the recombinantly expressed *Arabidopsis* GRX480 protein and those in *E.coli*.....79

5.6 Total protein concentration is drastically reduced in *E.coli* cultures recombinantly expressing GRX480 but a multiple injection method significantly increases isolate concentrations from the *Strep*-column.....84

CHAPTER 6 – CONCLUDING REMARKS.....86

REFERENCES.....87

APPENDIX.....101

LIST OF TABLES

CHAPTER 4

Table 1. Protein identities corresponding to the PDB Library ID codes listed in Figure 18.....67

APPENDIX

Supplemental Table 1. The activities and molecular weights (kDa) of *Escherichia coli* glutaredoxins, thioredoxins, and related proteins as provided by the UniProtKB database.....101

Supplemental Table 2. The activities and molecular weights (kDa) of *Escherichia coli* proteins involved in iron-sulfur [Fe-S] cluster assembly and redox sensing as provided by the UniProtKB database.....102

LIST OF FIGURES

CHAPTER 1

Figure 1. The hypothesized SWISS-MODEL of the monomeric *Arabidopsis* GRX480 protein (also known as ROXY19 or Glutaredoxin C9) based on the 137 amino acid sequence.....24

CHAPTER 3

Figure 2. The plasmid components used for recombinant expression of *Arabidopsis* GRX480 proteins in *E.coli* (DE3) competent cells.....30

CHAPTER 4

Figure 3. Recombinant expression of *Strep*-tagged wildtype and active site variants of the *Arabidopsis* GRX480 protein in *E.coli* DE3 cells causes an alteration in the expression profile of native *E.coli* proteins.....39

Figure 4. A single injection method is inefficient in isolating *Strep*- tagged GRX480 from a *Strep*-tag purification column.....42

Figure 5. A multiple injection method, consisting of 10 mL injections for a total of 60 mLs, results in *Strep*-column saturation and is sufficient in isolating the *Strep*- tagged GRX480 protein.....43

Figure 6. Successful isolations of the *Strep*- tagged wildtype GRX480 protein (CCMC) and single mutation active site variants(XXMX) using the FPLC- adapted multiple injection method.....46

Figure 7. Successful isolations of the *Strep*- tagged GRX480 double (XXMX) and triple mutation (SSMS) active site variants using the FPLC- adapted multiple injection method.....47

Figure 8. Mean total protein concentrations from crude recombinant *E.coli* expression and *Strep*-column protein isolates differ for wildtype GRX480 (CCMC) and active site variants.....48

Figure 9. SDS-PAGE and immunoblot analysis of wildtype GRX480 (CCMC) and active site variants (XXMX) *Strep*-column isolations.....50

Figure 10. Operational parameters of the S100 gel filtration column determined by use of protein standards with a known molecular weight (MW).....51

Figure 11. Results of 10 mL of injected *Strep*- tagged wildtype GRX480 protein (CCMC) and single mutation active site variants (XXMX) *Strep*-column isolates using a FPLC- adapted S100 gel filtration column.....55

Figure 12. SDS-PAGE and immunoblot analysis of wildtype GRX480 (CCMC) gel filtration fractions collected during the runs depicted in Figure 11.....56

Figure 13. SDS-PAGE and immunoblot analysis of single mutation active site variants(XXMX) of GRX480 gel filtration fractions collected during the runs depicted in Figure 11.....57

Figure 14. Results of 10 mL of injected *Strep*- tagged GRX480 double (XXMX) and triple mutation (SSMS) active site variants *Strep*-column isolates using a FPLC- adapted S100 gel filtration column.....58

Figure 15. SDS-PAGE and immunoblot analysis of double mutation active site variants (XXMX) of GRX480 gel filtration fractions collected during the runs depicted in Figure 14.....59

Figure 16. SDS-PAGE and immunoblot analysis of the triple mutation active site variant (SSMS) of GRX480 gel filtration fractions collected during the runs depicted in Figure 14.....60

Figure 17. The total gel filtration elution ranges and calculated molecular weights for the wildtype GRX480 protein and active site variants.....63

Figure 18. I-TASSER results for GRX480 protein sequence alignment, structural prediction, and ligand binding site residues.....66

Figure 19. The top five structural models of the GRX480 protein predicted by I-TASSER.....68

CHAPTER 5

Figure 20. The approximate cites of cleavage in the N-terminal domain of the SCMC, CCMS, CSMS, and CSMS variants as revealed by SDS-PAGE and immunoblot analysis of protein isolates from the *Strep* and gel filtration columns.....77

1. INTRODUCTION AND LITERATURE REVIEW

1.1 Reactive Oxygen Species and the Cellular Redox State

Reactive oxygen species (ROS) are essential to many developmental and physiological processes in both prokaryotes and eukaryotes. In plants, ROS are normally produced by chloroplasts and mitochondria during photosynthesis and carbon metabolism, however, stress conditions such as high temperature, drought, high salinity, metal stress, and pathogenic infection will significantly increase ROS levels within the cell (Scandalios, 2002; Vranová et al., 2002; Miller et al., 2009; Guo & Huang, 2010). The production of ROS during stress responses changes the internal redox state of cells. Most organisms contain glutathione (GSH) which play a crucial role in antioxidant biosynthetic pathways and redox homeostasis (Noctor et al., 2012). GSH keeps the intracellular buffer in a reduced state to protect the structure and function of proteins. Glutathione disulfide (GSSG) is reduced into two molecules of GSH by the enzyme glutathione reductase. GSSG is produced by antioxidant enzymes such as glutathione peroxidases during ROS scavenging by the reduction of peroxidases such as hydrogen peroxide to protect vital proteins from oxidative damage. When a plant is under these stress conditions, the GSH:GSSG ratio has been found to shift towards GSSG. This shift results in downstream activation of multiple pathways, including the initiation of programmed cell death to combat the infection and spread of disease (El-Shabrawi et al., 2004; Kocsy et al., 2004; Szalai et al., 2009; Noctor et al., 2012).

1.2 Glutaredoxins

Glutaredoxins (GRXs) are small redox proteins responsible for modulating activities of specific proteins by catalyzing the reversible reduction of disulfide bonds in the presence of NADPH and glutathione reductase. They interact with GSH to produce GSSG by using GSH as an electron donor (Fernandes & Holmgren, 2004; Buchanan et al., 2005; Song et al., 2013; Zagorchev et al., 2013) They possess conserved cysteine (Cys) residues in their active site and their activity is mediated by the ROS produced during oxidative stress (Gille and Sigler, 1995; Xing et al., 2006). The first GRX was discovered as a glutathione (GSH)-dependent hydrogen donor for ribonucleotide reductase in mutants of *E.coli* lacking thioredoxin (TRX), the protein normally displaying dithiol hydrogen donor properties (Holmgren, 1976). This *E.coli* GRX was found to be small in size, exhibited a general GSH-disulfide oxidoreductase activity, contained an active site sequence of amino acids Cys-Pro-Tyr-Cys, and showed similarity to eukaryotic GSH-disulfide oxidoreductases/ transhydrogenases (Racker, 1955; Nagai & Black, 1968; Askelöf et al., 1974; Holmgren, 1979). The three dimensional structure of this *E.coli* GRX was found to be similar to TRX, and contains a folding pattern that includes a binding site for GSH commonly found in other GSH-dependent enzymes such as GSH peroxidise (Bushweller et al., 1992; 1994). The first mammalian GRX was isolated from calf thymus and exhibited the same Cys-Pro-Tyr-Cys active site and served as a hydrogen donor for ribonucleotide reductase (Klintrot et al., 1984; Papayannopoulos,1989). Interestingly, proteins similar to GRXs are also found in some viruses and are thought to help mediate virus-host interaction (Johnson et al., 1991; Ahn & Moss, 1992). GRXs are now known to be recycled by GSH to form GSSG. This complex is reduced by NADPH and glutathione reductase to form the GSH/GRX reducing system. GRXs are

also known to be recycled by ferredoxin / NADPH dependent thioredoxin reductases (TR) to form a TRX/GRX reducing system(Reynolds et al., 2002; Johansson et al., 2004; Fernandes et al., 2005; Zaffaghini et al., 2008; Couturier and Jacquot, 2009).

GRXs are part of a thioredoxin (TRX) superfamily whose members are glutathione - dependent thiol oxidoreductases. Although both TRXS and GRXs are similar in their activity and active site residues in plants, GRXs are directly reduced by GSH to produce GSSG, while the reduction of TRX requires plant organ specific reductases. These are NADPH-dependent TRX reductases in the mitochondria and cytosol, and ferredoxin/TRX reductase in the plastid (Lemaire et al., 2007; Schürmann & Buchanan, 2008; Zagorchev et al., 2013). In humans, upregulation of the thioredoxin superfamily of proteins including a distinct CPYC motif glutaredoxin (Grx1) is found in proliferating lung cancer tissue (Fernandes et al., 2009).

1.3 The Glutaredoxin Reaction Mechanism

GRX mediated reactions are of two types, dithiol or monothiol, based on the amino acid sequence of their active site. These reduction reactions are thought to be in response to a change in cellular redox state and cause post-translational modifications to a target protein. These modifications are usually related to protein structure and regulate the activity of these target proteins. CXXC type GRXs can exert both dithiol and monothiol reaction, whereas CXXS types can only reduce mixed disulfides via the monothiol reaction (Xing et al., 2006). The dithiol reaction is catalyzed by two conserved cysteine residues. The N-terminal cysteine is responsible for directing a nucleophilic attack on one of the sulfur atoms contained within the disulfide region of the target protein, and a disulfide bridge is formed. The bridge between the two

proteins is disbanded when an intramolecular disulfide bridge is formed between the two cysteines of the GRX active site, which releases the reduced protein target (Xing et al., 2006). The monothiol reaction involves a target protein that has formed a disulfide bridge with glutathione (GSH). The N-terminal cysteine of the GRX possesses a high affinity for GSH and reacts directly with it. Protein reactivation can occur through a process called deglutathionylation, after the redox state of the cell has been normalized, as glutathionylation functions as a protective mechanism of protein sulfhydryl groups from damage during oxidative stress (Ghezzi, 2005; Xing et al., 2006). Cys residues in proteins are vulnerable to oxidative alterations caused by excessive ROS production under stress which can lead to loss of protein conformation and the associated activity. These Cys residues can be reformed through interaction with GRX. Extensive glutathionylation and increased GRX expression are thought to enhance stress tolerance, however, the exact mechanism of protein glutathionylation in plants is not fully understood (Kumar et al., 2009; Zaffagnini et al., 2012; Zagorchev et al., 2013).

1.4 Glutaredoxin Classes

GRXs are divided into CGFS, CPYC, and CC-type classes based on active site sequences (Yang et al., 2015). CPYC and CGFS type GRXs can be found in humans, yeast, *E.coli*, and both lower and higher plants. The CC-type class is entirely plant-specific (Xing et al., 2006).The CGFS type active site motifs were first characterized in yeast while the CPYC motif was originally identified in both *E. coli* and yeast (Rodríguez Manzaneque et al.,1999; Xing et al., 2006) .

Of the thirty one GRX proteins in the model plant *Arabidopsis*, twenty one possess the CC type motif; seven CCMC, two CCLC, ten CCMS, one CCLG and one CCLS. The CXXC motif is

found in three GRXs with a CPYC active site, one with CGYC, and one with CSYC. The monocysteine motif, CXXS, is represented by four GRXs with a CGFS type active site sequence and one with CSYS. (Rodríguez Manzaneque et al., 1999; Lemaire, 2004; Rouhier et al., 2004; Xing et al., 2006). Interestingly, a study involving transgenic expression of a plant chloroplast-targeted monothiol glutaredoxin from *Arabidopsis* (AtGRX4) in yeast revealed that not only did this glutaredoxin have a similar sequence to the yeast glutaredoxin Grx5, but was also able to localize to the mitochondria, suppress cell sensitivity to oxidants, reduce iron accumulation, and rescue lysine auxotrophy in *grx5* mutant yeast cells. These findings propose a highly evolutionary conserved antioxidant activity in monothiol glutaredoxins (Cheng et al., 2006; Cheng, 2008). In plants, the CPYC active site sequence, proline(P) can be replaced with a glycine (G) or a serine (S). The tyrosine (Y) can also be replaced by a phenylalanine (F), and the C-terminal cysteine(C) for a serine(S). The CGFS sequence however, is absolutely conserved in even distantly related species such as *Arabidopsis, Physcomitrella,* and *Agrobacterium tumefaciens* as a divergence in this sequence has yet to be discovered (Isakov et al., 2000; Xing et al., 2006). The hypothesis that the ability to modify target protein activity post-translationally was a critical development in land plant evolution is supported by the observations that only two CC-type GRXs exist in the "lower" bryophyte *Physcomitrella* and a significantly larger number exist in "higher" gymnosperm and angiosperm species (Xing et al., 2006). The emergence of the CC type GRX class is estimated to have occurred 450 million years ago with the evolution of the first nonvascular land plants. The increase in the number of CC type GRXs throughout plant evolutionary history is thought to correlate with an increase in plant floral complexity and the development of intricate signalling pathways to combat biotic and abiotic

stress factors (Kenrick and Crane, 1997; Xing et al., 2006). CCXC/S type glutaredoxins in *Arabidopsis*, also known as ROXYs, are most well known for their interaction with TGACG(TGA)motif-binding protein transcription factors to mediate stress related responses and floral development. Recently, ROXYs have also been shown to interact with transcriptional co-repressors of the TOPLESS (TPL) protein family which are related to Tup1 in fungi and Groucho/TLE in animals. (Uhrig et al., 2017).

The role of the conserved cysteine in CC-type GRX motifs in the second position next to the N-terminal cysteine (C**C**XC) still remains quite elusive, and it is not clear whether it functions through a monothiol or dithiol mechanism. However, this cysteine was found to be replaced in four GRXs of *Oryza* suggesting a possible species specific role (Xing et al., 2006).

1.5 Glutaredoxins in Abiotic Stress Responses

Transgenic expression of the fern GRX, PvGrx5, in *Arabidopsis* decreased accumulation and heightened tolerance to arsenic. It also conferred an increased tolerance to heat stress and reduced the effects of oxidative damage to proteins (Sundaram et al., 2009; Sundaram & Rathinasabapathi, 2010). A GRX in rice, Glutaredoxin C14, was found to be upregulated during copper induced stress (Song et al., 2013). In tomato, it was found that a GRX with a CGFS active site, SlGRX, was expressed in multiple tissue types including the leaf, root, stem and flower. SlGRX was found to be induced by oxidative, drought, and salt stresses. Virus-induced gene silencing of this gene caused an increased sensitivity to oxidative and salt stresses, decreased chlorophyll content, reduced tolerance to drought stress, and decreased water content. When this protein was transgenically over-expressed in *Arabidopsis*, it significantly increased

resistance of plants to oxidative, drought, and salt stress as well as causing an increase in expression of the native *Arabidopsis* drought and salt stress related genes *Apx2*, *Apx6*, and *RD22* (Guo et al., 2010). Organisms exposed to extreme fluctuations in the availability of water also suffer from extreme changes in cellular redox state which often leads to irreversible oxidation of free cysteine residues of proteins. Studies conducted on desiccation tolerant organisms , which can survive extreme loss of water and then be revived upon re-hydration, suggested that protein glutathionylation mediated by TRXs and GRXs was a likely contributor to this protection mechanism (Colville & Kranner, 2010).

1.6 Glutaredoxins in Floral Development

The *PERIANTHIA* gene (*PAN)*, regulates floral patterning in *Arabidopsis*. Plants lacking this gene display a phenotype containing an extra sepal and petal, fewer stamen, and a pentamerous arrangement of floral organs (Running and Meyerowitz, 1996; Chuang et al., 1999; Murmu et al., 2010). The PAN protein interacts with BTB-ankryin proteins, BLADE-ON-PETIOLE1 (BOP1) and BOP2, to control the number of sepal-whorl organs in flowers (Hepworth et al., 2005; Murmu et al., 2010). ROXY1 and ROXY2, two CC-type class GRX proteins in *Arabidopsis*, also play a role in flower development. ROXY1 has been shown to regulate *PAN* and both ROXY1 and ROXY2 are needed for anther cell and microspore development (Xing et al., 2005; Xing et al., 2008; Li et al., 2009).

Plants deficient in TGACG(TGA)motif-binding protein transcription factors, TGA9 and TGA10, were shown to have defects in male gametogenesis that are comparably similar to the phenotypes of *roxy1roxy2* mutants. Further analysis revealed that TGA9 and TGA10 expression

during anther development overlaps with ROXY1 and ROXY2 expression, and that these TGAS directly interact with ROXY proteins which are thought to modify the TGA cysteine residues and cause protein activation. (Murmu et al.,2010). Two monocot rice homologs of *Arabidopsis ROXY1*, *OsROXY1* and *OsROXY2*, were found to rescue the *roxy1* mutant floral phenotype despite *Arabidopsis* being an eudicot species. Overexpression of *OsROXY1*, *OsROXY2*, and *ROXY1* in *Arabidopsis* caused vegetative, developmental, and reproductive defects due to an imbalanced redox state within these mutants (Wang et al., 2009)

A distinct maize mutant, *Aberrant phyllotaxy2* (*Abph2*), displayed a phenotype in which the shoot meristem was enlarged and the phyllotactic pattern switched from alternate to decussate. This was caused by transposition of a glutaredoxin gene, *MALE STERILE CONVERTED ANTHER1* (*MSCA1*) and an altered expression pattern. *MSCA1* loss-of-function mutants show a reduced meristem size as *MSCA1* interacts with a TGA transcription factor, *FASCIATED EAR4*, the maize ortholog of PAN. These experiments suggest a role for glutaredoxins in regulating shoot meristem growth, size, and phyllotaxy (Yang et al., 2015). Interestingly, one of two regulatory Cys residues in the TGA1 transcription factor, a TGACG(TGA)motif-binding protein involved in the defense response against pathogens , is conserved in the PAN protein and both belong to the same subclade in the basic leucine-zipper (bZIP) superfamily of *Arabidopsis* (Jakoby et al., 2002; Li et al., 2009).

1.7 Glutaredoxins in Plant Disease Resistance and Iron Homeostasis

Salicylic acid (SA) is an important plant signalling molecule in the induction of the plant defense response known as “Systemic Acquired Resistance (SAR)” during pathogen infection

(Cao et al., 1997; Zhang et al., 2003). SA inducible genes, such as those encoding for glutathione-S-transferase and pathogenesis-related (PR) proteins, have been found to be under the control of TGA transcription factors which bind to *activating sequence-1*(*as-1)* type elements to induce transcription during the stress response (Lam et al., 1989; Liu and Lam, 1994; Ulmasov et al., 1994; Qin et al., 1994; Zhang et al., 2003; Thurow et al., 2005). These TGA transcription factors are also known to interact with *NPR1* (*non-expressor of PR genes 1*), which mediates SA-induced gene expression in the SAR response, but also represses genes in a secondary defense pathway that is triggered by the signalling molecule jasmonic acid (JA)(Zhang et al., 1999; Spoel et al., 2003; Beckers and Spoel, 2006). There exists a "cross-talk" between the SA and JA induced pathways in that there are both antagonistic and synergetic interactions between components of each. This allows the plant to protect itself from necrotrophic pathogens and insects through the JA-mediated pathway, and to confer immediate and long term resistance to biotrophic pathogens through the SA-mediated SAR pathway (Spoel et al., 2003). Interestingly, another study showed that overexpression of transgenic rice glutaredoxins *OsROXY1*/ *OsROXY2*, and native *ROXY1* in Arabidopsis (normally associated with floral development) caused an increased accumulation of ROS and a significant increase in susceptibility to infection from the necrotrophic pathogen *Botrytis cinerea* (Wang et al., 2009). Interaction between NPR1 and TGA transcription factors has been characterized in numerous studies. In *Arabidopsis*, SA-induced redox modifications of TGA1 and NPR1 have been proposed as the activating mechanism in defense response signalling cascades as both exist in non-inducing conditions and must be held under strict transcriptional control (Qin et al., 1994). Only the reduced form of TGA1, induced by SA treatment, was found to interact with NPR1

(Després et al., 2003). Reduction of cysteine residues in the NPR1 protein, also induced by SA treatment, causes a conformational change from an oligomer to a monomeric complex which is then imported into the nucleus where it directs TGA2 and TGA3 to sequences encoding defense related genes such as *PR-1*(Fan and Dong, 2002; Johnson et al., 2003; Mou et al., 2003). In one study, it was observed that transcription of a CC-type glutaredoxin in *Arabidopsis,* GRX480*,* is SA-inducible and requires NPR1. Interestingly, suppression of the JA-dependent defensin gene *PDF1.2* was facilitated by transgenically expressed GRX480, but only through interaction with the tobacco TGA2.2 transcription factor (Ndamukong et al., 2007). Conversely, one study found that GRX480 was indeed a stress related SA-responsive gene, but it was induced transiently by an NPR1-independent pathway. Analysis of the promoter region of *GRX480* indicated gene transcription was controlled through two *as-1* like elements. TGA2 and TGA3, but not TGA1, were found to bind to this promoter region (Herrera-Vásquez et al., 2015).

In a recent study, transgenic plants expressing GRX480 under the control of the constitutive *Cauliflower Mosaic Virus 35S (CaMV 35S)* promoter revealed that the repressive function of GRX480 on JA/ethylene-induced defense genes in the *ORA59* anti-microbial defense pathway required at least one of the redundant transcription factors TGA2, TGA5 or TGA6 and conferred higher susceptibility to the necrotrophic pathogen *Botrytis cinerea*. Mutation of the conserved CCMC active site motif of this GRX480 into CPYC or SSMS revealed that protein activity was retained in the CPYC mutant but lost with the SSMS mutation (Huang et al., 2016). In an attempt to isolate recombinant poplar CCxC/S motif glutaredoxin proteins from an *E.coli* expression system, Couturier et al. (2010) found that the proteins were either not expressed or insoluble due to the conserved hydrophobic GAWL C-terminal tail of the proteins. This tail is

suspected to be essential for these GRXs to interact with TGA transcription factors but unfortunately prevents expression in *E.coli* (Li et al., 2009). However, mutation of the CCXC/S poplar GRX (GrxS7.2) C-terminal tail and addition of a histidine tag allowed some degree of purification (Couturier et al., 2010).

In plants, some GRXs with CXXC/S active sites exhibit disulfide reductase activity, regenerate thiol-dependent antioxidant enzymes, and incorporate stable iron-sulfur [2Fe-2S] clusters (Rouhier et al., 2007; Rouhier, 2010). Plant, bacterial, yeast and human CGFS active site GRXs can exist as dimeric holoproteins which bind [2Fe-2S] clusters in assembly and the regulation of iron homeostasis , or as exist as monomeric apoforms that exhibit deglutathionylation activity (Rodríguez-Manzaneque et al., 1999; Picciocchi et al., 2007; Bandyopadhyay et al., 2008; Zaffagnini et al., 2008; Rouhier, 2010) . These homodimeric iron clusters are formed when two CCXC/S or CGFS type GRX monomers ligate one [2Fe-2S] moiety and two molecules of GSH via their N-terminal active site cysteine (Feng et al., 2006; Johansson et al., 2007; Rouhier et al., 2007; Iwema et al., 2009; Li et al., 2009). When poplar GRX active sites of GrxC1(CGYC) and C4 (CPYC) were mutated into CCMC or CCMS, the recombinant proteins were found to bind [2Fe-2S] centers into holodimers and the monomeric apoforms displayed glutathione –dependent reductase activity (Couturier et al., 2010).

1.8 The Structure and Expression of Glutaredoxins

Very little structural and stoichiometric data on the CC-type GRXs in *Arabidopsis* is currently available, more specifically regarding GRX480. TRXs, GRXs, and glutathione

transferases are known to have a distinct fold (belonging to the thioredoxin fold superfamily) with a conserved valine residue that interacts with GSH (Ren et al., 2009). X-ray crystallography and NMR spectroscopy studies of monothiol and dithiol GRXs from various organisms conclude that the motif generally consists of a four stranded beta sheet surrounded by three alpha helices. The Cys active site motif is located on the loop connecting the first beta sheet and alpha helix (Fig. 1). The N-terminal Cys residue in the active site is surface exposed with a pKa value 3 or more pH units below the pKa of a free Cys residue. The C-terminal Cys residue of the active site is buried within the protein structure and has a significantly higher pKa value (Lillig et al., 2008). A study of CGFS, CPYC, and CC-type GRXs in rice by Garg et al., (2010) found that the CPYC and CC-type were similar in that they each contained similar conformation of structural elements (alpha helices and beta sheets), and that they maintained three conserved regions known for GSH binding. The CGFS type differed slightly in the number of beta sheets and GSH binding site conservation. The most notable structural differences between these GRXS were found in the variable loop regions of the protein, where sequence similarity is low. Tissue and growth stage specific expression of GRX was found to be the most diverse in the CC-type class with expression in the SAM, and multiple stages of panicle and seed development. CGFS type GRXs were found to be expressed in the SAM and panicle, but to a significantly lesser degree. CPYC types were found to be most highly expressed in the leaf. The reason why plants exhibit redundancy and divergence in GRXS, more specifically the specialized activity yet sequence and structural similarity of CC-type GRXS, is proposed to be due to the need for duplicate genes that operate at non-, sub-, neo-, or hypo-functionalization under specific conditions such as those induced by stress responses (Lynch and Conery, 2000; Garg et al., 2010).

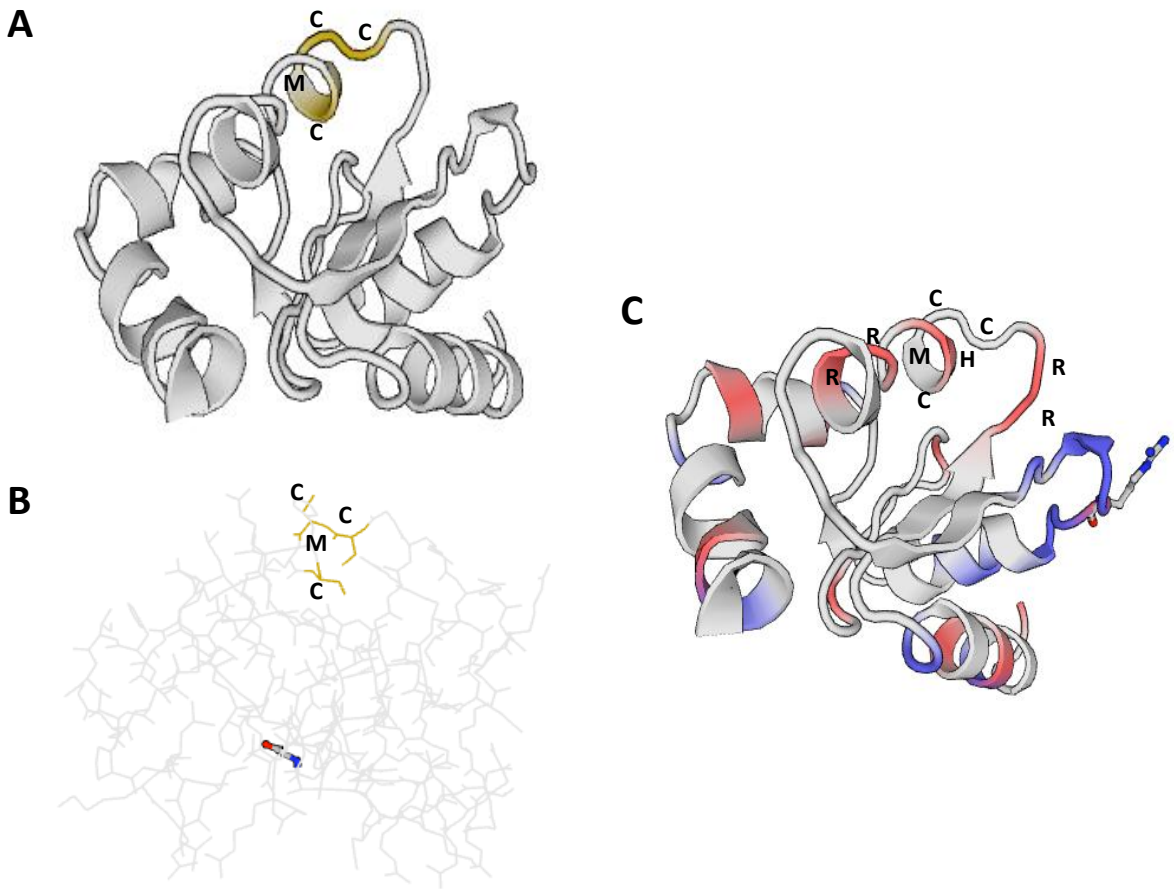

Figure 1. The hypothesized SWISS-MODEL of the monomeric *Arabidopsis* GRX480 protein (also known as ROXY19 or Glutaredoxin C9) based on the 137 amino acid sequence. **(A)** A 3D structural model depicting the protein active site sequence consisting of three cysteine (C) residues and one methionine (M) residue. **(B)** A line drawing of the model depicted in **(A)** showing the side chains of the cysteine residues **(C)** The active site motif is flanked by charged arginine (R) residues and a polar histidine (H) residue (indicated by shaded regions) which participate in salt bridge and hydrogen bond formation respectively (Arnold et al., 2006; Kiefer et al., 2009; Biasini et al., 2014; Bienert et al., 2017).

1.9 Glutaredoxins and related proteins in *Escherichia coli*

Escherichia coli bacteria is known to have four glutaredoxins, Grx1, Grx2, Grx3, and Grx4 (Fernandes & Holmgren, 2004). The Grx2 protein is approximately 24 kDa in size and contains an extra structural domain that makes it more similar to glutathione transferases. Grx4 is approximately 13 kDa in size with a highly conserved CGFS active site sequence and is involved in iron-sulfur [2Fe-2s] cluster assembly. Grx4 serves as a substrate for thioredoxin reductase and is highly expressed upon iron depletion. It forms FeS-bound homodimeric and heterodimeric complexes and acts as a scaffold protein for [2Fe-2S] transfer to apo-ferredoxin (Fernandes et al., 2005; Yeung et al., 2011). Both Grx2 and Grx4 are produced abundantly in *E.coli* cells (Sagemark et al., 2007; Iwema et al., 2009; Elgán et al., 2010). Grx3 contains a CPYC-active site sequence, is 9 kDa in size, and reduces glutathione–protein mixed disulfides. Grx1, 10 kDa in size with a CPYC active site sequence, is structurally similar to Grx3 with a 37 % sequence identity and also reduces glutathione-protein mixed disulfides. However, Grx1 is the only glutaredoxin that can efficiently reduce ribonucleotide reductase (RR) and 3'-phosphoadenylylsulfate (PAPS) which are essential to *E.coli* cell survival (Bushweller et al., 1992; Miranda-Vizuete , 1994; Prinz et al., 1997; Vlamis-Gardikas et al., 1997; Lillig et al., 1999; Nordstrand et al., 1999; Elgán et al., 2010). A Met^{43} side chain outside of the active site sequence is buried under the second helix in Grx3, where it interacts with numerous surrounding residues. Studies involving a mutation of this residue, Met43Val, revealed a 7-fold increase in V_{max} towards reducing RR, a 1.1 decrease in the pK_a value of the N-terminal cysteine of the active site, a 11 mV increase in the reducing power of the active cite cysteines, and no change in the structure of the mutant protein (Ortenberg et al., 2004; Porat et al., 2007; Elgán

et al., 2010). The Grx1-like activity of the Grx3 (Met43Val) mutant was further investigated by producing a Grx3 (M43V/C65Y) mutant which displayed enhanced intrinsic motion to allow for increased affinity for larger substrates such as RR (Elgán et al., 2010).

The thioredoxin system (thioredoxin, thioredoxin reductase, and NADPH) is also part of the antioxidant system in *E.coli* cells under oxidative stress. The *E.coli* thioredoxin, Trx1 (11.8 kDa), is well characterized and possesses a thioredoxin fold containing the CGPC active site at the end of the β_2 strand and beginning of a long α helix. Similar to glutaredoxins, the N terminal cysteine is the attacking nucleophile in the disulfide reduction of target proteins as it has the lowest pK_a value. Trx1 has a low redox potential and this allows thioredoxin-$(SH)_2$ to be the major dithiol reductant in the cytosol. Trx1 provides electrons to methionine sulfoxide reductase (MSR) which protects the cell against oxidative damage from reactive nitrogen intermediates (Holmgren, 1985; Eklund et al., 1991; Jeng et al., 1994; Holmgren, 1995; Arnér & Holmgren, 2000; John et al., 2001; Lu & Holmgren, 2014). Trx1 also acts as a specific reductase for the peroxidase Tpx in ROS scavenging. Together they form a Michaelis complex with affinity for hydrogen peroxide and cumene hydroperoxide (Holmgren, 1985; Jeong et al., 2000; John et al., 2001; Lu & Holmgren, 2014). Trx1, Trx2 (15.6 kDa thioredoxin in *E.coli* expressed during oxidative stress), Grx1 and Grx3 can also provide electrons to BCP peroxidase to catalyse hydrogen peroxide (Reeves et al., 2011; Holmgren, 2014). Expression of Trx2 and Grx1 is regulated by the OxyR transcription factor which is controlled by the formation of disulfide bonds between the Cys199 and Cys208 residues. Trx2 and Grx1 bound to GSH can reduce this disulfide bond to deactivate OxyR to form an autoregulatory response. Although it was found that the thioredoxin system was not necessary for bacterial growth under oxidative stress if a

functional GSH-Grx system was present, it was shown to be crucial in maintaining disulfide/dithiol redox control within the cell (Prinz et al., 1997; Zheng et al., 1998; Åslund et al., 1999; Ritz et al., 2000; Lu & Holmgren, 2014). Thioredoxin reductase exists as a 70 kDa dimeric flavoprotein (34.6 kDa monomer) in bacteria and can reduce thioredoxins as well as NrdH redoxin (Jordan et al., 1997; Arnér & Holmgren, 2000).

E.coli glutathione transferase (GST) is involved in oxidative stress pathways and possesses the ability to catalyse nucleophilic attack by the tripeptide glutathione (GSH) (Hayes et al., 2005; Kanai et al., 2006; Allocati et al., 2009). It exhibits a folding structure common among cytosolic GSTs which are homo- or hetero-dimers of 25 kDa subunits containing a N-terminal thioredoxin-like domain and a C-terminal alpha helices domain. Isolation of *E.coli* GST revealed a three dimensional homodimer of 40 kDa that exhibited GSH-dependent peroxidase activity toward cumene hydroperoxide (Nishida et al., 1998; Rossjohn et al., 1998; Kanai et al., 2006).

2. EXPERIMENTAL OBJECTIVES

The primary goal of the research presented in this thesis is to investigate the role of the conserved cysteine (C**C**MC) in the CC-type glutaredoxin GRX480 active site and whether it plays a central role in protein complex assembly or a structural role within the protein itself. As it has been shown that some plant, bacterial, yeast and human GRXs can exist as dimeric holoproteins in the regulation of iron homeostasis or as monomeric apoforms that exhibit deglutathionylation activity, uncovering the behaviour of the GRX480 protein may shed some light onto its not fully understood role during abiotic or biotic stress responses. As homodimeric iron clusters are formed when two CCXC/S or CGFS type GRX monomers ligate one [2Fe-2S] moiety and two molecules of GSH via their N-terminal active site cysteine (**C**XXX) and protein deglutathionylation activity requires a CXXC/CXXS active site, mutations (single, double, and triple) to the active site of the GRX480 protein were used as a means to uncover how each cysteine residue may contribute to three dimensional protein structure and complex assembly. Determining whether the difficulties experienced during previous studies in expressing plant glutaredoxins in *E.coli* is due to the presence of a GAWL C-terminal tail, the inability of the bacteria to transcribe/translate the uncommon codons of the genetic sequence, or if the synthesized protein is more likely to be degraded by the bacteria is also a subject of interest in this research. As such, the GAWL tail of the GRX480 protein was left unmodified and the genetic sequence was codon optimized for expression in *E.coli* cultures.

3. MATERIALS AND METHODS

3.1 *AtGRX480* Codon Optimization, Active Site Mutation, and Plasmid Construction

The genetic sequence of the *Arabidopsis* GRX480 protein (*AtGRX480*) was codon optimized to allow for recombinant protein expression in *E.coli* DE3 competent cells (Strain B/BL21-DE3) as the original sequence was previously shown to not allow for successful expression of the GRX480 protein. The subsequent amino acid sequence (Fig. 2) remained unchanged. GRX480 active site variants were created by site directed mutagenesis via point mutations in the genetic sequence of *AtGRX480* to encode for the amino acid serine (S) instead of cysteine (C). Single (SCMC, CSMC, CCMS), double (SSMC, CSMS, SCMS), and triple mutants (SSMS) were created for the purposes of this study.

The commercially available pET41a plasmid (Novagen)(Fig. 2) was modified to exclude all multiple cloning sites with the exception of *XhoI* and *NdeI* to allow for insertion and cloning of the *AtGRX480* genetic sequence. The *Strep*- tag II (Qiagen) was used to replace the original S-tag and His-tag sequences, and was fused to the C-terminal end of the amino acid sequence. The kanamycin (Km) antibiotic resistant gene remained in the plasmid and served as means for bacterial colony selection. The genetic sequence for glutathione transferase (GST) was removed as it possesses similar activity to glutaredoxins and may interfere or present false positives in experiments involving GRX480.

A

```
          10         20         30         40         50
MQGTISCARN YNMTTTVGES LRPLSLKTQG NGERVRMVVE ENAVIVIGRR

          60         70         80         90         100
GCCMCHVVRR LLLGLGVNPA VLEIDEERED EVLSELENIG VQGGGGTVKL

          110        120        130        140
PAVYVGGRLF GGLDRVMATH ISGELVPILK EVGALWLLESAWSHPQFEK
```

B

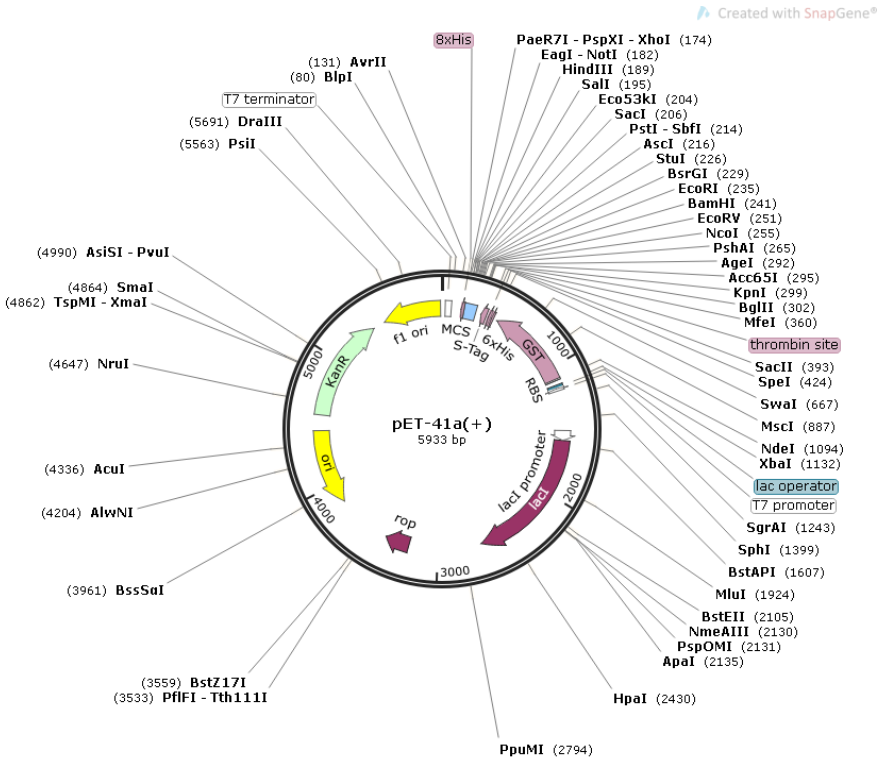

Figure 2. The plasmid components used for recombinant expression of *Arabidopsis* GRX480 proteins in *E.coli* (DE3) competent cells. (A) The amino acid sequence of the GRX480 protein with the active site sequence (CCMC) indicated by an arrow, and *Strep*-tag sequence indicated in red. **(B)** The commercially available pET41a plasmid that was modified to allow recombinant protein expression of GRX480 in *E.coli* (DE3) competent cells.

3.2 Bacterial Transformation

The plasmid DNA for GRX480, GRX480 active site variants, and a plasmid containing no gene sequence (empty vector for control) were transformed into *E.coli* DE3 competent cells (Strain B/BL21-DE3) through electroporation. A reaction mixture (5ul 1/100x diluted plasmid DNA, 25 uL competent cells, 20uL MQ H_2O) was subjected to a 5 second pulse (2.5 kV, 25 uF capacitance, 200Ω resistance, 2mm gap). The transformed reaction mix was inoculated into a culture tube containing growth medium (882 uL 2YT (16g/L tryptone, 10g/L yeast extract, 5g/L NaCl) + 18 uL of 20% D-glucose) and incubated at 37^o C while shaking at 250 rpm for 1 hr. 50 uL and 850 uL were used on two separate solid culture plates containing LB Medium (10g/L tryptone, 5g/L yeast extract, 10g/L NaCl, 15 g/L agar) and a 10 ug/mL working concentration of the kanamycin(Km) antibiotic and incubated for 24 hrs at 37^o C. A single isolated colony was used to make a 5mL 2YT culture containing a 10 ug/mL concentration of Km that was incubated for 24 hrs at 37^o C and 250 rpm. 700 uL of this culture was then mixed with 300uL of filter-sterilized 50% glycerol and stored in a cryovial at -80^o C as a cell stock.

3.3 Bacterial Culture and Recombinant Protein Expression

A sterile pipette tip was used to scrape the surface of the frozen cell stock and was placed in 5mL 2YT culture containing a 10 ug/mL concentration of Km that was incubated for 24 hrs at 37^o C and 250 rpm. Two 50 uL aliquots were used to inoculate plates containing LB medium/ Km and incubated for 24 hrs at 37^o C. These plates were then placed at 4^o C for a

maximum of 3 weeks, at which time the process was repeated to ensure viable cell cultures and to exclude those that had possibly grown resistant to the antibiotic without actually containing the plasmid. Culture of *E.coli* cells containing an empty vector were performed in the absence of Km. 3 x 10mL aliquots of 2YT/Km were each inoculated with a single isolated colony each from these plates and incubated for 24 hrs at 37^{o} C and 250 rpm. 5 mL of these cultures were then used to inoculate 6 x 500mL aliquots each of 2YT/Km for a total of 3L of culture. These cultures were incubated for approximately 1.5 to 2hrs at 37^{o} C and 250 rpm until an optical density (OD) of 0.4 – 0.6 at 600 nm was reached. Protein expression was then induced by addition of 1 mL of 0.5M IPTG (with the exception of one trial of the empty vector control) to each 500 mL culture which were then incubated at 37^{o} C and 250 rpm for 3 hrs. Cells were then collected by centrifugation at 4^{o} C. Each 500 mL culture was found to yield a pellet weighing 1.1g on average. Each 1.1g pellet required resuspension in 17 mL of Buffer NP (50 mM NaH_2PO_4, 300 mM NaCl, pH 8.0) to ensure optimum equipment performance during cell lysation and protein extraction using the Emulsiflex C3(AVENSTIN) for an elapsed time of 4 mins per 34 mL of cell suspension. Due to a large amount of cell debris and lipids, especially when large volumes of pellet were being processed, protein samples often had to be centrifuged more than once to retrieve a supernatant pure enough to pass through a syringe filter. The filtered protein extract was then used for *Strep*-column purification and 3 mLs were saved for further analysis.

3.4 FPLC- adapted *Strep*-Column Protein Purification

A 1mL *Strep*-Tactin Superflow Plus Column (Qiagen) was adapted to the ÄKTA purifier 10 FPLC (GE Healthcare Bio-Sciences) and operated with UNICORN Version 5.31 software. To determine the optimal conditions needed to purify the *Strep*-tagged GRX480 protein sufficiently, a number of different experimental variables were tested (see below). In each case the FPLC system was filled with Buffer NP and the column was equilibrated with 10mL. The protein isolate was injected through the *Strep*-Tactin column via a sample loop with a pressure maximum set to 0.4 MPa. Absorbance (mAU) was measured at 215, 280, and 330 nm wavelengths and protein concentration was found to be indicated by changes in absorbance at 215nm. Samples of protein flowthrough were collected and stored at -20^{o} C. Once all protein had cleared through the column (absorbances returned to baseline values), elution of the *Strep*-tagged protein was performed using Buffer NPD (50 mM NaH_2PO_4, 300 mM NaCl, 2.5 mM desthiobiotin, pH 8.0). Protein elution was found to span over a large range of volume so the first 15 mL starting at the point of a steady increase in absorbance at 215 nm were collected. The total protein concentration of these peak fractions was determined by the Bradford Assay (see below). 10 mL was used immediately for gel filtration while 5 mL was stored at -20^{o} C for protein concentration determination and analysis by SDS-PAGE. The *Strep*-Tactin column was then disconnected from the FPLC and regenerated. Regeneration involved three syringe washes of 5 mL of *Strep*-Tactin Regeneration Buffer (50 mM NaH_2PO_4, 300 mM NaCl, 1 mM HABA, pH 8.0) followed by two washes of 4mL of Buffer NP. This process was repeated until successful regeneration of the column by displacement of desthiobiotin was indicated by a colour change

of the resin from white to red. Samples of the Regeneration Buffer were collected and stored at -20^{o} C for SDS-PAGE analysis. The column was then stored at 4^{o} C for re-use.

Experimental variables tested during trouble-shooting :

Culture volume and pellet weight: 1L (2.2g), 1.5L (3.3g), and 3L (6.6g)

Injection volume/method: single injections of 10mL or 50 mL and multiple injections (10 mL injections for a 40, 50, 60 ,70 ,80, and 170 mL total volume).

Flow rates: 1.0 mL/min (standard) and 0.8 mL/min

Elution buffer concentration: fixed and gradient

3.5 Bradford Protein Assay

Bradford dye reagent was prepared by diluting one part Protein Assay Dye Reagent Concentrate (Bio-Rad) with four parts MQ filtered H_2O. 10 dilutions (0.1 mg/mL to 1 mg/mL) of BSA were prepared to encompass the known linear range (0.2 to 0.9 mg/mL). 100 uL of each BSA standard and crude extracts taken from *E.coli* cells recombinantly expressing GRX480 proteins were added to 5mL of diluted dye reagent and mixed. The solution was allowed to incubate at room temperature for 5 mins and then absorbances were measured at 595 nm. Protein concentrations were calculated using the equation provided from the linear regression line of the BSA standards (Fig. 8). Absorbances of GRX480 crude extracts that did not fall within this range were repeated with a 1/10 dilution of the protein sample. This method was found to be insufficient in determining *Strep*-column isolate protein concentrations so a Bradford Micro-Assay was performed. 10 dilutions (1ug/mL to 10 ug/mL) of BSA were prepared to encompass the known linear range (1.2 to 10 ug/mL). 800 uL of each BSA standard and *Strep*-column

isolates taken were added to 200 uL of dye reagent concentrate and mixed. The solution was allowed to incubate at room temperature for 5 mins and then absorbances were measured at 595 nm. Protein concentrations were calculated using the equation provided from the linear regression line of the BSA standards (Fig. 8).

3.6 FPLC- adapted Gel Filtration

All buffers and MQ H_2O were filtered and de-gased prior to use and protein samples were syringe filtered before injection. A Sephacryl S-100 column (GE Healthcare Bio-Sciences) with a total volume of 100mL was adapted to the ÄKTA purifier 10 FPLC (GE Healthcare Bio-Sciences) and operated with UNICORN Version 5.31 software. 0.5 mL of gel filtration standards blue dextran (2000 kDa, 1mg/mL), ferritin (440 kDa, 5mg/mL), BSA (66kDa, 5mg/mL), ovalbumin (44 kDa, 5mg/ml), and equine skeletal muscle myoglobin (17 kDa, 5mg/mL) were injected into the column using S-100 Running Buffer (50 mM HEPES, 250 mM NaCl, pH 7.4) in separate runs with a flow rate of 0.2 mL/min and a max pressure of 0.4 MPa. The protein elution volume (Ve) of blue dextran and ferritin were used to estimate the void volume (Vo) of the column while the Ve of the remaining standards were used to calculate the gel phase distribution coefficient (Kav). A plot of the Kav and the log of the molecular weight (Log MW) of the proteins were used to generate a linear regression equation (Fig. 10) for use in estimating the 3D molecular weight of the GRX480 proteins. 10 mL of each GRX480 *Strep*-Column protein isolate was injected into the column in separate runs using the same conditions as the standards. Due to an extremely low protein concentration of *Strep*-column isolates (2.0 to 3.4ug/mL), a volume of 10 mL (10%

of total column volume) was used for injection. Typically volumes up to 30% of the total column volume can be applied for group separations and 4% for high resolution fractionation; however a minimum of 8 mg of protein is typically needed (Biotech, 1998). Consequently, no significant or consistent changes in absorbance were observed during gel filtration, so all collected 0.5 mL fractions were incubated with1.5 cold acetone for 24hrs at -20^{o} C and then analyzed by SDS-PAGE.

3.7 SDS-PAGE, Immunoblot, and Protein Visualization

All samples analyzed by SDS-PAGE were acetone precipitated for 24hrs at -20^{o} C. Samples were then centrifuged for 30 mins at 4^{o} C. The acetone was removed from these samples and left to dry for 5 mins. Both samples containing protein pellets and those without one visible were resuspended in SDS-PAGE Sample Buffer (0.06 M Tris, 10% glycerol, 0.025% bromophenol, 2% SDS, 5% Mercapto EtOH) and boiled at 100 ^{o} C for 5 mins. Due to large differences in protein concentration and pellet size, crude protein extracts, *Strep*-Column protein isolations, and gel filtration fractions were resuspended in 400 ul, 200ul, and 50ul of Sample Buffer respectively. In all cases, 50 uL was loaded into each well of a hand-cast SDS-PAGE (4% stacking, 12 % resolving) gel. 15 uL of PiNK Plus Prestained Protein Ladder (GeneDireX) was also loaded in each gel as a molecular weight marker. Gels were run at 100 V in a tank containing Electrode Buffer (0.025 M Tris, 0.192 M glycine, 0.1% SDS, pH 8.3) until samples passed through the stacking gel, and then at 120 V until proper separation and resolution was obtained. Transfer to a nitrocellulose membrane was conducted at 20 V for 1 hr

in a Trans-Blot SD Semi-Dry Transfer Cell (Bio-Rad) in Transfer Buffer (25 mM Tris, 192 mM glycine, 20% methanol, pH 8.3). Membranes were stained with Ponceau S to confirm presence of proteins. Antibody detection (immunoblot) was achieved using an anti-*strep* antibody raised in rabbit (GenScript) as the primary antibody and a fluorophore coupled goat anti-rabbit (Mandel) antibody as the secondary antibody. Protein bands were then detected by infrared imaging using an Odyssey Imager (LI-COR). Molecular weights and band intensities were estimated using Image Studio (LI-COR) software and background saturation was optimized for each membrane to increase visibility.

3.8: Protein Structure Prediction

The amino acid sequence of GRX480 depicted in Figure 2 was submitted to the online I-TASSER (Iterative Threading ASSEmbly Refinement) server for sequence alignment and structural prediction.

4. RESULTS

4.1 Recombinant expression of *Strep*-tagged wildtype and active site variants of the *Arabidopsis* GRX480 protein causes an alteration in the expression profile of native *E.coli* proteins.

When *Strep*-tagged wildtype GRX480 was recombinantly expressed in *E.coli* DE3 cells, there was a marked decrease in the presence of proteins of approximately 36, 32, 20, 16, and 12 kDa in size (Fig. 3A (I)) when compared to *E.coli* cultures containing an empty vector. Control colonies containing the empty vector were also subjected to IPTG induced protein expression to observe for any possible additional protein products and to verify that the protein bands corresponding to GRX480 expression (Fig. 3A (II)) were genuine and not a product of the empty vector. The total protein expression profiles of colonies containing the empty vector and the IPTG induced empty vector did not show any obvious differences (Fig. 3A (I)). Immunoblot analysis revealed protein bands with slight affinity for the anti-*Strep* antibody in both the control colonies and colonies expressing wildtype GRX480 with band sizes of 36,34, and 32 kDa (Fig.3A (II)). The protein bands with the highest affinity for the anti-*Strep* antibody were approximately 14.7 kDa in size and identified as GRX480 as they were absent in the control colonies (Fig.3A (II)). When single (SCMC, CSMC, CCMS) double (SSMC, CSMS, SCMS), and triple (SSMS) mutations in the active site of GRX480 (CCMC) were examined, similar patterns were observed (Fig. 3B). There was a marked decrease in the presence of proteins of approximately 36, 20, and 16 kDa in size (Fig. 3B (I)) when compared to *E.coli* cultures containing an empty vector. Immunoblot analysis revealed protein bands with slight affinity for the anti-*Strep*

antibody in both the control colonies and colonies expressing GRX480 proteins with band sizes of 36,34, and 32 kDa (Fig. 3B (II)). The protein bands with the highest affinity for the anti-*Strep* antibody were approximately 14.7 kDa in size and identified as GRX480 as they are absent in the control colonies (Fig. 3B (II)).

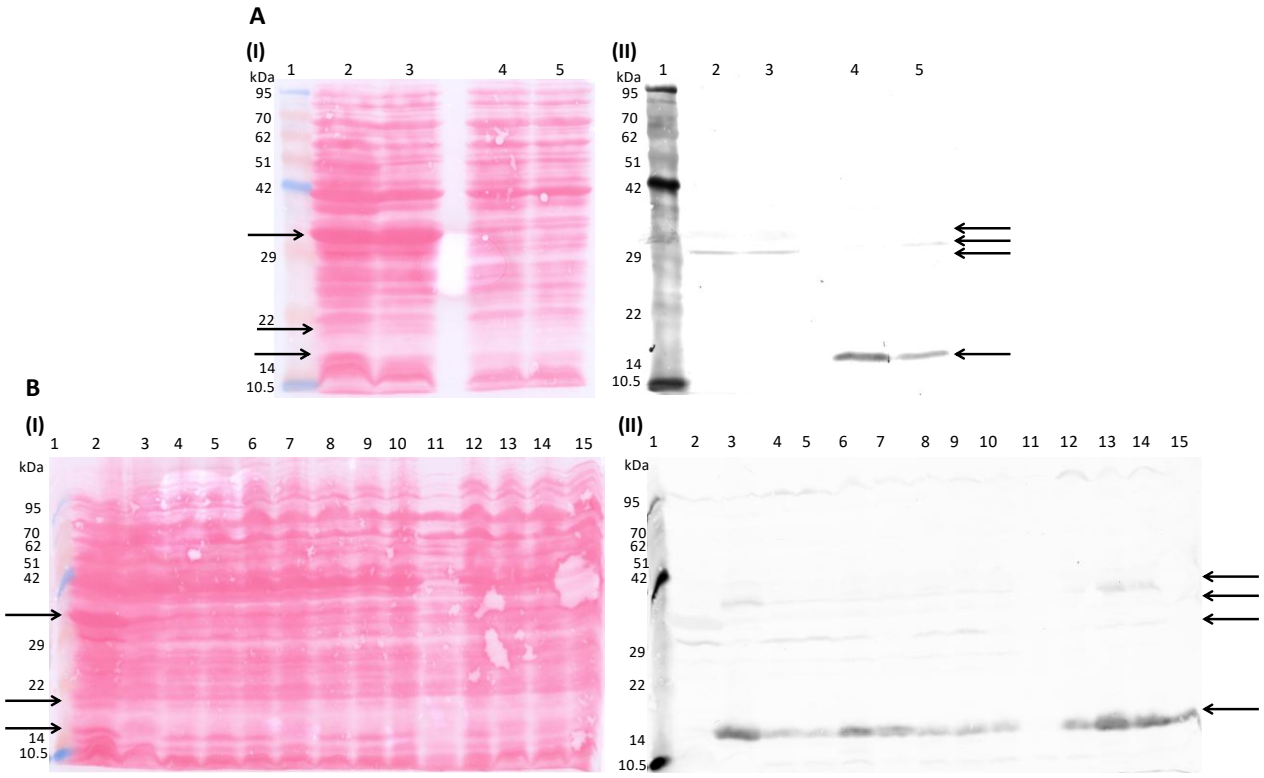

Figure 3. Recombinant expression of *Strep*-tagged wildtype and active site variants of the *Arabidopsis* GRX480 protein in *E.coli* DE3 cells causes an alteration in the expression profile of native *E.coli* proteins. 500 ul of precipitated crude extract taken from recombinant *Strep*-tagged GRX480 protein (XXMX active site) expression in *E.coli* cultures and cultures containing an empty vector (EV) were resuspended in 400 ul SDS-PAGE Sample Buffer and boiled. 50 ul of the indicated protein sample was loaded onto a 4% stacking/12 % resolving SDS-PAGE gel alongside 15 uL of a pre-stained protein ladder (Lane 1, A(I)(II) & B (I)(II)). Molecular weights are indicated in kilodaltons (kDa). After running, proteins were transferred to a nitrocellulose membrane and then stained with Ponceau S to visualize the total protein expression profile (A (I) & B (I)). Immunoblot with a rabbit anti-*Strep* primary antibody and goat anti-rabbit secondary antibody was used to visualize the GRX480 proteins (A (II) and B (II)). **A(I):** Lane 2**:** culture containing empty vector**;** Lane 3**:** culture containing empty vector induced by IPTG; Lanes 4 & 5: cultures containing the recombinant wildtype GRX480 protein (CMCC active site). Arrows (in descending order) indicate approximate protein sizes of 36, 20, and 14.7 kDa

respectively. **A(II):**Immunoblot of the membrane depicted in A(I). Arrows (in descending order) indicate approximate protein sizes of 36, 34, 32, and 14.7 kDa respectively. **B(I):** Lane 2**:** culture containing empty vector**;** Lanes 3 to 5**:** cultures containing the recombinant wildtype GRX480 protein (CMCC active site); Lanes 6 to 15: cultures containing the recombinant GRX480 protein active site variants (XXMX). Arrows (in descending order) indicate approximate protein sizes of 36, 20, 14.7 kDa respectively. **B(II):** Immunoblot of the membrane depicted in B(I). Arrows (in descending order) indicate approximate protein sizes of 36, 34, 32, and 14.7 kDa.

4.2 A multiple injection method is needed to isolate GRX480 from a *Strep*-tag purification column.

During attempts to purify GRX480 from filtered crude protein extract, a single injection method proved to be inefficient in isolating the protein. Figure 4 shows two examples of the volumes tested. A single injection of 10 mL of crude protein extract and elution using a gradient concentration yielded a slight increase in absorbance at 215 nm (Fig.4A (I)), but when the fractions were analyzed by SDS-PAGE and immunoblot, no protein band could be detected (Fig. 4A(II)). When the single injection volume was increased to 50 mL with a fixed volume of elution buffer concentration, a more noticeable increase in absorbance was detected at 215 nm (Fig. 4B (I)), however only faint protein bands were detected by immunoblot (Fig. 4B (II)). In both cases, protein bands corresponding to the GRX480 protein were instead observed in the column flowthrough prior to the use of the elution buffer (Fig. 4A/B(II)).

Multiple injections of 10mL of crude protein extract, with time allowed for the absorbance to return to near baseline, yielded more successful results. Figure 5 shows two examples of the volumes tested. A multiple injection for a total of 60 mLs (Fig. 5A) and 180 mLs (Fig. 5B) with a fixed elution buffer concentration yielded the same magnitude of change in

absorbance at 215 nm. The intensity of the protein bands corresponding to the GRX480 protein after column isolation were analyzed by immunoblot (Fig. 5C). It was concluded that 60 mL of total injected crude protein extract was sufficient in saturating the column with enough protein to be isolated with the use of elution buffer. Although this multiple injection method was more successful than the single injection method in terms of purifying GRX480, an unknown protein of approximately 36 kDa with high affinity for the *Strep*-tag antibody was also present in these column isolates (Fig. 5C). It was also revealed that a large amount of the GRX480 protein remained bound to the column when treated with a column regeneration buffer as depicted in Figure 5C. Doubling the concentration of desthiobiotin in the elution buffer did not increase the amount of GRX480 protein eluted from the column (results not shown).

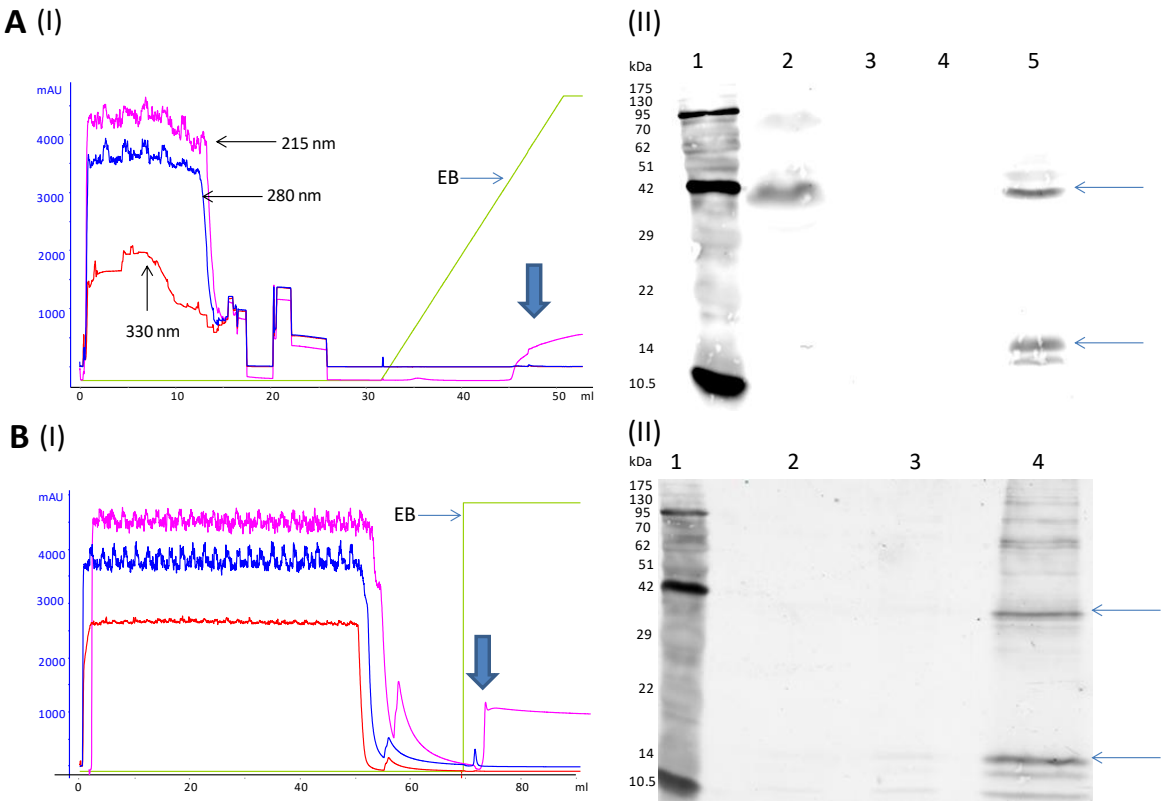

Figure 4. **A single injection method is inefficient in isolating *Strep*- tagged GRX480 from a *Strep*-tag purification column.** The results of a single injection of crude protein extract from *E.coli* colonies containing GRX480 protein through a FPLC- adapted 1mL *Strep*-Tactin Superflow Plus Column (Qiagen) and elution of GRX480 (indicated by large arrow) with an elution buffer (EB) containing 2.5 mM desthiobiotin. Absorbances (in mAU) were monitored at 215, 280, and 330 nm. **A(I)**: Experimental parameters: Protein extraction from 2.2g of *E.coli* pellet, 10mL of crude extract injection, 1 mL/min flow rate, gradient elution (to 100% concentration). **B(I)**: Experimental parameters: Protein extraction from 3.3g of *E.coli* pellet , 50 mL of crude extract injection, 0.8 mL/min flow rate, and fixed concentration elution . 500 ul of precipitated protein column eluate were resuspended in 200 ul SDS-PAGE Sample Buffer and boiled. 50 ul was loaded onto a 4% stacking/12 % resolving SDS-PAGE gel alongside 15 uL of a pre-stained protein ladder (Lane 1, A(II) & B(II)). After running, proteins were transferred to a nitrocellulose membrane. Immunoblot with a rabbit anti-*Strep* primary antibody and goat anti-rabbit secondary antibody was used to visualize the GRX480 proteins (A (II) and B (II))Molecular weights are indicated in kilodaltons (kDa). **A(II)**: Immunoblot of protein fractions from A(I). Lane 2: Ovalbumin protein standard (44 kDa); Lanes 3 & 4: *Strep*-column eluate; Lane 5: *Strep*-column flowthrough. **B(II):** Immunoblot of protein fractions from B(I). Lanes 2 & 3: *Strep*-column eluate; Lane 4: *Strep*-column flowthrough. Arrows (in descending order) in both A(II) and B(II) indicate approximate protein sizes of 36 and 14.7 kDa.

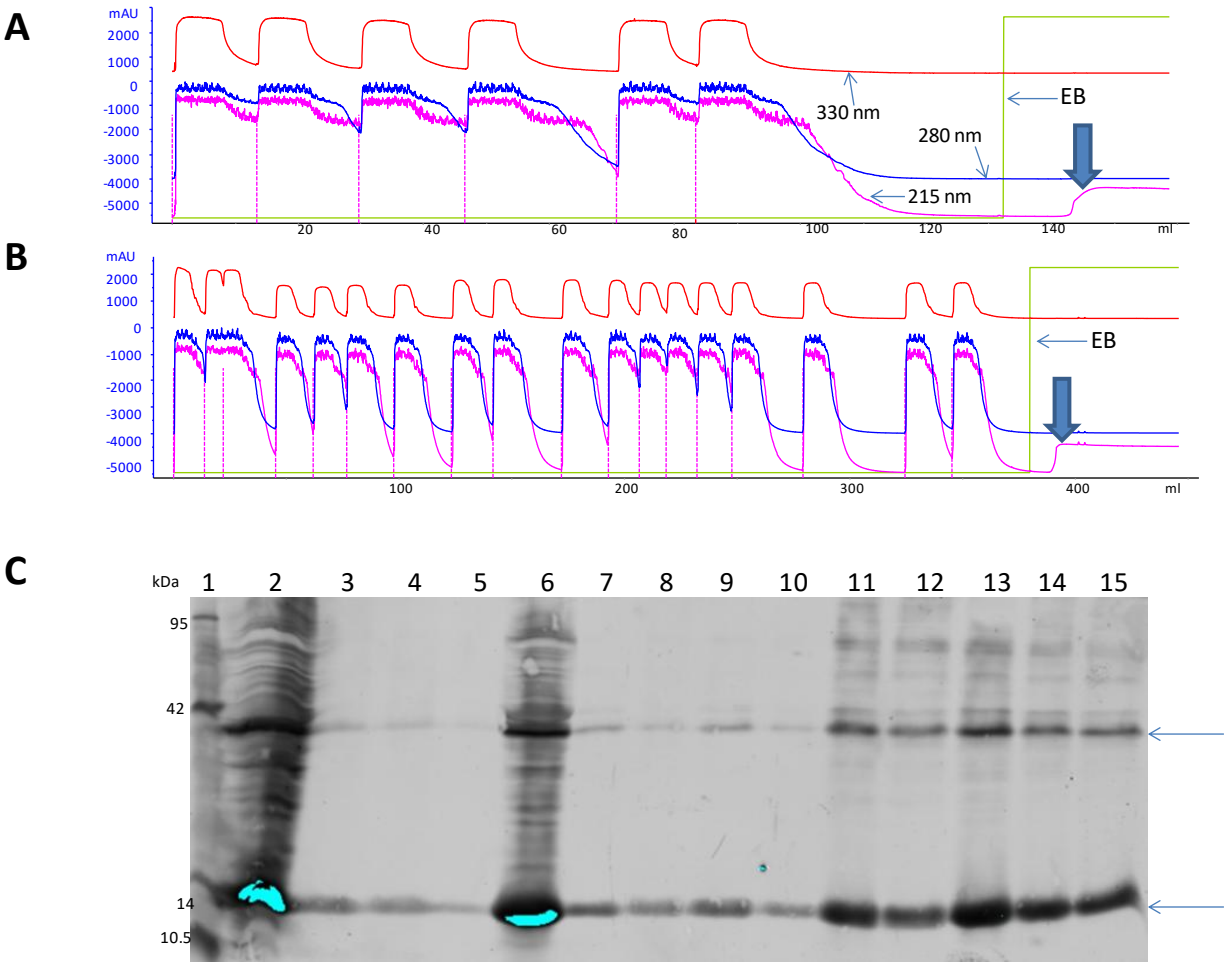

Figure 5. A multiple injection method, consisting of 10 mL injections for a total of 60 mLs, results in *Strep*-column saturation and is sufficient in isolating the *Strep*- tagged GRX480 protein. The results of a multiple injection method of crude protein extract from *E.coli* colonies containing GRX480 protein through a FPLC- adapted 1mL *Strep*-Tactin Superflow Plus Column (Qiagen) and elution of GRX480 (indicated by large arrow) with an elution buffer (EB) containing 2.5 mM desthiobiotin. Absorbances (in mAU) were monitored at 215, 280, and 330 nm. **(A)**: Experimental parameters: Protein extraction from 3.3 g of *E.coli* pellet , 6 x 10 mL (60 mL total) of crude extract injection, 0.8 mL/min flow rate, and fixed concentration elution. **(B)**: Experimental parameters: Protein extraction from 3.3 g of *E.coli* pellet , 18 x 10 mL (180 mL total) of crude extract injection, 0.8 mL/min flow rate, and fixed concentration elution. 500 ul of precipitated protein column eluate were resuspended in 200 ul SDS-PAGE Sample Buffer and boiled. 50 ul was loaded onto a 4% stacking/12 % resolving SDS-PAGE gel alongside 15 uL of a pre-stained protein ladder (**C**, Lane 1). After running, proteins were transferred to a nitrocellulose membrane. Immunoblot with a rabbit anti-*Strep* primary antibody and goat anti-rabbit secondary antibody was used to visualize the GRX480 proteins(**C**).Molecular weights are

indicated in kilodaltons (kDa). **(C)**: Lanes 2 & 6: Crude extracts from (A) and (B) respectively; Lanes 3-5 & 7-10: *Strep*-column protein eluate from (A) and (B) respectively; Lanes 11-12 & 13-15; *Strep*-column eluate when washed with a regeneration buffer (1 mM HABA) to remove proteins still bound to the column. Arrows (in descending order) indicate approximate protein sizes of 36 and 14.7 kDa.

4.3 The active site variants of the GRX480 protein require differing volumes of crude protein extract for *Strep*-column isolation and successful use in gel filtration.

During Strep-column isolation of the GRX480 protein, it was found that different volumes of crude protein extract were required to observe an increase of 1000 mAU or greater at 215 nm during elution for each active site variant. Figures 6 and 7 depict the FPLC-adapted multiple injection runs that resulted in isolation of the protein and also yielded results during the subsequent gel filtration. Wildtype GRX480 (CCMC) required 50 mLs of crude extract while the single variants SCMC, CSMC, and CCMS required 70, 80, and 70 mLs respectively (Fig. 6). The double variants CSMS, SCMS, and SSMC required 70, 70, and 60 mLs respectively (Fig. 7). The triple variant, SSMS, yielded results after use of only 40 mLs but 60 mLs improved results in terms of *Strep*-column yield (Fig. 7).

4.4 Mean total protein concentrations from crude recombinant *E.coli* expression and *Strep*-column protein isolates differ for GRX480 active site variants.

When total protein concentrations of crude *E.coli* culture extract containing the GRX480 protein were determined by Bradford assay, it was found that concentration differed for each active site variant and all were drastically lower than the empty vector containing colonies, a

measured concentration of 5.99 mg/mL (Fig. 8). The CSMS variant exhibited the greatest mean concentration at 3.10 mg/mL, while the SSMS and SCMC variants produced concentrations of 2.04 and 1.75 mg/mL respectively. The SCMS variant and wildtype(CCMC) cultures produced a much lower yield at 1.12 and 0.92 mg/mL respectively. The lowest protein concentrations were those of the SSMC, CCMS, and CSMC variants at 0.71, 0.64, and 0.47 mg/mL respectively. Analysis of *Strep*-column isolates by the Bradford micro-assay revealed that the trends differed from those observed for the crude protein concentrations (Fig. 8). Use of the multiple injection method allowed for a more uniform protein concentration to be eluted for each of the GRX480 proteins. The SCMC and CSMC variants had the highest mean total protein concentrations at 3.36 and 3.05 ug/mL respectively. Mid-range concentrations of 2.86, 2.67, and 2.56 ug/mL were observed for the CSMS, CCMS, and SSMS variants respectively. The lowest protein concentrations from were exhibited by SCMS, wildtype(CCMC), and SSMC at 2.21, 2.20, and 2.0 ug/mL respectively.

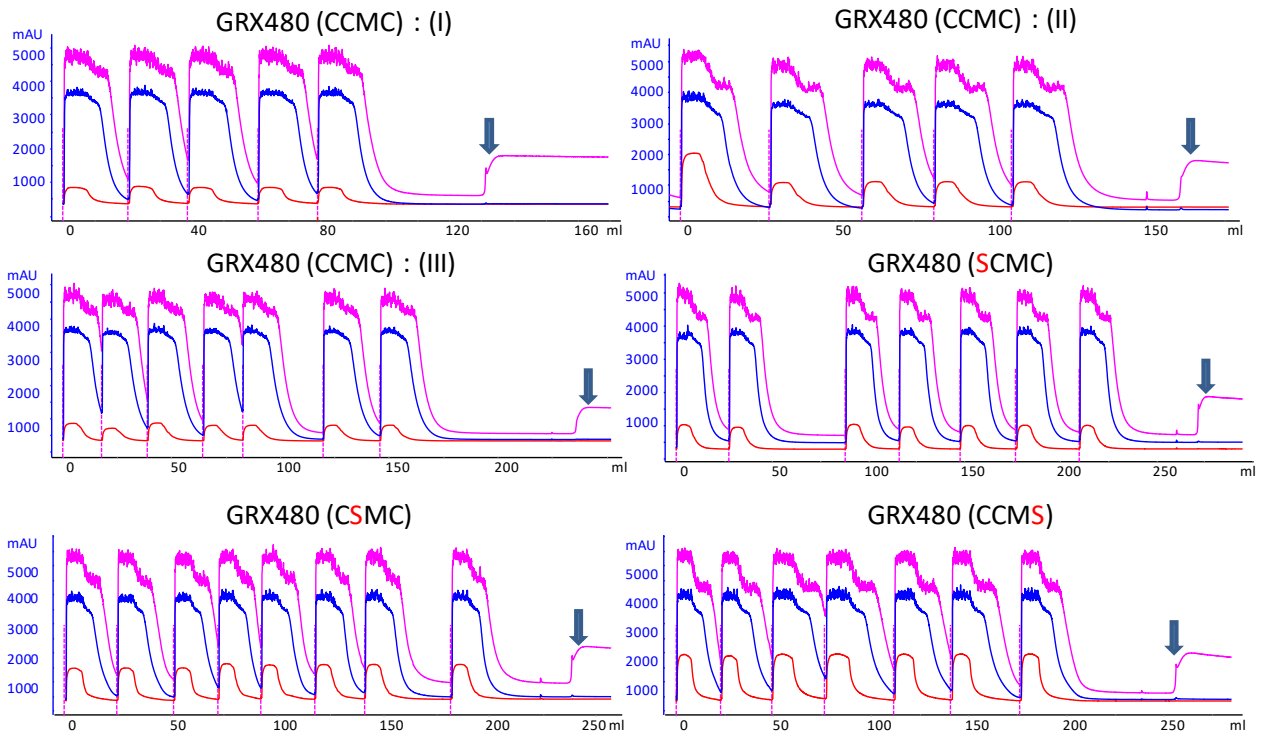

Figure 6. **Successful isolations of the *Strep*- tagged wildtype GRX480 protein (CCMC) and single mutation active site variants(XXMX) using the FPLC- adapted multiple injection method.** The results of a multiple injection method of crude protein extract from *E.coli* colonies containing GRX480 protein through a FPLC- adapted 1mL *Strep*-Tactin Superflow Plus Column (Qiagen) and elution of GRX480 (indicated by large arrow at 215 nm) with an elution buffer containing 2.5 mM desthiobiotin. Absorbances (in mAU) were monitored at 215 (highest peaks), 280 (mid-range peaks), and 330 (lowest peaks) nm. All runs depicted required extraction from 3.3g of *E.coli* pellet, a 0.8 mL/min flow rate, and a fixed concentration elution. 10 mL injections for a total of 50 mL and 70 mLs for wildtype GRX480 (CCMC), 70 mLs for the single variants (SCMC and CCMS), and 80 mLs for the CSMC variant were required for observable GRX480 isolation and for subsequent use in gel filtration.

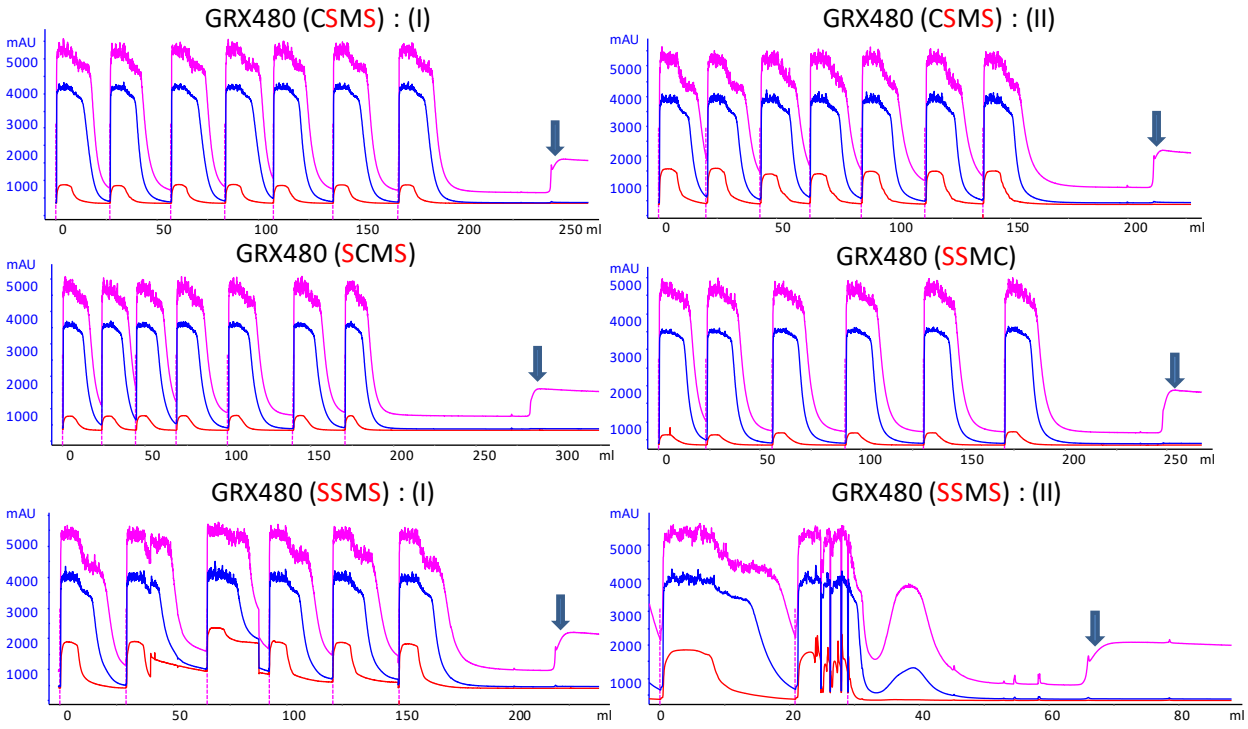

Figure 7. **Successful isolations of the *Strep*- tagged GRX480 double (XXMX) and triple mutation (SSMS) active site variants using the FPLC- adapted multiple injection method.** The results of a multiple injection method of crude protein extract from *E.coli* colonies containing GRX480 protein through a FPLC- adapted 1mL *Strep*-Tactin Superflow Plus Column (Qiagen) and elution of GRX480 (indicated by large arrow at 215 nm) with an elution buffer containing 2.5 mM desthiobiotin. Absorbances (in mAU) were monitored at 215 (highest peaks), 280 (mid-range peaks), and 330 (lowest peaks) nm. All runs depicted required extraction from 3.3g of *E.coli* pellet, a 0.8 mL/min flow rate, and a fixed concentration elution . 10 mL injections for a total of 70 mLs were required for the CSMS and SCMS variants while 60 mLs was required for the CSMC. The SSMS triple variant yielded results with just 40 mLs of crude extract, however yield was improved when 60 mLs was used.

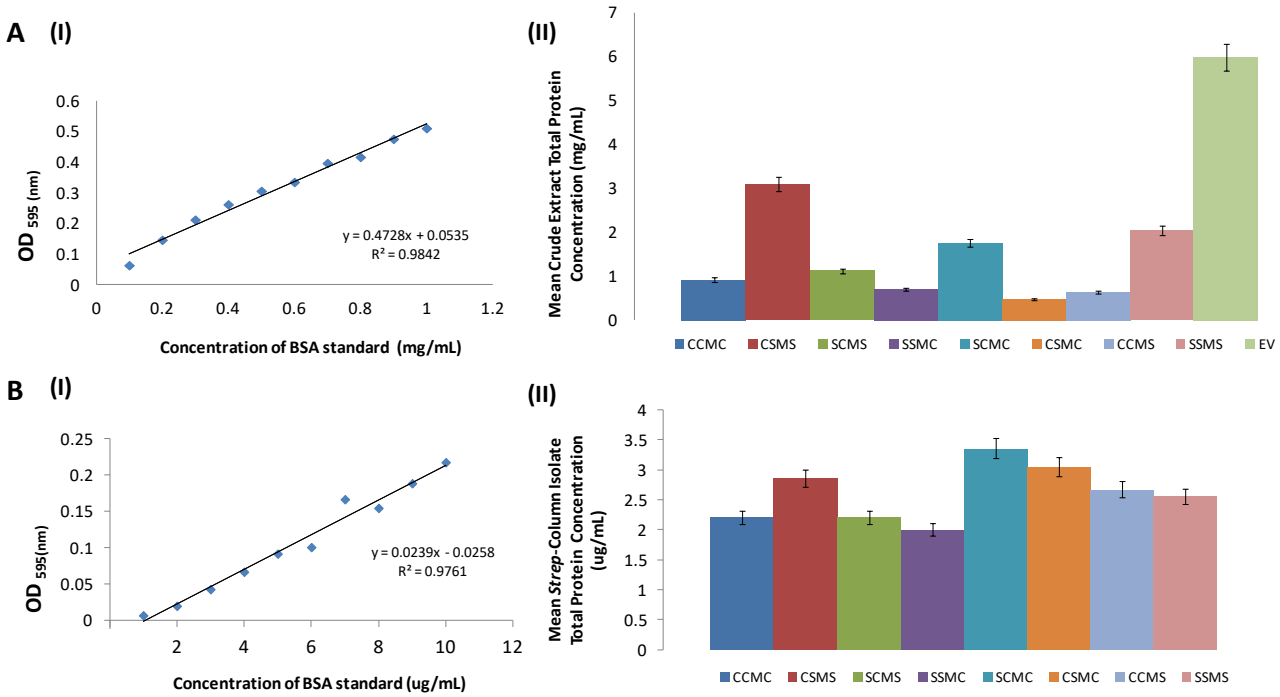

Figure 8. Mean total protein concentrations from crude recombinant *E.coli* expression and *Strep*-column protein isolates differ for wildtype GRX480 (CCMC) and active site variants. Bradford Assay **(A)** to determine the mean crude extract protein concentration (mg/mL) from *E.coli* cultures and the Bradford Micro-Assay **(B)** to determine the mean *Strep*-column isolate total protein concentration (ug/mL). Known concentrations of bovine serum albium (BSA) standard were used to determine absorbance at 595 nm (**A(I)** & **B(I)**). The linear regression equation was used to determine concentrations of GRX480 protein isolates from multiple experiments and all active site variants, the values of which were then averaged (**A(II)** & **B(II)**). Crude protein concentrations of colonies containing an empty vector (EV) served as a control.

4.5 The GRX480 SCMC, CCMS, CSMC, and CSMS active site variants exhibit a distinct degradation pattern and the highest concentration of the GRX480 protein when purified from the *Strep*-column.

SDS-PAGE and Immunoblot analysis of *Strep*-column purified GRX480 samples revealed that the CSMC, CCMS and CSMS active site variants exhibited a distinct degradation pattern and also the highest concentration of the GRX480 protein (Fig. 9). Wildtype GRX480 (CCMC) and all other active site variants displayed a single band at approximately 14.7 kDa. The double variant, CSMS, showed a significantly more intense band at 14.7 kDa with additional degradation bands at 13, 12 and 10.8 kDa. The single variants, SCMC, CSMC and CCMS, also displayed a more intense band at 14.7 kDa when compared to the wildtype and other variants with CSMC closer to the intensity to that of CSMS than SCMC or CCMS. The SCMC, CSMC and CCMS variants also showed degradation similar to that of CSMS with degradation bands at 13 and 10.8 kDa, but with the 12 kDa band noticeably absent from SCMC and CCMS and very faint in the CSMC sample. Interestingly, the unknown contaminating/ co-eluting protein is noticeably present at 36 and 34 kDa in the CSMS, CSMC, and CCMS samples as it displays an affinity for the *Strep*-tag antibody.

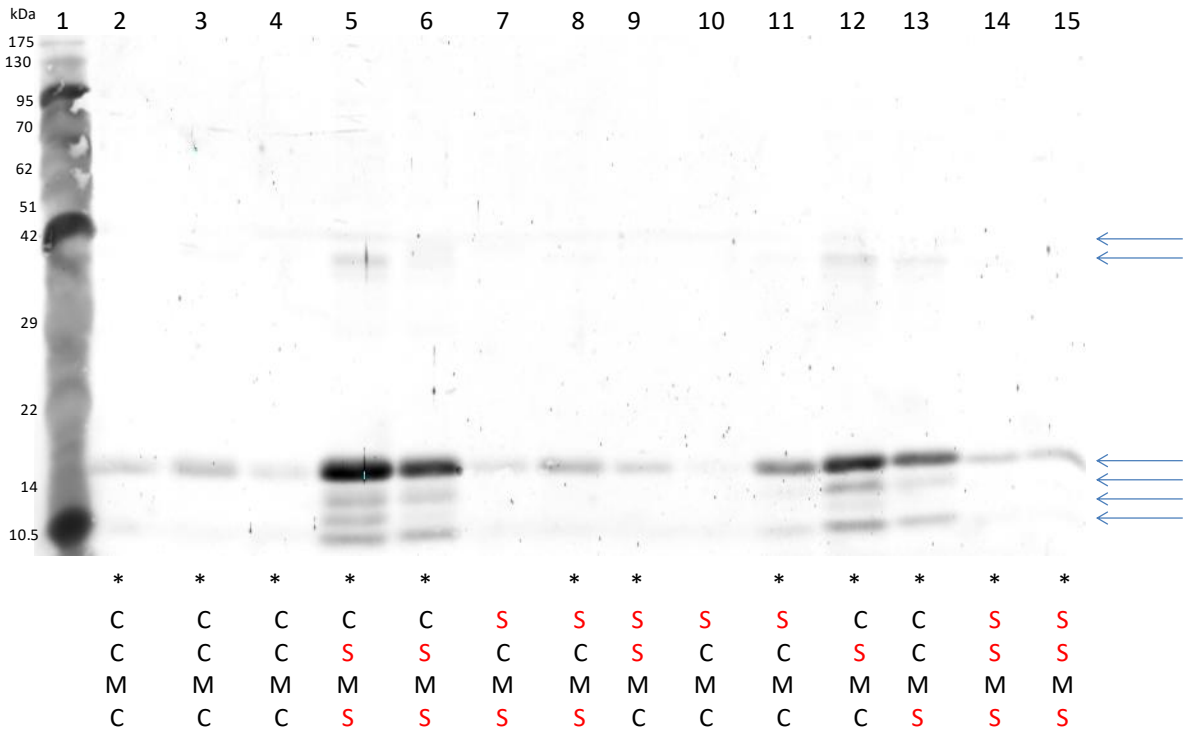

Figure 9. **SDS-PAGE and immunoblot analysis of wildtype GRX480 (CCMC) and active site variants (XXMX) *Strep*-column isolations.** 500 ul of precipitated protein column eluate were resuspended in 200 ul SDS-PAGE Sample Buffer and boiled. 50 ul was loaded onto a 4% stacking/12 % resolving SDS-PAGE gel alongside 15 uL of a pre-stained protein ladder (Lane 1). After running, proteins were transferred to a nitrocellulose membrane. Immunoblot with a rabbit anti-*Strep* primary antibody and goat anti-rabbit secondary antibody was used to visualize the GRX480 proteins. Molecular weights are indicated in kilodaltons (kDa). Lanes 2-15 contain isolated GRX480 protein but only those marked with an asterisk(*) indicate the *Strep*-column isolations depicted in Figures 5 & 6 that were subsequently used and generated results for gel filtration (Figs. 10-15). Arrows (in descending order) indicate approximate protein sizes of 36, 34, 14.7,13, 12 and 10.8 kDa.

4.6 The wildtype GRX480 protein and active site variants display atypical behaviour when analyzed by gel filtration.

Five standard proteins with known molecular weights were used to calculate the experimental parameters of the gel filtration column (Fig. 10A). Blue Dextran (2000 kDa) and Ferritin (440

kDa) exceeded the bead size of the gel filtration column and thus were used to estimate a column void volume of 34.5 mL. Bovine serum albium (66 kDa), ovalbumin (44 kDa), and equine skeletal muscle myoglobin (17 kDa) were found to elute at 45, 50, and 62 mL respectively. The total bed volume of the column was measured to be 100 mL. From these variables the gel phase distribution coefficient was calculated and plotted against the LogMW of the protein standards (Fig. 10B). From this linear regression, an equation was generated to determine the molecular weight of the GRX480 protein using the experimental elution volumes obtained.

A

Protein Standard	MW (kDa)	Log MW	V_e (mL)	K_{av}
Bovine Serum Albium	66	1.8195	45	0.1603
Ovalbumin	44	1.6435	50	0.2366
Equine Skeletal Muscle Myoglobin	17	1.2304	62	0.4198

V_0 (void volume of the column evaluated with Blue Dextran (2000 kDa) and Ferritin (440 kDa) = 34.5 mL

V_t (total bed volume of the column) = 100 mL

V_e (protein elution volume)

K_{av} (gel phase distribution coefficient) = (V_e - V_0) / (V_t - V_0)

B

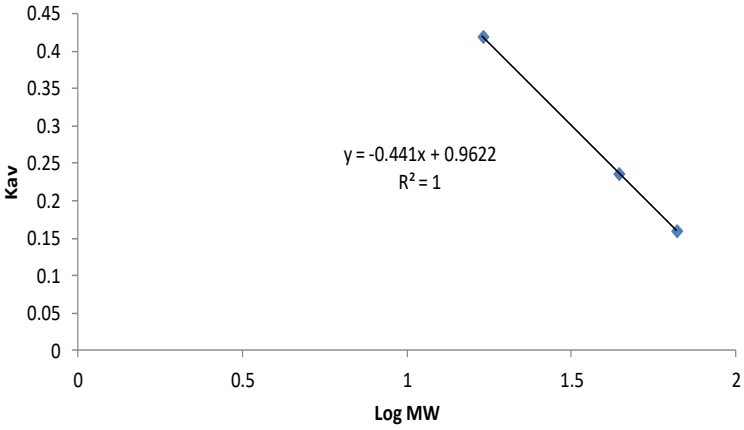

Figure 10. Operational parameters of the S100 gel filtration column determined by use of protein standards with a known molecular weight (MW). (A) The identities, molecular weights (measured in kilodaltons), and observed and calculated properties of the protein standards used in gel filtration. (B) The linear regression used to generate the equation to determine the molecular weights of the GRX480 protein based on the observed experimental elution volumes of the protein.

After *Strep*-column isolation, samples containing the GRX480 protein were immediately run through the FPLC-adapted gel filtration column. The entire elution range (mL) of the column was monitored for changes in absorbance at 215, 280, and 330 nm (Figs. 11 & 14). For the majority of the gel filtration runs, no visible changes in absorbances at any wavelength could be observed. For the CCMS variant, a sharp increase in absorbance at 280 and 330nm at 86 mL was observed (Fig. 11). The CSMS and SSMS variants showed a slight increase in absorbance at 280 and 330nm at 66.5 and 78 mL respectively (Fig.14). As analysis using UNICORN software did not provide comprehensive results, the fractions collected during column elution were precipitated and then screened for presence of the GRX480 protein by SDS-PAGE and immunoblot analysis (Figs. 12-13, 15-16). Immunoblot analysis revealed that the GRX480 protein eluted over a range of volumes correlating to protein complex disassociation and then eventually the degradation of the monomeric protein. After the membrane was scanned, the background saturation was optimized using Image Studio (LI-COR) software to increase the visibility of the protein bands. As such, comparison between band intensity can only be analyzed for bands on the same membrane. As outlined in previous results, the linearized monomeric GRX480 protein is approximately 14.7 kDa in size when analyzed by SDS-PAGE. The elution volume during gel filtration for a protein this size was calculated to be approximately 63.5 mL. Protein bands eluting earlier indicate a larger three dimensional size and those eluting later than 63.5 mL, a smaller size. Diffusion of protein into neighbouring fractions corresponding to slightly smaller or larger molecular weight is common when injecting large volumes of protein concentrate and this was observed during some runs despite the extremely low protein concentration of the *Strep*-column isolates (Figure 8). This can be observed for wildtype GRX480 and all active site

variants (Figs. 12-13, 15-16) with the exception of the CCMS variant which could not be successfully observed as an intact protein (Fig. 13). In these figures, bands appearing after the 63.5 mL elution volume also exhibit molecular sizes of 10.8 kDa or less and are representative of degradation products of the monomer where the *Strep*-tag has remained intact or protein monomers that degraded after capture. Degradation of the monomeric protein after capture can actually be observed in fractions that contain more than one protein band of 14.7 kDa or less such as those of wildtype GRX480 (CCMC)(Fig.12), CSMC (Fig.13), CSMS (Fig. 15) and SSMS(Fig. 16). The absorbance peak observed by the UNICORN software during gel filtration of CCMC (Fig. 11) at 85 mL, corresponding to a molecular weight of 2.5 kDa, reveals presence of a protein band of less than 10.5 kDa (Fig. 13) when analyzed by SDS-PAGE and immunoblot. The absorbance peak of CSMS (Fig. 14) at 66.5 mL, corresponding to a molecular weight of 11.9 kDa, reveals the darkest protein band on the membrane (Fig.15) at approximately 14.7 kDa. The absorbance peak of SSMS (Fig.14) at 78 mL, corresponding to a molecular weight of 4.7 kDa, reveals a presence of two fainter bands at 36 kDa and 14.7 kDa (Fig. 16). As these absorbance peaks were revealed to not correlate to peak elution of the GRX480 protein from the gel filtration column, the selection of fractions to analyze by SDS-PAGE and immunoblot were instead chosen based on screening fractions for precipitation of protein, testing the full range of column elution beginning at the void volume, and then narrowing this range as protein elution patterns became clearer.

The unknown contaminating protein of approximately 34-36 kDa in previous experiments was found to elute in the majority of gel filtration runs as a dimeric complex in the 45-46 mL fractions, corresponding to a molecular weight of 65.8-60.8 kDa (Figs. 12, 15, & 16).

Degradation of the dimeric complex and/or diffusion of the monomeric protein are observed in the 50 mL (44.2 kDa) fraction and 58 mL or greater fractions (23.4 kDa and less) respectively (Figs. 12, 13, 16). The results of gel filtration of the GRX480 protein are summarized in Figure 17 which includes the elution volume of all protein bands and the calculated three dimensional molecular weights. Elution ranges were established by accounting for variation in the size of the 14.7 kDa linearized monomer of the protein observed by SDS-PAGE and immunoblot, as the actual size can vary up to 20%. This categorization also helps to account for any diffusion from the true elution volume, as this was observed in all gel filtration experiments.

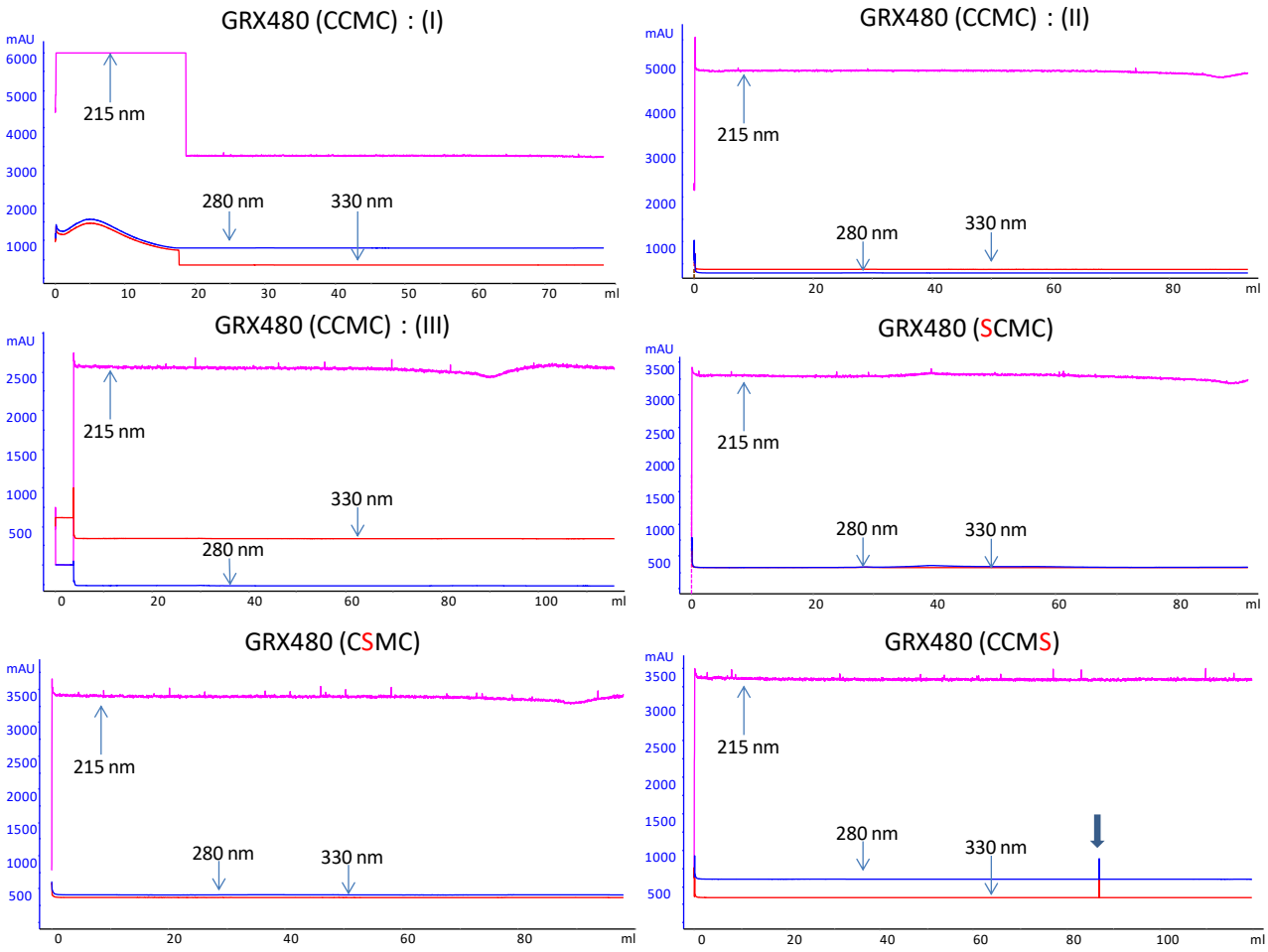

Figure 11. **Results of 10 mL of injected *Strep*- tagged wildtype GRX480 protein (CCMC) and single mutation active site variants(XXMX) *Strep*-column isolates using a FPLC- adapted S100 gel filtration column.** All results depicted correspond to the successful Strep-column isolation depicted in Figure 6. Absorbances (in mAU) were monitored at 215 ,280, and 330 nm over elution of the protein from the column (measured in mL). The thicker arrow depicted in the lower right figure depicts an increase in absorbance at 86 mL corresponding to presence of protein a band confirmed by immunoblot analysis in Figure 13.

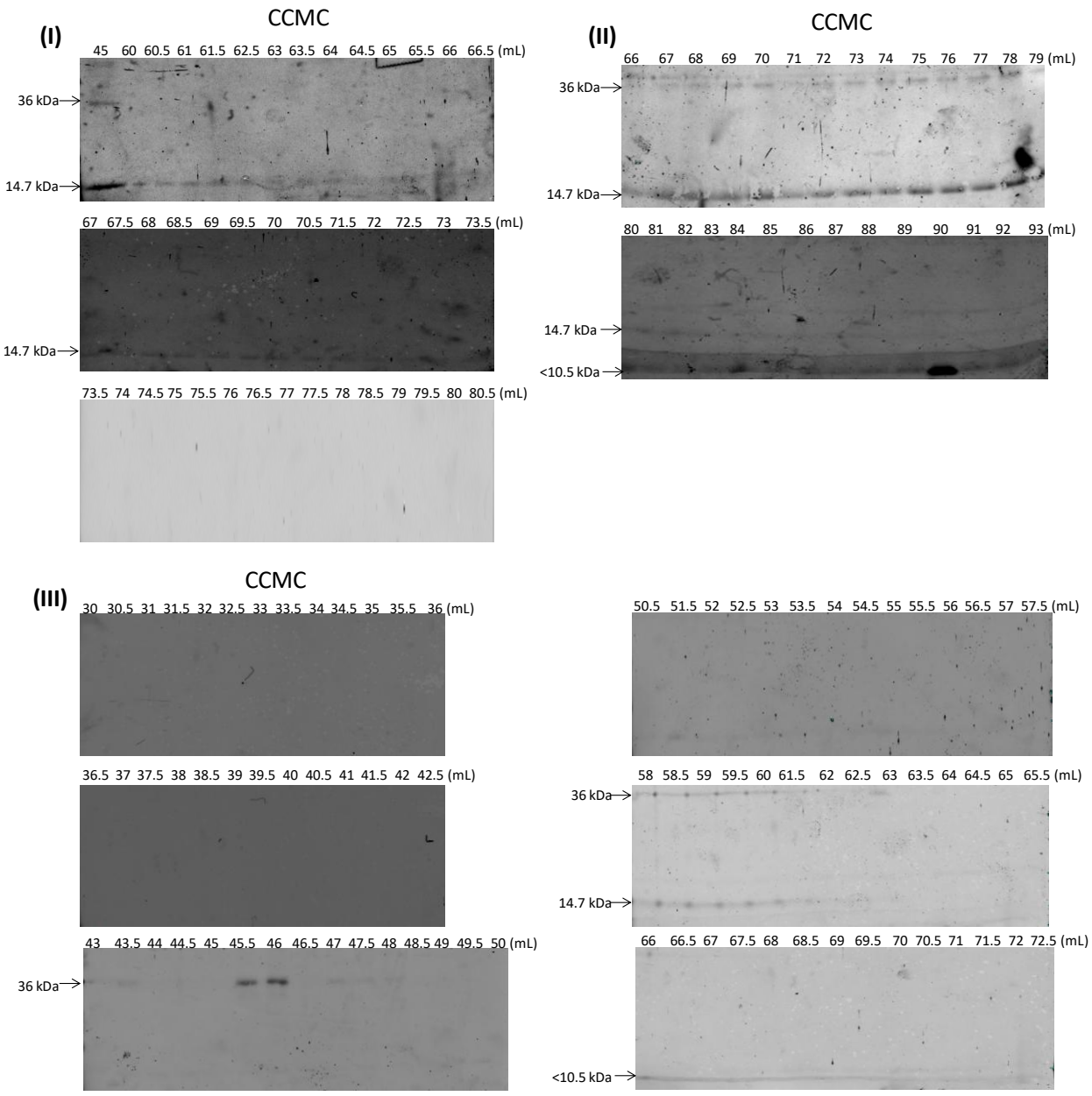

Figure 12 . **SDS-PAGE and immunoblot analysis of wildtype GRX480 (CCMC) gel filtration fractions collected during the runs depicted in Figure 11.** 500 ul of precipitated S100 gel filtration eluate were resuspended in 50 ul SDS-PAGE Sample Buffer and boiled. 50 ul was loaded onto a 4% stacking/12 % resolving SDS-PAGE gel alongside 15 uL of a pre-stained protein ladder. After running, proteins were transferred to a nitrocellulose membrane. Immunoblot with a rabbit anti-*Strep* primary antibody and goat anti-rabbit secondary antibody was used to visualize the GRX480 proteins. Molecular weights where protein bands were observed are indicated in kilodaltons (kDa).

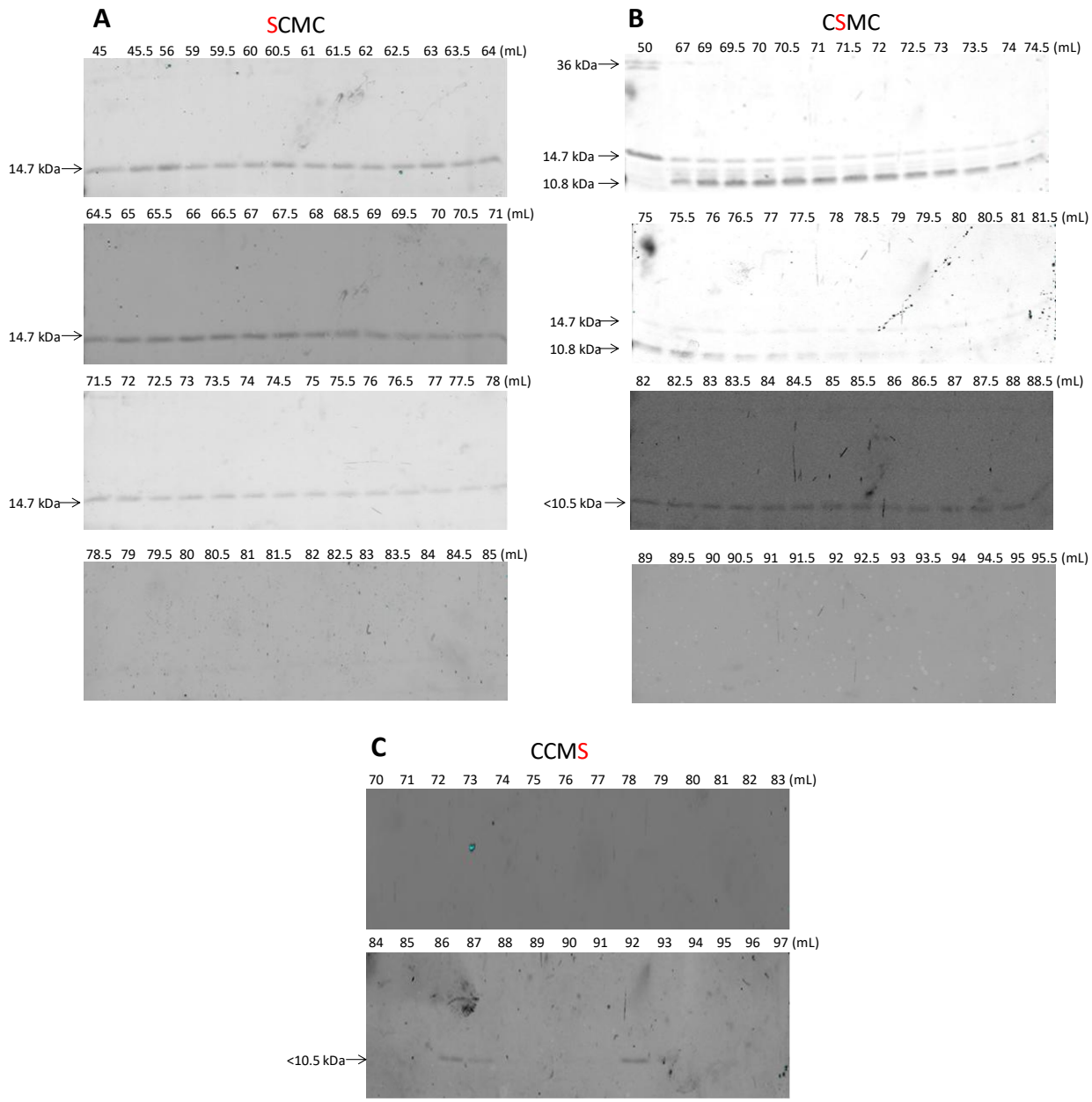

Figure 13. SDS-PAGE and immunoblot analysis of single mutation active site variants(XXMX) of GRX480 gel filtration fractions collected during the runs depicted in Figure 11. 500 ul of precipitated S100 gel filtration eluate were resuspended in 50 ul SDS-PAGE Sample Buffer and boiled. 50 ul was loaded onto a 4% stacking/12 % resolving SDS-PAGE gel alongside 15 uL of a pre-stained protein ladder. After running, proteins were transferred to a nitrocellulose membrane. Immunoblot with a rabbit anti-*Strep* primary antibody and goat anti-rabbit secondary antibody was used to visualize the GRX480 proteins. Molecular weights where protein bands were observed are indicated in kilodaltons (kDa).

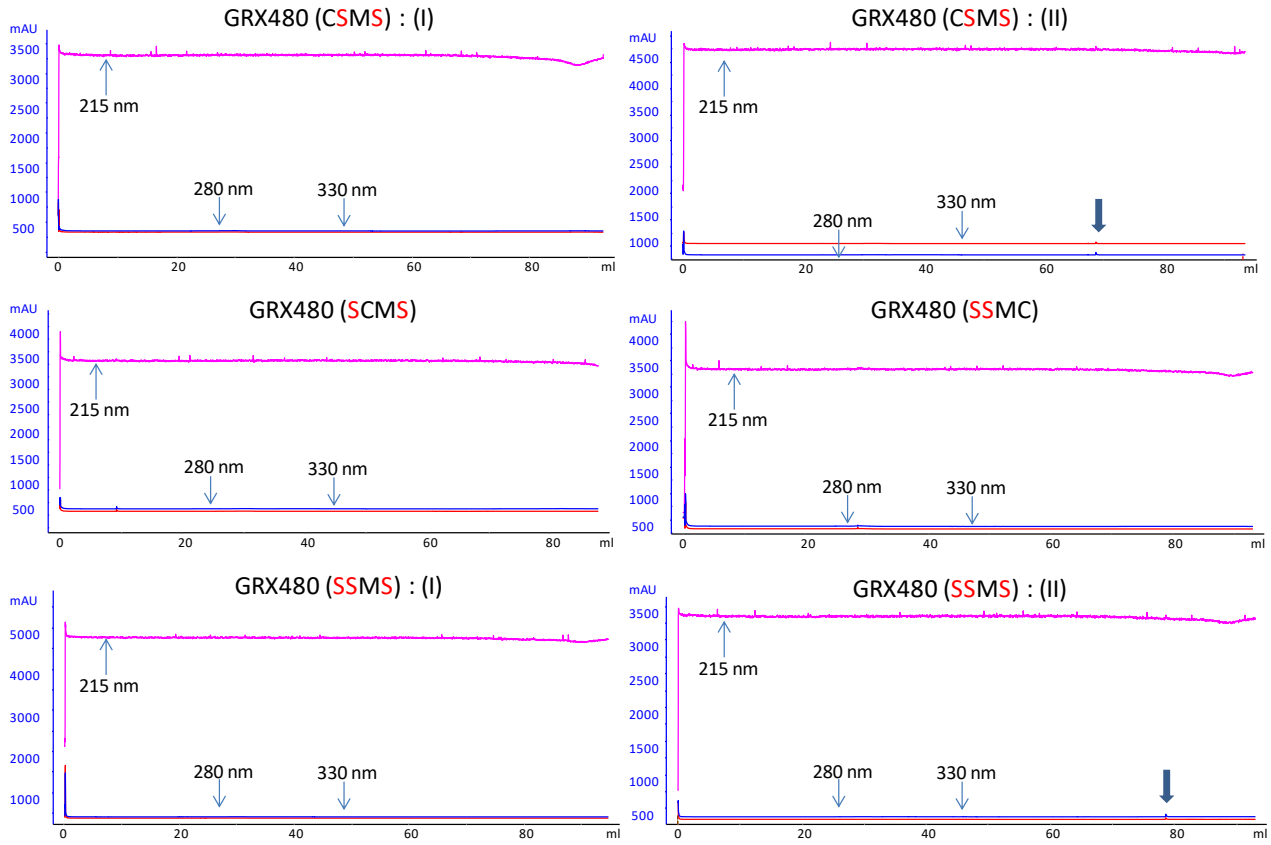

Figure 14. **Results of 10 mL of injected *Strep*- tagged GRX480 double (XXMX) and triple mutation (SSMS) active site variants *Strep*-column isolates using a FPLC- adapted S100 gel filtration column.** All results depicted correspond to the successful Strep-column isolation depicted in Figure 7. Absorbances (in mAU) were monitored at 215 ,280, and 330 nm over elution of the protein from the column (measured in mL). The thicker arrow depicted in the upper and lower right figures depict an increase in absorbance at 66.5 and 78 mL corresponding to presence of protein a band confirmed by immunoblot analysis in Figures 15 and 16 respectively.

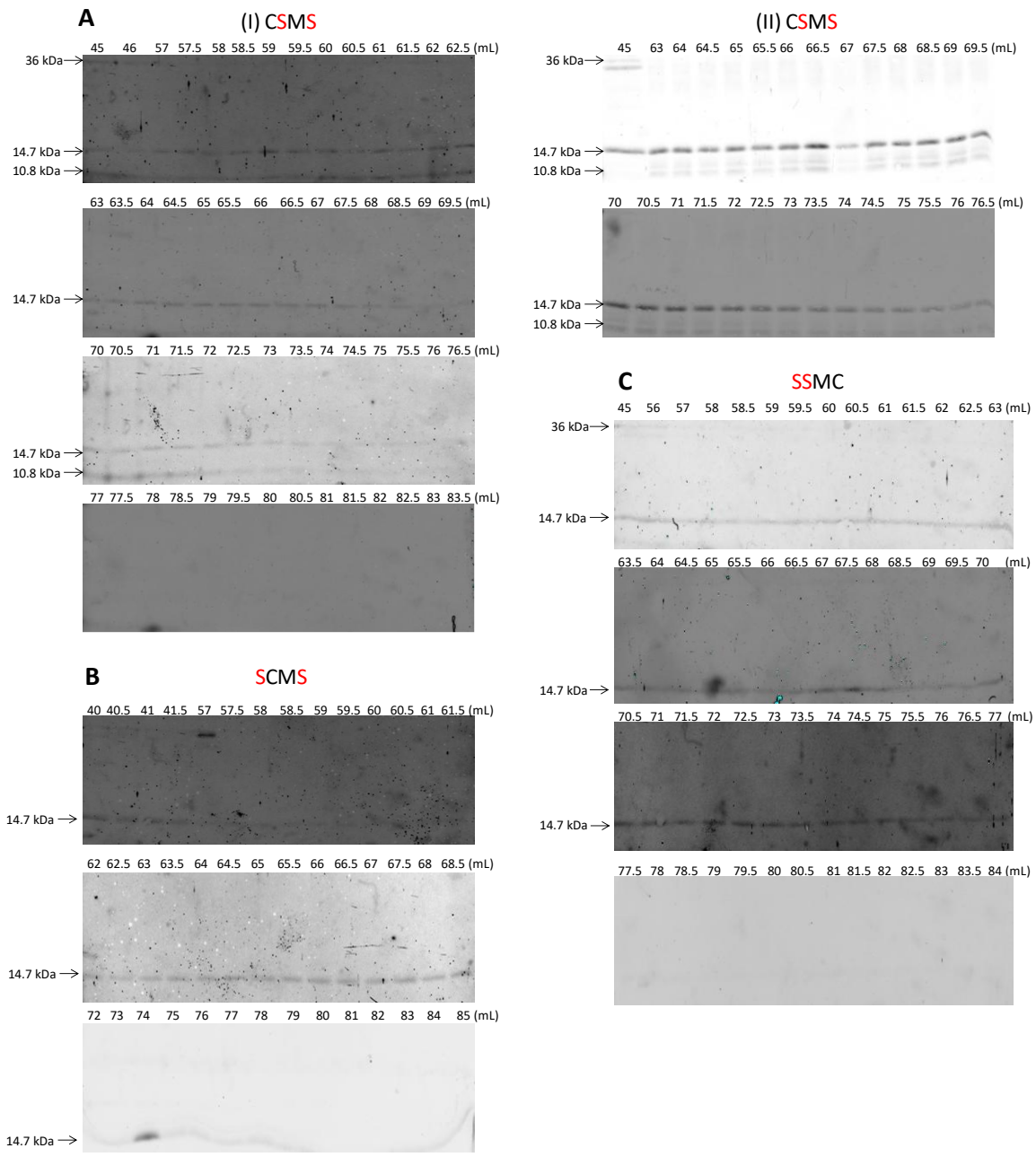

Figure 15. SDS-PAGE and immunoblot analysis of double mutation active site variants(XXMX) of GRX480 gel filtration fractions collected during the runs depicted in Figure 14. 500 ul of precipitated S100 gel filtration eluate were resuspended in 50 ul SDS-PAGE Sample Buffer and boiled. 50 ul was loaded onto a 4% stacking/12 % resolving SDS-PAGE gel alongside 15 uL of a pre-stained protein ladder. After running, proteins were transferred to a nitrocellulose membrane. Immunoblot with a rabbit anti-*Strep* primary antibody and goat anti-rabbit secondary antibody was used to visualize the GRX480 proteins. Molecular weights where protein bands were observed are indicated in kilodaltons (kDa).

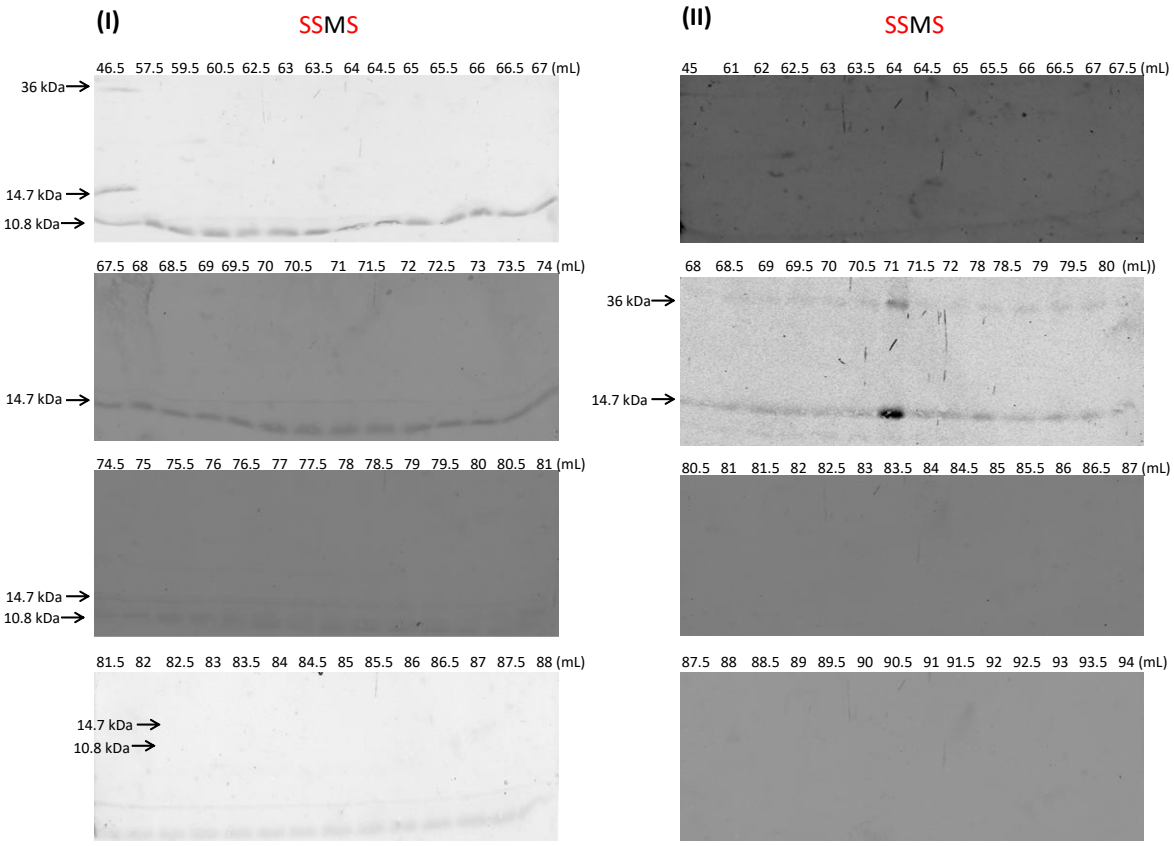

Figure 16. **SDS-PAGE and immunoblot analysis of triple mutation active site variants(SSMS) of GRX480 gel filtration fractions collected during the runs depicted in Figure 14.** 500 ul of precipitated S100 gel filtration eluate were resuspended in 50 ul SDS-PAGE Sample Buffer and boiled. 50 ul was loaded onto a 4% stacking/12 % resolving SDS-PAGE gel alongside 15 uL of a pre-stained protein ladder. After running, proteins were transferred to a nitrocellulose membrane. Immunoblot with a rabbit anti-*Strep* primary antibody and goat anti-rabbit secondary antibody was used to visualize the GRX480 proteins. Molecular weights where protein bands were observed are indicated in kilodaltons (kDa).

4.7 Wildtype GRX480 and the SCMC, CSMS, SSMC, and SSMS variants form a tetrameric complex *in vitro*.

Wildtype GRX480 (CCMC) was found to elute most abundantly at 45 mL (Fig.12) indicated by an intense band and linearized molecular weight of 14.7 kDa. Elution at this volume corresponds to a calculated molecular weight of 65.8 kDa (Fig. 17), indicating a tetrameric complex of GRX480 monomers each having a three dimensional molecular mass of approximately 16.45 kDa. Results representing degradation of a dimeric complex and the monomeric protein are represented by bands that fall within the 23.51- 17.65 kDa and 17.64-11.76 kDa ranges respectively while those 11.76 kDa or smaller are representative of protein degradation products. The cluster of data points in the upper portion of the monomer size range were calculated to be 16.31 and 16.98 kDa, consistent with the 16.45 calculated monomer size given by the observed size of the tetrameric complex (Fig. 17) and the amino acid sequence (Fig.2) encoding for a monomeric GRX480 protein of approximately 16.39 kDa in size. Similar size range patterns are observed for the SCMC, CSMS, SSMC, and SSMS variants where bands corresponding to a tetramer, dimer degradation, monomer, and monomeric protein diffusion/degradation are present (Fig. 17). Some differences between these variants and the wildtype protein are that the SCMC and CSMS variants contain an additional degradation band in the tetramer range, and the SSMS tetramer was observed at the lower end of the tetramer size range. The SCMC, CSMS, SSMC, and SSMS variants also exhibit bands that fall within the actual size range of a dimeric complex, albeit at the lowest end (Fig. 17).

4.8 The CSMC and SCMS variants of GRX480 exhibit differences in complex formation *in vitro*.

Interestingly, the variants with the only the conserved cysteine present (SCMS) or absent (CSMC) exhibit differences in complex formation. The SCMS variant was similar to wildtype (CCMC) in the size and range of the protein monomer, but was found to elute from the column much earlier exhibiting multiple bands corresponding to molecular weights of 98.05, 94.22, 90.54, and 87.0 kDa (Fig. 17). The CSMC variant was found to elute at a volume corresponding to a size of 44.18 kDa within the trimeric range and only degradation products of the protein monomer could be observed (Fig. 17).

4.9 The CSMC and CSMS variants exhibit the same distinct degradation pattern after elution from the gel filtration column as observed after *Strep*-column isolation

The distinct degradation patterns observed for the CSMC and CSMS variants after *Strep*-column isolation (Fig. 9) were again observed post capture from the gel filtration column (Figs. 13 & 15). The CSMS variant similarly showed the darkest band as the protein monomer at 14.7 kDa and multiple fragmentation bands at 13, 12, and 10.8 kDa (Fig.15). The CSMC variant also exhibited bands at these sizes; however the 10.8 kDa fragmentation band was the darkest (Fig.13). Unfortunately the CCMS variant could not be studied as an intact protein on the gel filtration column (Fig.13).

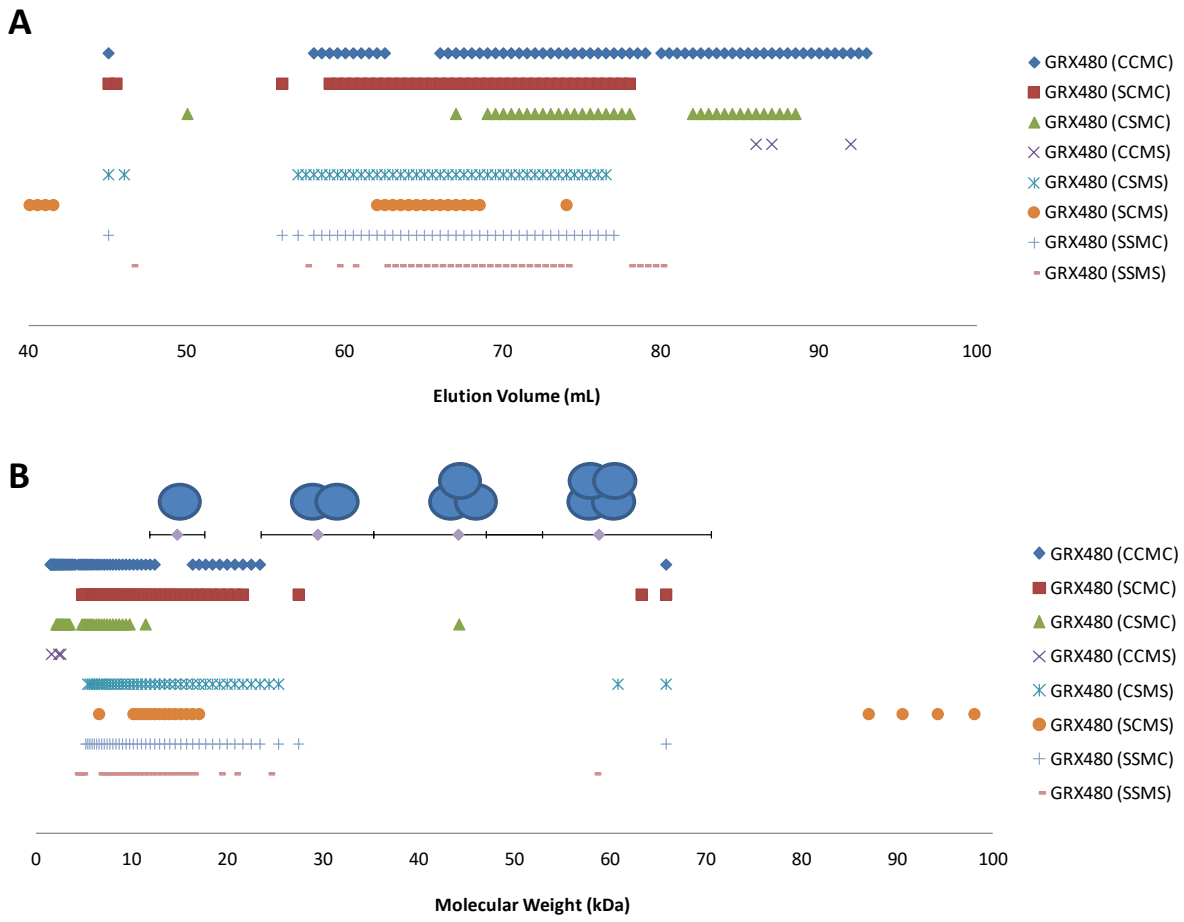

Figure 17. The total gel filtration elution ranges and calculated molecular weights for the wildtype GRX480 protein and active site variants. (A) Observed elution volume **(B)** Calculated molecular weight measured in kilodaltons (kDa). Elution ranges were established by accounting for variation in the size of the 14.7 kDa linearized monomer of the protein observed by SDS-PAGE and immunoblot, as the actual size can vary up to 20%. This categorization also helps to account for any diffusion from the true elution volume, as this was observed in all gel filtration experiments. Cartoon representations of a protein monomer, dimer, trimer, and tetramer are placed above their respective range bars. Each data point corresponds to the presence of a protein band in Figures 12, 13, 15 and 16.

4.11 I-TASSER results suggest that *Arabidopsis* GRX480 has high sequence homology and predicted structural similarities to glutaredoxins involved in iron-sulfur [Fe-S] cluster assembly and may bind glutathione (GSH) through amino acid residues other than the N-terminal active site cysteine.

Of the top 10 sequence alignments reported by I-TASSER (Fig. 18A), zebrafish glutaredoxin 2 (Table 1) was identified as the top match to GRX480 by 6 out of the 10 threading programs. The normalized Z-scores of 3.13, 2.64, 2.75, 1.97, 2.36, and 2.63 indicate an excellent alignment with a number of conserved amino acid residues in the active site sequence and other regions of the protein. Two of the threading programs also indicate a high sequence homology with yeast glutaredoxin 6 (Table 1) with Z-scores of 1.45 and 2.03. The remaining two threading programs suggest similarities to the glutaredoxin domain of human thioredoxin reductase 3 and the glutathionylated glutaredoxin Grx1p C30S mutant from yeast with Z-scores of 2.73 and 1.43 respectively. The N-terminal cysteine, Cys52, is conserved in all of the aligned proteins. Comparison of the predicted structure of GRX480 (Fig. 18A) to proteins in the PDB database reveals that zebrafish glutaredoxin 2 ranks the highest for structural similarity (Fig. 18B) with a high TM-score of 0.740. The nine other proteins listed in Figure 18B in order of decreasing TM-score (0.707 to 0.678) are human glutaredoxin 2, glutaredoxin C1 from *Populus tremula x tremuloides*, poplar glutaredoxin S12, the glutaredoxin domain of human thioredoxin reductase 3, glutaredoxin C1 from *Populus tremula x tremuloides*, Grx1 from *Plasmodium falciparum,* yeast glutaredoxin 2, Glutaredoxin C5 from *Arabidopsis thaliana,* and the N-terminal domain of human glutaredoxin 2 (Table 1). The structural properties and activities of these proteins are discussed in section 5.1. When estimating possible ligand binding sites on the GRX480 protein, only glutathione (GSH) is found to be significant with a high C-score of 0.74

(Fig. 18C). The amino acids estimated to bind glutathione in the active site are the Cys52 (N-terminal) and Met54 residues. The Arg49, Asn88, Lys99, Leu100, Pro101, Gly112, Leu113, and Asp114 amino acid residues are also predicted to bind GSH. Interestingly, the Pro101 and Gly112 residues are highly conserved in all proteins in Figure 18A, while the Asp114 residue is only conserved in the glutaredoxin domain of human thioredoxin reductase 3 and the glutathionylated glutaredoxin Grx1p C30S mutant from yeast. The predicted helix, stand/sheet, and coil regions of the GRX480 from Figure 18A are visualized in Figure 19. I-TASSER predicts 5 alpha helical and 4 beta strand/sheet structures within the GRX480 protein. One helix and one strand exist in the N-terminal region to the left of the CCMC active site . The N-terminal cysteine is located on a coiled part of the protein at the end of the first beta sheet while the rest of the active site is located on the second helix to form the distinct fold. This is followed by three more helical and strand regions on the C-terminal region of the protein. The top five three dimensional models (Fig. 19) and their associated C-scores are ordered from most likely to least likely as follows: Model 1 (-1.53), Model 5 (-1.92), Model 2 (-1.93), Model 4 (-2.36), and Model 3 (-2.74). The TM-score for these models was calculated to be 0.53±0.15 with a root mean square deviation (RMSD) of 7.8±4.4Å. The three dimensional organization of the alpha helices (pink) and beta strands (yellow) of the protein are pictured in Figure 19A. These models are similar in that two of the large beta strands run in parallel and one anti-parallel in the center of the protein with the fourth and smallest strand running perpendicular. They mostly differ in the organization and distance of the alpha helices and coiled regions (blue/white) around this central point. In model 5, the beta strands are densely clustered in the center of the protein and more three dimensional space exists between them and the alpha helices/

associated coiled domains. Figure 19B shows the location of the active site sequence and of the approximate location of the other amino acid residues in respect to one another. The position and proximity of the C-terminal domain in relation to the active cite remains rather constant while the N-terminal domain is what varies between these models. In models 1,2,4 and 5 the N-terminal domain of the protein is not in close proximity to the active site and is nestled behind or between areas of the C-terminal domain that flank the active site. In model 3, the N-terminal tail is positioned directly over the active site sequence.

A

B

Rank	PDB Hit	TM-score	RMSD[a]	IDEN[a]	Cov
1	3uiwA	0.740	1.46	0.227	0.803
2	2ht9B	0.707	1.52	0.181	0.766
3	1z7rA	0.706	2.20	0.241	0.781
4	3fz9A	0.700	1.42	0.276	0.759
5	3h8qA	0.699	2.07	0.222	0.781
6	2e7pD	0.689	1.19	0.267	0.737
7	4kjeA	0.682	1.54	0.202	0.745
8	3ctgA	0.681	1.80	0.231	0.752
9	3rhcA	0.680	1.28	0.265	0.730
10	2cq9A	0.678	1.86	0.161	0.766

C

Rank	C-score	Cluster size	PDB Hit	Lig Name	Ligand Binding Site Residues
1	0.74	97	4i2uA	GSH	49,52,54,88,99,100,101,112,113,114
2	0.03	5	4n11A	CPT	49,51,52,100
3	0.01	2	2X8GA	2X8GA03	14,37,41
4	0.01	1	2X99A	2X99A12	31,34,77,79,83
5	0.01	1	2HT9A	2HT9A00	59,63,68

Figure 18. I-TASSER results for the GRX480 protein sequence alignment, structural prediction, and ligand binding site residues. (A) Protein structure of GRX480 and proteins (identified by PDB Library Hit codes) with a similar structure predicted by the top 10 threading templates used by I-TASSER and LOMETS from the PDB library**.** The top 10 alignments reported above (in order of their ranking) are from the following threading programs: 1:MUSTER 2: FFAS-3D 3: SPARKS-X 4: HHSEARCH2 5: HHSEARCH I 6: Neff-PPAS 7: HHSEARCH 8: pGenTHREADER 9: wdPPAS 10: cdPPAS. The GRX480 amino acid sequence (**Seq**) and its predicted secondary structure (**Sec. Str**) (C= coil, H=helix, S= sheet/strand). The percentage sequence identity of the

templates in the threading aligned region **(Iden1)** and whole template chains **(Iden2)** with the query sequence. **Cov** represents the coverage of the threading alignment and is equal to the number of aligned residues divided by the length of the query protein. **Norm. Z-score** is the normalized Z-score of the threading alignments. Alignment with a Normalized Z-score >1 means a good alignment. **(B)** Proteins structurally close to the target in the PDB (as identified by TM-align). **TM-score** is a metric for measuring the structural similarity of two protein models. TM-score has the value in (0,1], where 1 indicates a perfect match between two structures. A score higher than 0.5 generally has the same fold in SCOP/CATH. **RMSD**[a] is the root mean square deviation between residues that are structurally aligned by TM-align. **IDEN**[a] is the percentage sequence identity in the structurally aligned region. **(C)** Possible ligand binding sites on GRX480. **C-score** is the confidence score of the prediction. C-score ranges [0-1], where a higher score indicates a more reliable prediction. **Cluster size** is the total number of templates in a cluster. **Lig Name** is name of possible binding ligand from the BioLiP database. **Rep** is a single complex structure with the most representative ligand in the cluster, i.e., the one listed in the **Lig Name** column. **Ligand Binding Site Residues** are identified by their position in the query sequence (Zhang, 2008; Roy et al., 2010; Yang et al., 2015). Protein identities corresponding to the PDB Library hit codes are listed in Table 1.

Table 1. Protein identities corresponding to the PDB Library ID codes listed in Figure 18.

PBD Library ID	Protein Identity
3uiwA	Zebrafish glutaredoxin 2
3h8qA	Glutaredoxin domain of human thioredoxin reductase 3
5j3rA	Yeast monothiol glutaredoxin Grx6 in complex with a glutathione-coordinated [2Fe-2S] cluster
2jadA	Glutathionylated glutaredoxin Grx1p C30S mutant from yeast
2ht9B	Dimeric human glutaredoxin 2
1z7rA	Glutaredoxin C1 from *Populus tremula x tremuloides*
3fz9A	Poplar glutaredoxin S12 in complex with glutathione
2e7pD	Holo form of glutaredoxin C1 from *Populus tremula x tremuloides*
4kjeA	Grx1 from *Plasmodium falciparum*
3ctgA	Reduced yeast glutaredoxin 2
3rhcA	Glutaredoxin C5 from *Arabidopsis thaliana*
2cq9A	N-terminal domain of human glutaredoxin 2

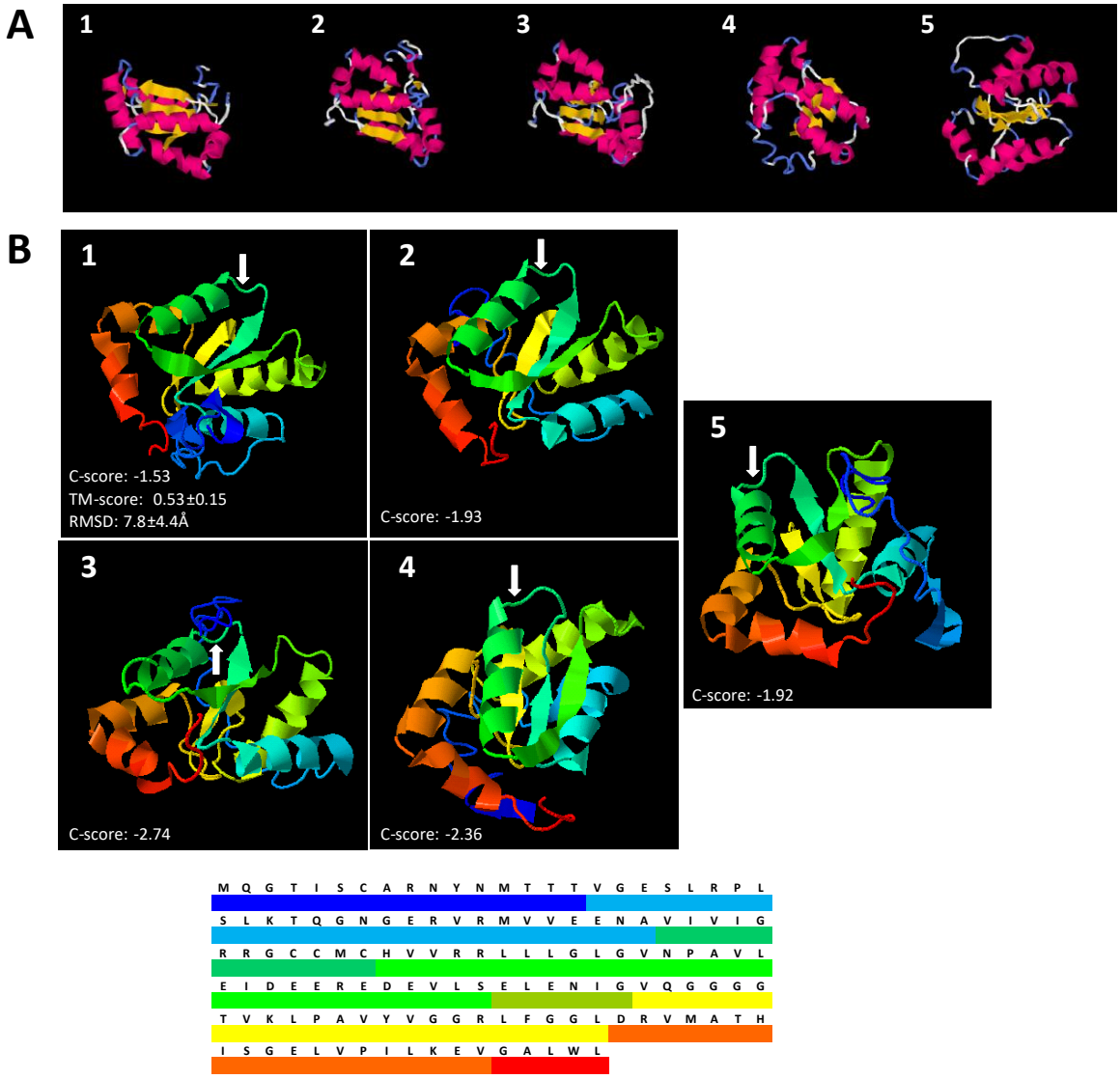

Figure 19. The top five structural models of the GRX480 protein predicted by I-TASSER. (A) A structural overview of how the folded protein occupies three dimensional space. Beta strands are represented as broad yellow arrows in which the arrowhead is the carboxyl end of the peptide and pink regions are the alpha helices **(B)** The specific locations of amino acid residues within the folded structure. The arrow in each figure of **(B)** indicates the location of the CCMC active site. For each target, I-TASSER simulations generate a large ensemble of structural conformations, called decoys. To select the final models, I-TASSER uses the SPICKER program to cluster all the decoys based on the pair-wise structure similarity, and reports up to five models which corresponds to the five largest structure clusters. The confidence of each model is quantitatively measured by C-score that is calculated based on the significance of threading template alignments and the convergence parameters of the structure assembly simulations. C-

score is typically in the range of [-5, 2], where a C-score of a higher value signifies a model with a higher confidence. TM-score and RMSD are estimated based on C-score and protein length following the correlation observed between these qualities. Distance deviation between residue positions in the model is measured in Angstrom(Å)(Zhang, 2008; Roy et al., 2010; Yang et al., 2015). A colourized legend is provided to locate specific amino acid regions of the protein. N-terminus (blue) and C-terminus (red).

5. DISCUSSION AND FUTURE DIRECTIONS

5.1 Tetrameric complex formation is normally associated with monothiol glutaredoxins involved in iron-sulfur [Fe-S] cluster assembly.

The most surprising of these experimental results was that not only did the wildtype GRX480 (CCMC) protein form a tetrameric complex *in vitro*, but that the SCMC, CSMS, SSMC, and SSMS active site mutations were also able to do so. This taken with the results from I-TASSER that showed high predicted structural similarity of the *Arabidopsis* GRX480 protein to zebrafish, human, yeast, and poplar glutaredoxins prompted thorough investigation into the known properties of these proteins in hopes of being able to better understand and interpret the other results obtained during this experimentation.

Several glutaredoxins from different species have been shown to form iron-sulfur [2Fe-2S] clusters including Grx5 and Grx6 from yeast, human Grx2 and Grx5/GLRX5, poplar GrxC1, *P. falciparum* Grx1, and *E. coli* Grx4 (Lillig et al., 2005; Picciocchi et al., 2007; Rouhier et al., 2007; Mesecke et al., 2008; Iwema et al., 2009; Luo et al., 2010). As a general rule, it has been suggested that monothiol (CXXX) Grxs are involved in iron homeostasis and [FeS]-cluster biosynthesis and that dithiol (CXXC) Grxs serve as [Fe-S] redox sensors during oxidative stress.

The GSH in holo forms of Grxs are in constant exchange with free GSH which is thought to connect the stability of the cluster to the cellular redox potential in the cell. However, recent studies on the activity of glutaredoxins that contain atypical structural components suggest that some glutaredoxins may not be confined to these strict classifications of activity based on active site sequences and may possess different modes of binding GSH and [Fe-S] co-factors (Lillig et al., 2005; Berndt et al., 2007; Mulenhoff et al., 2010;Rouhier et al., 2010; Li et al., 2012; Bräutigam et al., 2013).

Fe-S cluster formation in dithiol human Grx2 (CSYC) and dithiol poplar GrxC1 (CGYC) both require the formation of a Grx dimer and the presence of two GSH molecules (Johansson et al., 2007; Rouhier et al., 2007). Under non-stress conditions, human glutaredoxin 2 (GRX2) exists in a holoform until conditions such as the loss of the [2Fe-2S] cluster or a decrease in the GSH/GSSG ratio cause it to be activated by GSSG. Grx2 then reduces low molecular-mass disulfide molecules and protein GSH-mixed disulfides by using GSH as an electron donor (Johansson et al., 2004; Lillig et al., 2005). The apoform of poplar GrxC1 exists as a monomer and behaves like a typical glutaredoxin, while the dimeric holoform is an iron-sulfur protein with a bridging [2Fe-2S] cluster dependent on the first cysteine at the active site from each subunit and two cysteines from two glutathione molecules. Mutagenesis studies also suggested that incorporation of an iron-sulfur cluster could be a shared feature of plant glutaredoxins possessing a glycine adjacent to the active site cysteine residues. (Feng et al., 2006; Rouhier et al., 2007). The ortholog of poplar GrxC1, Arabidopsis GrxC1, formed a holodimeric [Fe-S] cluster that acted as a redox sensor to reduce downstream pathways under oxidative conditions *in planta*, but was unable to form clusters *in vitro*. The Arabidopsis GrxC2 paralogue was shown to

be unable to form a cluster *in vitro*. Single mutants *grxc1* and *grxc2* showed similar phenotypes, while the double *grxc1 grxc2* mutant produced a lethal phenotype suggesting some functional redundancy between GrxC1 and GrxC2. These researchers also showed that orthologs of GRXC2 are present in all seed producing plants including gymnosperms and flowering plants. Interestingly, GRXC1 orthologs are absent in monocots, gymnosperms and mosses and are only present in the dicot species that have been sequenced to date (Riondet et al., 2011).

The yeast monothiol (CSYS) GRX6, which differs from all monothiol glutaredoxins and shares features with dithiol glutaredoxins, was found to be a tetramer in solution when binding two iron-sulfur clusters. GRX6 dimerizes noncovalently and the [Fe-S] cluster is stabilized by reduced GSH. Loss of reduced GSH and [Fe-S] components causes the tetrameric complex to degrade into a 46 kDa dimer. Noncovalent dimerization of the GRX6 monomers requires an N-terminal domain, but this domain is not needed for glutathione disulfide reductase and glutathione S-transferase activity. The C-terminal Grx domain was found to be responsible for assembly of the Fe–S cluster, specifically involvement of Cys136 residue. Interestingly, trypsin digestion of the protein completely removed the N-terminal domain. These results suggested that the N-terminal and C-terminal domains exist independently and that the N-terminal domain is highly sensitive to protease mediated degradation (Mesecke et al., 2008; Luo et al., 2010).

The single-domain monothiol (CGFS active site) human glutaredoxin 5 (GLRX5) is known to form a holotetrameric complex during mitochondrial iron-sulfur cluster assembly while the apoprotein exists as a monomer. GLRX5 was found to bind two [2Fe–2S] clusters and four GSH

molecules with the [2Fe–2S] clusters buried in the interior of the complex and shielded from the solvent by the conserved β1-α2 loop, a Phe^{69} residue, and the GSH molecules. The N-terminal active site cysteine ligates each [2Fe–2S] cluster along with two cysteine thiols from two GSH molecules. The formation of the complex involved the conserved cysteine residues of the monomer subunits with more extensive intersubunit interactions than iron–sulfur-bound human glutaredoxin 2 (GLRX2). Interestingly, glutathionylation of the cysteine residues occurs even in the absence of the [2Fe–2S] clusters which is thought to facilitate transfer of the cluster and to prevent further oxidation (Johansson et al., 2011). The N-terminal domain of this protein was found to be highly susceptible to degradation, specifically the segment prior to the Arg108 and Lys111 residues. GLRX5 bound GSH through its Cys136 in a highly conserved "GSH-binding groove." In humans, GLRX5 is suggested to aid in the transfer and insertion of iron-sulfur clusters into target protein after their assembly on the IscU scaffold protein (Vilella et al., 2004; Johansson et al., 2011).

In recent years, the three dimensional structure and behaviour of dithiol zebrafish glutaredoxin 2, a homologue of human Grx2 that is important in embryonic brain development, has been characterized. Zebrafish Grx2 contains eight conserved cysteine residues. Two exist in the dithiol C-P-Y-C active site (Cys 37 and Cys 40), two structural and vertebrate-specific cysteines (Cys 28 and Cys113) which are similar to the intra-molecular disulfide forming cysteine residues in human Grx2, and four cysteines of unknown function (Cys16, Cys90, Cys116 and Cys117). The N-terminal active site cysteine residues in all other holo glutaredoxins normally required for [FeS]-cluster bridged dimers using two molecules of non-covalently bound glutathione were not required for [Fe-S] cluster coordination with zebrafish Grx2.

However, the non-active site cysteines, two of the vertebrate-specific cysteines, and two of the cysteine residues of unknown function were proposed to have a potential role in [Fe-S]cluster coordination as mutations to them abolished the ability to bind the [Fe-S] cofactor (Lillig et al., 2005; Johansson et al., 2007; Bräutigam et al., 2011; 2013). Additionally, the cluster formation activity observed seemed to be a cross between Grxs and ferredoxins, showing similarities to cluster formation in the *Aquifex aeolicus* ferredoxin that possesses Trx-fold where cluster formation is governed by four cysteine residues (Yeh et al., 2000; Bräutigam et al., 2013).

Interestingly, the only other *Arabidopsis* glutaredoxin (C5) that was identified by I-TASSER is also involved in [Fe-S] cluster binding. It possesses a CSYC active site and exists as two forms when recombinantly expressed in *E.coli.* The monomeric apoprotein exhibits deglutathionylation activity in the recycling of plastidial methionine sulfoxide reductase B1 and peroxiredoxin IIE. The dimeric holoprotein incorporates a [2Fe-2S] cluster which is dependent on the second cysteine residue in the active site. Interestingly, this cysteine was not involved in ligation of the protein despite the presence of a dithiol active site and did not form any inter- or intramolecular disulfide bonds. It was also discovered activity of the enzyme exclusively relies on a monothiol mechanism (Couturier et al., 2011).

The unique, enigmatic, and recently characterized behaviour of these proteins and the role of each cysteine in the active site may help to shed some light onto the unexpected experimental results obtained for the GRX480 protein and its active site variants. The formation of a tetrameric complex in the CCMC, SCMC, CSMS, SSMC, and SSMS variants despite the absence of the N-terminal cysteine in some variants shows that GRX480 is capable of binding

GSH through other amino acid residues in the sequence. This compounded with the observation that the N-terminal region of the protein was more noticeably susceptible to degradation may be due to shared features of the GRX480 protein with the proteins outlined above. Whether the wildtype GRX480 protein and each active site variant is capable of binding a [Fe-S] cofactor should be of high importance in future research endeavours. Whether GRX480 is involved in iron homeostasis and [FeS]-cluster biosynthesis or acts as a [Fe-S] redox sensor during oxidative stress may help to explain some of controversy surrounding its exact involvement in disease resistance pathways. The results of the I-TASSER sequence alignment and structural similarities between GRX480 and [Fe-S] cluster proteins indicates that GRX480 may share features of both monothiol and dithiol glutaredoxins. The possible role of each cysteine in the active site of GRX480 is further described below.

5.2 The SSMS active site variant can form a tetrameric complex *in vitro* despite complete absence of the active cite Cys residues, suggesting alternate modes of binding GSH.

Of all the results obtained during this experimentation, the ability of the SSMS variant to form a tetrameric complex was the most surprising. This indicates that the complex formation happens independently of the cysteines in the active site of the protein, but still requires GSH as described by previous researchers (see Section 5.1). It is interesting however that the band corresponding to the SSMS tetramer was found in the lower end of the size range (Fig. 17) and suggests partial disassociation of the complex or some degree of degradation. This may be due to the absence of the cysteines which normally stabilize the complex. Of the possible GSH

binding sites of the GRX480 protein (Fig.18), only the Cys52 (N-terminal) and Met54 residues in the active site are predicted to do so. As the Met54 residue was not mutated, it may still be capable of binding GSH as well as the Arg49, Asn88, Lys99, Leu100, Pro101, Gly112, Leu113, and Asp114 residues. Whether this GRX480 variant and others missing the N-terminal cysteine of the active site are capable of binding [Fe-S] clusters or displaying the glutaredoxin activities described in Section 5.1 should be of great interest for future research.

5.3 The CSMC and CSMS variants reveal an increase in specific regions of the N-terminal domain of the protein that are prone to degradation when the conserved Cys and the C-terminal Cys are absent.

As demonstrated in Figure 9, the single variants SCMC, CCMS, CSMC and the double variant CSMS exhibit a distinct degradation pattern after isolation from the *Strep*-column. Interestingly, the variants involving the conserved cysteine residue (CSMC and CSMS) show an additional degradation band. These variants are also the only ones to prominently display this degradation pattern post isolation from the gel filtration columns in Figures 13 & 15. All of the GRX480 proteins exhibit some degree of degradation post isolation as the band is found at approximately 14.7 kDa rather than the 16.39 kDa indicated by the amino acid sequence and gel filtration results. As the *Strep*-tag is C-terminally fused, any band that is exposed by immunoblot still contains the tag and degradation has happened from the N-terminal end. Figure 20 depicts the approximated sites of cleavage of the GRX480 proteins based on the size of the fragmentation bands observed during SDS-PAGE and immunoblot. Interestingly, the

additional cleavage site and associated band exhibited by the CSMC variant was more intense in the CSMS variant in Figure 9. Although the *E.coli* BL21 (DE3) strain was specifically created to be deficient of lon and omp-t proteases, it seems that these GRX480 variants are still particularly sensitive to degradation. This may be caused by the fact that *E.coli* is unable to perform many of the posttranslational modifications that may normally confer protection of the GRX480 protein *in planta*. *E.coli* also lack a secretion mechanism for the release of recombinant protein into the culture medium which traps the GRX480 protein within the cell where it is more likely to be degraded by *E.coli* proteases before it can be recovered. The *E.coli* may also have a limited ability to facilitate extensive disulfide bond formation in the recombinant GRX480 protein which is critical in folding and structural integrity of the protein (Makrides, 1996). As the distinct degradation pattern was also seen post capture for CSMC and CSMS from the gel filtration column, where it is impossible to have two bands of differing sizes in the same fraction, this indicates that the protein degraded after it was isolated. This is unlikely due to direct *E.coli* protease interaction as the sample had already been strictly purified from the *Strep*-column and remained intact as it travelled through the gel filtration column. However, the cleavage site directly before the active site sequence may pose a problem if these variants are to be used for activity assays in the future. These results strongly suggest that the conserved and C-terminal cysteines of the active site are important in maintaining structural integrity of the N-terminal domain of the protein. When looking at the predicted three dimensional structure of the GRX480 protein in Figure 19, the N-terminal domain is only in close proximity to the active site sequence in Model 3, the model which has the lowest C-score. However, it may be that the conserved and C-terminal cysteines form important intramolecular

bonds that are disrupted in the above mutations. This could cause changes to the overall folding pattern of the protein that further exposes these regions to the solvent or weakens bonds between the active site, C-terminal regions, and the N-terminus of the protein.

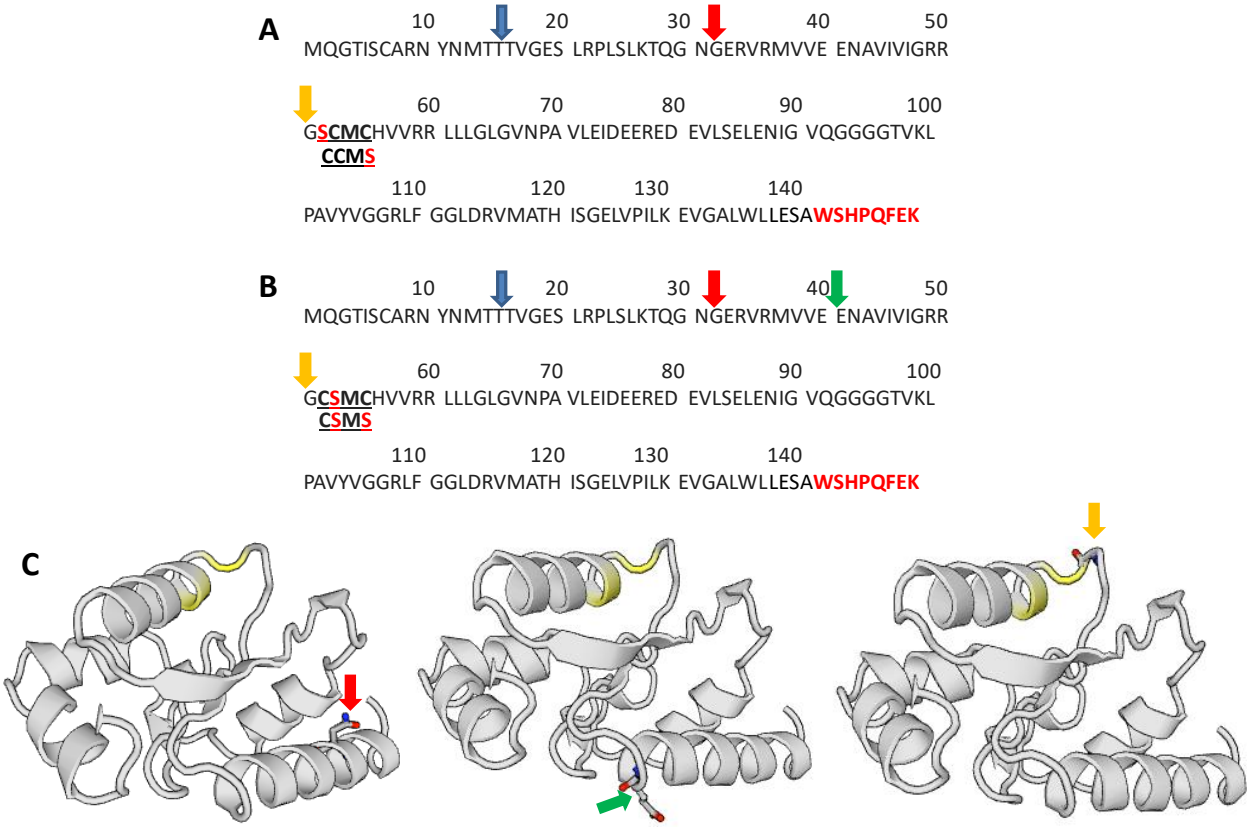

Figure 20. The approximate cites of cleavage in the N-terminal domain of the SCMC, CCMS, CSMS, and CSMS variants as revealed by SDS-PAGE and immunoblot analysis of protein isolates from the *Strep* and gel filtration columns. As each amino acid has an average molecular weight of 110 Da, the cleavage sites indicated produce a protein fragment of **(A)** 14.7, 13, and 10.8 kDa for SCMC and CCMS and **(B)** 14.7, 13, 12, and 10.8 kDa for CSMC and CSMS. **(C)** The location of the unique cleavage sites on the N-terminal domain of the hypothesized SWISS-MODEL of the GRX480 protein. The active site sequence is highlighted in yellow.

5.4 The incomplete and/or unstable formation of a tetrameric complex in CSMS, the fragility of the CCMS protein, and the unexplainably large complex formed by the SCMS variant during gel filtration suggests an interplay between the Cys residues of the active site sequence.

Although the CSMS variant was similar to the wildtype GRX480 protein and other variants in terms of the range in which its monomer was found (Fig. 17), the largest protein structure was found within a range indicating a trimeric complex. As outlined in Section 5.3, this specific mutant was the most prone to degradation and the band observed in this trimeric region may be the result of the more rapid degradation of an unstable tetrameric complex. It may also indicate a partial or incomplete formation of a tetrameric complex due to the changes induced by mutation to the active site sequence of the protein.

The inability to observe the CCMS protein intact on the cell filtration column (Fig. 13) is likely due to low protein yield (Fig. 8) and/or a higher likeliness of degradation (Fig.20). What is interesting is that faint protein bands corresponding to the GRX480 SCMS variant were found at much earlier elution volumes than those of the wildtype GRX480 and other variants (Figs. 15 & 17) indicting formation of an extremely large that is either trailing from elution from the void or is indeed present at those specific volumes. Subsequent experimental replicates of the gel filtration of SCMS were unsuccessful but are needed to clarify this result. If this can be replicated it would suggest that the conserved cysteine is involved in binding to other proteins and is regulated by the N-terminal and C-terminal cysteines of the active site. When they are

absent, the conserved cysteine is free to bind to other proteins, and in this case it may be either specific or nonspecific binding to *E.coli* proteins that are not visible by immunoblot analysis.

5.5 The changes observed in the expression profile of native *E.coli* proteins may be the result of similarities in activity or interaction between the recombinantly expressed *Arabidopsis* GRX480 protein and those in *E.coli*.

Of the most noticeable differences in the *E.coli* total protein expression when recombinantly expressing Arabidopsis GRX480 (Fig. 3) was the drastic decrease of a protein bands in the 36-32, 20, 16, and 12 kDa range. Interestingly, despite the drastic reduction in total protein concentration (Fig. 8) observed for wildtype GRX480 and active site variants, the band intensities of other proteins remained mostly unchanged. Therefore it is likely that the affected proteins are normally highly expressed. The molecular weight and activities of proteins involved in *E.coli* oxidative stress (covered in the literature review) and proteins involved in Fe-S cluster assembly (described below) have been summarized in Supplemental Tables 1 and 2 as they may provide some insight into the behaviour and role of the GRX480 protein.

Two major systems have been described in *E.coli* that assist in the assembly of Fe-S clusters: the ISC (Iron Sulfur Cluster) and SUF (SUlFur assimilation) systems. The 34-36 kDa *E.coli* IspH protein contains four cysteines, with three absolutely conserved Cys residues at amino acid positions 12, 96, and 197. This enzyme is involved in the nonmevalonate isoprenoid biosynthesis pathway and catalyzes the conversion of 1-hydroxy-2-methyl-2-(*E*)-butenyl diphosphate into a mixture of isopentenyl diphosphate (IPP) and dimethylallyl diphosphate

(DMAPP). Over-expression of the *isc* (iron-sulfur cluster) operon increased the catalytic activity of IspH and $[3Fe\text{-}4S]^{+}$ clusters were found to be bound to the IspH protein (Gräwert et al., 2004). Many researchers have observed that recombinant expression of complex eukaryotic proteins containing Fe-S clusters is difficult in *E.coli* as formation of these clusters was found to be dependent on *isc* genes where all individual components are important for their expression. Often it was found that that co-expression of the *isc* operon was needed for achieving high yields of active recombinant Fe-S proteins. Cluster inactivation due to stress conditions led to a significant decrease in protein expression and the growth rate of *E.coli* (Beinert et al., 1997; Zheng et al., 1998; Nakamura et al.,1999; Takahashi & Nakamura,1999; Agar et al., 2000; Hoff et al., 2000; Schwartz et al., 2000; Ollagnier-de-Choudens et al., 2000; Silberg et al., 2001; Kriek et al., 2003; Grawert et al., 2004; Jaganaman et al., 2007). One group of researchers found that recombinant expression of *Burkholderia cepacia* phthalate dioxygenase (PDO) and phthalate dioxygenase reductase (PDR), two iron-sulfur proteins, was not dependent on the co-expression of the *isc* gene cluster. These proteins possess a [2Fe-2S] Rieske center and [2Fe-2S] plant-type ferredoxin domain respectively (Jaganaman et al., 2007)

Interestingly, when the *isc* operon is disrupted due to oxidative stress or iron starvation, the *suf* operon becomes activated for Fe-S cluster synthesis which encodes for a cysteine desulfurase that has a cysteine residue in the active site (Loiseau et al., 2003; Ollagnier-de-Choudens et al., 2003; Outten et al., 2004; Jaganaman et al., 2007). The SUF system is composed of six proteins (Loiseau et al., 2003). The SoxR and YteF proteins are also iron-sulfur containing and known to function in redox sensing/transcriptional activation and [Fe-S] cluster

repair respectively during oxidative/nitrosative stress in *E.coli* (Hidalgo et al., 1995; Justino et al., 2006).

Of the proteins listed in Supplemental Table 1, thioredoxins 1 (11.8 kDa) and 2 (15.6 kDa) as well as glutaredoxin 4 (13 kDa) fit well into the 12-16 kDa size range for the affected protein bands. Thioredoxin reductase (34.6) is a strong candidate for the 34-36 kDa region. Interestingly, Grx4 is the most recently characterized glutaredoxin in *E.coli* and the only one known to be involved in [Fe-S] cluster assembly and to serve as a substrate for thioredoxin reductase. As thioredoxin reductase interacts with Trxs 1 & 2, it is entirely possible that the recombinant expression of GRX480 causes a downregulation in expression of these proteins. It may be that GRX480 has a similar structure and function to *E.coli* Grx 4 or the Trxs and may serve as a substrate for thioredoxin reductase, which was still produced (albeit in lower concentrations) in the recombinant protein cultures and may be the "contaminating" protein observed during the *Strep*-column isolation and gel filtration experiments. This may also explain how this protein was able to be present in large concentrations to exhibit non-specific affinity for the anti-*Strep* antibody during immunoblot if it is able to bind GRX480 on the *Strep*-column and to be co-purified. It is also interesting to note that this contaminating protein in present in the tetrameric and monomeric regions of CCMC and SSMS (Figs. 12 & 16) and in the tetrameric regions of CSMC and CSMS (Figs. 13 & 15). Whether this protein was a part of the complexes formed is unknown and should be explored as the CSMS and CSMC variants mimic the monothiol and dithiol active site sequences of native *E.coli* glutaredoxins.

Another possible protein candidate for the 34-36 kDa region in Supplemental Table 2 is the *E.coli* IspH protein, a protein also exhibiting a highly conserved Cys region necessary for activity. Activity of this protein is upregulated with the overexpression of *isc* operon proteins involved in [Fe-S] cluster assembly. Interestingly, The IscR (17.3 kDa), IscU (13.8 kDa), IscA (11.6 kDa), and [2Fe-2S] ferredoxin (12.3 kDa) proteins are within the 12-16 kDa affected range, and the HscB/Hsc20 protein (20.1 kDa) in the 20 kDa affected range. The IscS (45 kDa) and HscA/Hsc66 (65.7 kDa) that function as a sulfur delivery protein during [Fe-S] cluster assembly and a chaperone during cluster maturation respectively, are within the unaffected range. As the IscR protein is in the affected range and is a repressor of the *iscRSUA* operon and also the activator of the *suf* operon, it is interesting to note that the majority of the SUF proteins (Table 3) are within the unaffected range with the exception of the SufA (13.3 kDa) and SufE(15.8 kDa) proteins which are a scaffold/[Fe-S] delivery protein and a cysteine desulfurase(SufS) stimulator protein respectively. It is worth nothing that the "unaffected" regions in which some of these proteins reside may indeed be upregulated in response to recombinant GRX480 expression. Although the bands in these regions have similar intensities to those containing an empty vector, the total protein decrease is likely due to fewer cells surviving in the recombinant cultures. Thus, despite fewer cells contributing to the total protein expression profile, the intensities remain unchanged which would suggest upregulation of the expression of proteins within these regions.

The monothiol CSMS variant has a significantly higher total protein concentration (Fig. 8) in comparison to the wildtype GRX480 and all other variant proteins. This could be due to a similarity in the active site sequence to that of *E.coli* Grx4, the only glutaredoxin that has a

monothiol active site (CGFS) and that is involved in [Fe-S] cluster assembly. Similarly, the dithiol CSMC variant, mimicking the CPYC active sites of E.coli Grxs 1, 2 and 3, has the lowest total protein concentration. This may suggest that the GRX480 protein has similar activity to the Grx4 protein and acts synergistically to improve survival of the cell when its active site more closely resembles that of the native Grx4. The CSMC variant may be unable to function normally or through different mechanisms and its presence is thus a burden to the *E.coli* cell. The proteins listed in Supplemental Tables 1 & 2 and their homologues in *Arabidopsis thaliana* should be considered for future experimentations involving GRX480 protein-protein interactions and gene co-expression studies to further explore this hypothesis.

These observations together suggest that the GRX480 protein may alter, interfere, or be involved in some aspects of [Fe-S] cluster assembly/delivery, or oxidative stress pathways when recombinantly expressed in the *E.coli* cell. The difficulty in obtaining good experimental yield of the recombinant GRX480 protein may be similarly due to the problems experienced by previous researchers trying to express [Fe-S] related proteins in *E.coli* cultures and is something to consider in future studies. Supplementation of the *E.coli* growth media with iron or sulfur as well as altering the anaerobic/aerobic growth conditions of the bacterial colonies may help to improve survival and growth of the cells, and also to prevent from oxidative stress or iron starvation. It is a possibility that the GRX480 protein itself exhibits a negative effect on the growth of *E.coli* cultures and the decrease in total protein concentration may be the result of fewer surviving cells in the culture medium. It is also entirely possible that despite codon optimization of the *AtGRX480* genetic sequence, it is still too difficult for the bacteria to assemble a protein with a CC-type active site.

5.6 Total protein concentration is drastically reduced in *E.coli* cultures recombinantly expressing GRX480 but a multiple injection method significantly increases isolate concentrations from the *Strep*-column.

Although the *Strep*-tag offers very specific column binding conditions and high purity of column extracts, difficulties in obtaining a sufficient amount of the GRX480 proteins was a major issue during this experimentation that was exacerbated by poor yield from *E.coli* cultures. If future experiments involving protein activity or determining the crystallized structure of this protein are to be conducted, a pure sample is needed. The presence of the "contaminating" protein observed during this experimentation may present an issue. As discussed previously, this specific instance may be due to strong protein-protein interaction and may not be reflective of the true amount of contaminating proteins co-eluted with the target protein. Nevertheless, obtaining a purer protein sample would involve a second column isolation which runs the risk of losing a large amount of the protein to the column or protein degradation as observed in this study.

Implementation of a "multiple injection" method (Figs. 5, 6,& 7) versus the traditional single injection (Fig 4.) during *Strep*-column isolation was shown to efficiently increase the amount of the protein isolated so that it could be used in further experimentation. The multiple injection method serves to fully saturate the *Strep*-column with the target protein so that elution yields greater results. However, as observed in Figure 5 , the majority of the protein remains strongly bound to the column media and it seems that desthiobiotin is a poor competitor and thus not an efficient substrate for elution. The use of biotin as the eluting

substrate would offer better protein yield, however this would not allow for re-use of the column and may represent a costly alternative. As increasing the concentration of desthiobiotin did not offer any improvement, future experimentation with this protein should utilize the use of a more easily purified tag. The polyhistidine(*His)*-tag exhibits a very strong interaction with metal ion matrices and may interfere with [Fe-S] protein activity so this tag should be used with caution. The glutathione-S-transferase tag should also be avoided as it exhibits similar activity to glutaredoxins and may present false positives during enzyme activity assays (Terpe, 2003).

As the low recombinant protein yields of GRX480 in *E.coli* may be unavoidable due to the reasons previously discussed, purifying the protein directly from *Arabidopsis thaliana* may be necessary. This however may be difficult as it would require a genetic knockout or RNAi line in which *Agrobacterium* carrying a plasmid containing the tagged GRX480 protein would facilitate gene transfer and complementation. As a complete knockout or significant downregulation of the GRX480 protein may be lethal or impact survival of the plant, and complementation with potential non-active variants may also cause major issues, it is uncertain whether this option is viable. As GRX480 is suspected to be involved in oxidative stress or disease resistance pathways, sufficient expression levels for isolation of this protein may require these plants to be subjected to conditions detrimental to survival, especially if they contain a mutant variant of the protein.

6. CONCLUDING REMARKS

All together these results offer novel and previously unreported features of the GRX480 protein in terms of complex formation, the effects of specific mutations to the active site, and the changes observed in *E.coli* protein expression patterns when the GRX480 protein and its active site variants were recombinantly expressed. The "multiple injection" method utilized during this experimentation also offers a potentially useful tool to future researchers hoping to isolate recombinant protein from low yielding cultures. I-TASSER results along with those observed during experimentation suggest that GRX480 may share features with both monothiol and dithiol glutaredoxins that are involved in iron-sulfur [Fe-S] cluster assembly and redox sensing during stress responses. Although it is likely that the N-terminal cysteine of GRX480 is still necessary for glutaredoxin activity, the cysteine rich active site is not needed for tetrameric complex formation. These results also show that the conserved cysteine and C-terminal cysteine are important in maintaining structural integrity of the N-terminal region of the protein and stability of the tetrameric complex. Although this hypothesis needs to be further tested, the conserved cysteine may be involved in some aspects of specific binding to other proteins and is mediated by the presence of the N-terminal and C-terminal cysteines. The high sequence homology and predicted structural similarities to monothiol and dithiol glutaredoxins from different species that are involved in [Fe-S] cluster assembly is also not something to be overlooked. This presents an exciting new direction for future research involving this protein and whether the apo- and holo- forms both exhibit activities in SA-mediated plant disease resistance pathways is of great interest and wholly worth pursuing

REFERENCES

Agar, J. N., Zheng, L., Cash, V. L., Dean, D. R., & Johnson, M. K. (2000). Role of the IscU Protein in Iron− Sulfur Cluster Biosynthesis: IscS-mediated Assembly of a [Fe2S2] Cluster in IscU. *J. Am Chem. Soc.* **122**: 2136-2137.

Ahn, B. Y., & Moss, B. (1992). Glutaredoxin homolog encoded by vaccinia virus is a virion-associated enzyme with thioltransferase and dehydroascorbate reductase activities. *Proc. Natl. Acad. Sci. USA* **89**: 7060-7064.

Allocati, N., Federici, L., Masulli, M., & Di Ilio, C. (2009). Glutathione transferases in bacteria. *FEBS J.* **276:** 58-75.

Apweiler, R., Bairoch, A., Wu, C. H., Barker, W. C., Boeckmann, B., Ferro, S., ... & Martin, M. J. (2004). UniProt: the universal protein knowledgebase. *Nucleic Acids Res.* **32**: D115-D119.

Arnér, E. S., & Holmgren, A. (2000). Physiological functions of thioredoxin and thioredoxin reductase. *FEBS J.***267:** 6102-6109.

Arnold, K., Bordoli, L., Kopp, J., & Schwede, T. (2006). The SWISS-MODEL workspace: a web-based environment for protein structure homology modelling. *Bioinformatics **22***: 195-201.

Askelöf, P., Axelsson, K., Eriksson, S., & Mannervik, B. (1974). Mechanism of action of enzymes catalyzing thiol—disulfide interchange. Thioltransferases rather than transhydrogenases. *FEBS Lett. **38***: 263-267.

Åslund, F., Zheng, M., Beckwith, J., & Storz, G. (1999). Regulation of the OxyR transcription factor by hydrogen peroxide and the cellular thiol—disulfide status. *Proc. Natl. Acad. Sci. USA **96***: 6161-6165.

Atkinson, H. J., & Babbitt, P. C. (2009). Glutathione transferases are structural and functional outliers in the thioredoxin fold. *Biochemistry **48***: 11108-11116.

Bandyopadhyay, S., Gama, F., Molina-Navarro, M. M., Gualberto, J. M., Claxton, R., Naik, S. G., ... & Rouhier, N. (2008). Chloroplast monothiol glutaredoxins as scaffold proteins for the assembly and delivery of [2Fe–2S] clusters. *EMBO J. **27***: 1122-1133.

Beckers, G.J. and Spoel, S.H. (2006) Fine-tuning plant defence signalling: salicylate versus jasmonate*. Plant Biol*. **8**: 1–10

Beinert, H., Holm, R. H., & Münck, E. (1997). Iron-Sulfur Clusters: Nature's Modular, Multipurpose Structures. *Science* **277**: 653-659.

Berndt, C., Hudemann, C., Hanschmann, E. M., Axelsson, R., Holmgren, A., & Lillig, C. H. (2007). How does iron–sulfur cluster coordination regulate the activity of human glutaredoxin 2?. *Antioxid. Redox Signaling* **9**: 151-157.

Biasini, M., Bienert, S., Waterhouse, A., Arnold, K., Studer, G., Schmidt, T., ... & Schwede, T. (2014). SWISS-MODEL: modelling protein tertiary and quaternary structure using evolutionary information. *Nucleic Acids Res.***340**.

Bienert, S., Waterhouse, A., de Beer, T. A., Tauriello, G., Studer, G., Bordoli, L., & Schwede, T. (2017). The SWISS-MODEL Repository—new features and functionality. *Nucleic Acids Res.***45**: D313-D319.

Biotech, A. P. (1998). Gel filtration principles and methods.

Bräutigam, L., Johansson, C., Kubsch, B., McDonough, M. A., Bill, E., Holmgren, A., & Berndt, C. (2013). An unusual mode of iron–sulfur-cluster coordination in a teleost glutaredoxin. *Biochem. Biophys. Res. Commun.* **436:** 491-496.

Bräutigam, L., Schütte, L. D., Godoy, J. R., Prozorovski, T., Gellert, M., Hauptmann, G., ... & Berndt, C. (2011). Vertebrate-specific glutaredoxin is essential for brain development. *Proc. Natl. Acad. Sci. USA* **108**: 20532-20537.

Buchanan, B. B. and Balmer, Y. (2005). REDOX REGULATION: a broadening horizon. *Ann. Rev. Plant Biol.* **56**: 87 – 220.

Bushweller, J. H., Aslund, F., Wuethrich, K., & Holmgren, A. (1992). Structural and functional characterization of the mutant *Escherichia coli* glutaredoxin (C14----S) and its mixed disulfide with glutathione. *Biochemistry* **31:** 9288-9293.

Bushweller, J. H., Billeter, M., Holmgren, A., & Wüthrich, K. (1994). The nuclear magnetic resonance solution structure of the mixed disulfide between *Escherichia coli* glutaredoxin (C14S) and glutathione. *J. Mol. Biol.* **235**: 1585-1597.

Cao, H., Glazebrook, J., Clarke, J.D., Volko, S. and Dong, X. (1997) The Arabidopsis NPR1 gene that controls systemic acquired resistance encodes a novel protein containing ankyrin repeats. *Cell* **88**: 57–63.

Cheng, N. H., Liu, J. Z., Brock, A., Nelson, R. S., & Hirschi, K. D. (2006). AtGRXcp, an *Arabidopsis* chloroplastic glutaredoxin, is critical for protection against protein oxidative damage. *J. Biol. Chem.* **281**: 26280-26288.

Cheng, N. H. (2008). AtGRX4, an Arabidopsis chloroplastic monothiol glutaredoxin, is able to suppress yeast grx5 mutant phenotypes and respond to oxidative stress. *FEBS Lett.* **582**: 848-854.

Chuang, C. F., Running, M. P., Williams, R. W., & Meyerowitz, E. M. (1999). The PERIANTHIA gene encodes a bZIP protein involved in the determination of floral organ number in *Arabidopsis thaliana*. *Genes and Development* **13**: 334-344.

Colville, L., & Kranner, I. (2010). Desiccation tolerant plants as model systems to study redox regulation of protein thiols. *Plant Growth Reg.* **62:** 241-255.

Couturier, J., Jacquot, J. P., & Rouhier, N. (2009). Evolution and diversity of glutaredoxins in photosynthetic organisms. *Cell. Mol. Life Sci.* **66:** 2539-2557.

Couturier, J., Didierjean, C., Jacquot, J. P., & Rouhier, N. (2010). Engineered mutated glutaredoxins mimicking peculiar plant class III glutaredoxins bind iron–sulfur centers and possess reductase activity. *Biochem. Biophys.Res. Commun.* **403**: 435-441.

Couturier, J., Ströher, E., Albetel, A. N., Roret, T., Muthuramalingam, M., Tarrago, L., ... & Dietz, K. J. (2011). *Arabidopsis* chloroplastic glutaredoxin C5 as a model to explore molecular determinants for iron-sulfur cluster binding into glutaredoxins. *J. Biol. Chem.* **286**: 27515-27527.

Després, C., Chubak, C., Rochon, A., Clark, R., Bethune, T., Desveaux, D. and Fobert, P.R. (2003) The Arabidopsis NPR1 disease resistance protein is a novel cofactor that confers redox regulation of DNA binding activity to the basic domain/leucine zipper transcription factor TGA1. Plant Cell **15**: 2181–2191.

Eklund, H., Gleason, F. K., & Holmgren, A. (1991). Structural and functional relations among thioredoxins of different species. *Proteins: Structure, Function, and Bioinformatics* **11**: 13-28.

Elgán, T. H., Planson, A. G., Beckwith, J., Güntert, P., & Berndt, K. D. (2010). Determinants of activity in glutaredoxins: an in vitro evolved Grx1-like variant of Escherichia coli Grx3. *Biochem. J.* **430**: 487-495.

El-Shabrawi, H., Kumar, B., Kaul, T., Reddy, M. K., Singla-Pareek, S. L., & Sopory, S. K. (2010). Redox homeostasis, antioxidant defense, and methylglyoxal detoxification as markers for salt tolerance in Pokkali rice. *Protoplasma* **245**: 85-96.

Fan, W. and Dong, X. (2002) *In vivo* interaction between NPR1 and transcription factor TGA2 leads to salicylic acid-mediated gene activation in *Arabidopsis*. Plant Cell **14**: 1377–1389.

Feng, Y., Zhong, N., Rouhier, N., Hase, T., Kusunoki, M., Jacquot, J. P., ... & Xia, B. (2006). Structural Insight into Poplar Glutaredoxin C1 with a Bridging Iron− Sulfur Cluster at the Active Site†. *Biochemistry* **45**: 7998-8008.

Fernandes, A.P., and Holmgren, A. (2004). Glutaredoxins: glutathione-dependent redox enzymes with functions far beyond a simple thioredoxin backup system. *Antioxid. Redox Signal*. **6**: 63–74.

Fernandes, A. P., Fladvad, M., Berndt, C., Andrésen, C., Lillig, C. H., Neubauer, P., ... & Vlamis-Gardikas, A. (2005). A novel monothiol glutaredoxin (Grx4) from *Escherichia coli* can serve as a substrate for thioredoxin reductase. *J. Biol. Chem.* **280**: 24544-24552.

Fernandes, A. P., Capitanio, A., Selenius, M., Brodin, O., Rundlöf, A. K., & Björnstedt, M. (2009). Expression profiles of thioredoxin family proteins in human lung cancer tissue: correlation with proliferation and differentiation. *Histopathology* **55**: 313-320.

Fernandes, A. P., Fladvad, M., Berndt, C., Andrésen, C., Lillig, C. H., Neubauer, P., ... & Vlamis-Gardikas, A. (2005). A novel monothiol glutaredoxin (Grx4) from Escherichia coli can serve as a substrate for thioredoxin reductase. *J. Biol. Chem.* ***280***: 24544-24552.

Garg, R., Jhanwar, S., Tyagi, A. K., & Jain, M. (2010). Genome-wide survey and expression analysis suggest diverse roles of glutaredoxin gene family members during development and response to various stimuli in rice. *DNA Res.* **17**: 353-367.

Ghezzi, P.(2005)Regulation of protein function by glutathionylation. *Free Radical Res.***39**: 573–580.

Gille G. and Sigler K. (1995) Oxidative stress and living cells. *Folia Microbiol*. **40**:131–152.

Guo, Y., Huang, C., Xie, Y., Song, F., & Zhou, X. (2010). A tomato glutaredoxin gene *SlGRX1* regulates plant responses to oxidative, drought and salt stresses. *Planta* **232**: 1499-1509.

Gräwert, T., Kaiser, J., Zepeck, F., Laupitz, R., Hecht, S., Amslinger, S., ... & Buchner, J. (2004). IspH Protein of *Escherichia coli*: Studies on Iron− Sulfur Cluster Implementation and Catalysis. *J. Am. Chem. Soc.* **126**: 12847-12855.

Hayes, J. D., Flanagan, J. U., & Jowsey, I. R. (2005). Glutathione transferases. *Annu. Rev. Pharmacol. Toxicol.* **45**: 51-88.

Hepworth, S. R., Zhang, Y., McKim, S., Li, X., & Haughn, G. W. (2005). BLADE-ON-PETIOLE–dependent signaling controls leaf and floral patterning in *Arabidopsis*. *Plant Cell* **17**: 1434-1448.

Herrera-Vásquez, A., Carvallo, L., Blanco, F., Tobar, M., Villarroel-Candia, E., Vicente-Carbajosa, J., ... & Holuigue, L. (2015). Transcriptional control of glutaredoxin GRXC9 expression by a salicylic acid-dependent and NPR1-independent pathway in *Arabidopsis*. *Plant Mol. Biol. Rep.***33**: 624-637.

Hidalgo, E., Bollinger, J. M., Bradley, T. M., Walsh, C. T., & Demple, B. (1995). Binuclear [2Fe-2S] clusters in the *Escherichia coli* SoxR protein and role of the metal centers in transcription. *J. Biol. Chem.* **270**: 20908-20914.

Hoff, K. G., Silberg, J. J., & Vickery, L. E. (2000). Interaction of the iron–sulfur cluster assembly protein IscU with the Hsc66/Hsc20 molecular chaperone system of *Escherichia coli*. *Proc. Natl. Acad. Sci. USA* **97**: 7790-7795.

Holmgren, A. (1976). Hydrogen donor system for *Escherichia coli* ribonucleoside-diphosphate reductase dependent upon glutathione. *Proc. Natl. Acad. Sci. USA* **73**: 2275-2279.

Holmgren, A. (1979). Glutathione-dependent synthesis of deoxyribonucleotides. Purification and characterization of glutaredoxin from *Escherichia coli*. *J. Biol. Chem.* **254**: 3664-3671.

Holmgren, A. (1979). Glutathione-dependent synthesis of deoxyribonucleotides. Characterization of the enzymatic mechanism of *Escherichia coli* glutaredoxin. *J. Biol. Chem.* **254**: 3672-3678.

Holmgren, A. (1985). Thioredoxin. *Ann. Rev. Biochem.* **54**: 237-271.

Holmgren, A. (1995). Thioredoxin structure and mechanism: conformational changes on oxidation of the active-site sulfhydryls to a disulfide. *Structure* **3**: 239-243.

Huang, L. J., Li, N., Thurow, C., Wirtz, M., Hell, R., & Gatz, C. (2016). Ectopically expressed glutaredoxin ROXY19 negatively regulates the detoxification pathway in *Arabidopsis thaliana*. *BMC Plant Biol.* **16**: 200.

Isakov, N., Witte, S., and Altman, A. (2000) PICOT-HD: a highly conserved protein domain that is often associated with thioredoxin and glutaredoxin modules. *Trends Biochem. Sci.* **25**: 537–539.

Iwema, T., Picciocchi, A., Traore, D. A., Ferrer, J. L., Chauvat, F., & Jacquamet, L. (2009). Structural basis for delivery of the intact [Fe2S2] cluster by monothiol glutaredoxin. *Biochemistry **48***: 6041-6043.

Jakoby, M., Weisshaar, B., Dröge-Laser, W., Vicente-Carbajosa, J., Tiedemann, J., Kroj, T., & Parcy, F. (2002). bZIP transcription factors in *Arabidopsis*. *Trends Plant Sci.* **7**: 106-111.

Jaganaman, S., Pinto, A., Tarasev, M., & Ballou, D. P. (2007). High levels of expression of the iron–sulfur proteins phthalate dioxygenase and phthalate dioxygenase reductase in *Escherichia coli*. *Protein Expression and Purification* **52**: 273-279.

Jeng, M. F., Campbell, A. P., Begley, T., Holmgren, A., Case, D. A., Wright, P. E., & Dyson, H. J. (1994). High-resolution solution structures of oxidized and reduced *Escherichia coli* thioredoxin. *Structure* **2**: 853-868.

Jeong, W., Cha, M. K., & Kim, I. H. (2000). Thioredoxin-dependent hydroperoxide peroxidase activity of bacterioferritin comigratory protein (BCP) as a new member of the thiol-specific antioxidant protein (TSA)/alkyl hydroperoxide peroxidase C (AhpC) family. *J. Biol. Chem.* **275**: 2924-2930.

Johansson, C., Kavanagh, K. L., Gileadi, O., & Oppermann, U. (2007). Reversible sequestration of active site cysteines in a 2Fe-2S-bridged dimer provides a mechanism for glutaredoxin 2 regulation in human mitochondria. *J. Biol. Chem.* **282**:3077-3082.

Johansson, C., Lillig, C. H., & Holmgren, A. (2004). Human mitochondrial glutaredoxin reduces S-glutathionylated proteins with high affinity accepting electrons from either glutathione or thioredoxin reductase. *J. Biol. Chem.* **279**: 7537-7543.

Johansson, C., Roos, A. K., Montano, S. J., Sengupta, R., Filippakopoulos, P., Guo, K., ... & Kavanagh, K. L. (2011). The crystal structure of human GLRX5: iron–sulfur cluster co-ordination, tetrameric assembly and monomer activity. *Biochem. J.* **433**: 303-311.

John, G. S., Brot, N., Ruan, J., Erdjument-Bromage, H., Tempst, P., Weissbach, H., & Nathan, C. (2001). Peptide methionine sulfoxide reductase from *Escherichia coli* and *Mycobacterium tuberculosis* protects bacteria against oxidative damage from reactive nitrogen intermediates. *Proc. Natl. Acad. Sci. USA* **98**: 9901-9906.

Johnson, G. P., Goebel, S. J., Perkus, M. E., Davis, S. W., Winslow, J. P., & Paoletti, E. (1991). *Vaccinia* virus encodes a protein with similarity to glutaredoxins. *Virology* **181**: 378-381.

Johnson, C., Boden, E. and Arias, J. (2003) Salicylic acid and NPR1 induce the recruitment of trans-activating TGA factors to a defense gene promoter in *Arabidopsis*. *Plant Cell* **15**:1846–1858.

Jordan, A., Åslund, F., Pontis, E., Reichard, P., & Holmgren, A. (1997). Characterization of Escherichia coli NrdH A GLUTAREDOXIN-LIKE PROTEIN WITH A THIOREDOXIN-LIKE ACTIVITY PROFILE. *J. Biol. Chem.* **272**: 18044-18050.

Justino, M. C., Almeida, C. C., Gonçalves, V. L., Teixeira, M., & Saraiva, L. M. (2006). *Escherichia coli* YtfE is a di-iron protein with an important function in assembly of iron–sulphur clusters. *FEMS Microbiol. Lett.* **257**: 278-284.

Kanai, T., Takahashi, K., & Inoue, H. (2006). Three distinct-type glutathione S-transferases from Escherichia coli important for defense against oxidative stress. *J. Biochem.* **140**: 703-711.

Kiefer, F., Arnold, K., Künzli, M., Bordoli, L., & Schwede, T. (2009). The SWISS-MODEL Repository and associated resources. *Nucleic Acids Res.* **37**: D387-D392.

Kenrick, P. and Crane, P. R. (1997) The origin and early evolution of plants on land. Nature **389**: 33–38.

Klintrot, I. M., Hoog, J. O., Jornvall, H., Holmgren, A., and Luthman, M. (1984). The primary structure of calf thymus glutaredoxin. *FEBS J.* **144**: 417-423.

Kocsy, G., Kobrehel, K., Szalai, G., Duviau, M. P., Buzás, Z., & Galiba, G. (2004). Abiotic stress-induced changes in glutathione and thioredoxin h levels in maize. *Environmental and Experimental Botany* **52**: 101-112.

Kriek, M., Peters, L., Takahashi, Y., & Roach, P. L. (2003). Effect of iron–sulfur cluster assembly proteins on the expression of *Escherichia coli* lipoic acid synthase. *Protein Expression and Purification* **28**: 241-245.

Kumar, B., Singla-Pareek, S. L., & Sopory, S. K. (2009). Glutathione homeostasis: crucial for abiotic stress tolerance in plants. In *Abiotic Stress Adaptation in Plants* (pp. 263-282). Springer Netherlands.

Lemaire,S. D. (2004) The glutaredoxin family in oxygenic photosynthetic organisms. *Photosynth. Res.***79**: 305–318.

Lemaire, S. D., Michelet, L., Zaffagnini, M., Massot, V., & Issakidis-Bourguet, E. (2007). Thioredoxins in chloroplasts. *Current Genetics* **51**: 343-365.

Li, S., Lauri, A., Ziemann, M., Busch, A., Bhave, M., & Zachgo, S. (2009). Nuclear activity of ROXY1, a glutaredoxin interacting with TGA factors, is required for petal development in *Arabidopsis thaliana*. *Plant Cell* **21**: 429-441.

Li, H., & Outten, C. E. (2012). Monothiol CGFS glutaredoxins and BolA-like proteins:[2Fe-2S] binding partners in iron homeostasis. *Biochemistry* **51**: 4377-4389.

Lillig, C. H., Berndt, C., & Holmgren, A. (2008). Glutaredoxin systems. *Biochimica et Biophysica Acta (BBA)-General Subjects* **1780**: 1304-1317.

Lillig, C. H., Berndt, C., Vergnolle, O., Lonn, M. E., Hudemann, C., Bill, E. & Holmgren, A. (2005). Characterization of human glutaredoxin 2 as iron– sulfur protein: a possible role as redox sensor. *Proc. Natl Acad. Sci*. USA **102**: 8168–8173.

Lillig, C. H., Prior, A., Schwenn, J. D., Åslund, F., Ritz, D., Vlamis-Gardikas, A., & Holmgren, A. (1999). New thioredoxins and glutaredoxins as electron donors of 3'-phosphoadenylylsulfate reductase. *J. Biol. Chem* **274**: 7695-7698.

Liu, X. and Lam, E. (1994). Two binding sites for the plant transcription factor ASF-1 can respond to auxin treatments in transgenic tobacco. *J. Biol. Chem.* **269**: 668–675.

Loiseau, L., Ollagnier-de-Choudens, S., Nachin, L., Fontecave, M., & Barras, F. (2003). Biogenesis of Fe-S cluster by the bacterial suf system sufs and sufe form a new type of cysteine desulfurase. *J. Biol. Chem* **278**: 38352-38359.

Lu, J., & Holmgren, A. (2014). The thioredoxin antioxidant system. *Free Rad. Biol. Med.* **66**: 75-87.

Luo, M., Jiang, Y. L., Ma, X. X., Tang, Y. J., He, Y. X., Yu, J., ... & Zhou, C. Z. (2010). Structural and biochemical characterization of yeast monothiol glutaredoxin Grx6. *J. Mol. Biol.* **398**: 614-622.

Lynch, M., & Conery, J. S. (2000). The evolutionary fate and consequences of duplicate genes. *Science* **290**: 1151-1155.

Makrides, S. C. (1996). Strategies for achieving high-level expression of genes in *Escherichia coli*. *Microbiol.Rev.* **60**: 512-538.

Mesecke, N., Mittler, S., Eckers, E., Herrmann, J. M., & Deponte, M. (2008). Two novel monothiol glutaredoxins from *Saccharomyces cerevisiae* provide further insight into iron-sulfur cluster binding, oligomerization, and enzymatic activity of glutaredoxins. *Biochemistry* **47**: 1452-1463.

Meyer, Y., Belin, C., Delorme-Hinoux, V., Reichheld, J. P., & Riondet, C. (2012). Thioredoxin and glutaredoxin systems in plants: molecular mechanisms, crosstalks, and functional significance. *Antioxid. Redox Signaling* **17:** 1124-1160.

Miller, G. A. D., Suzuki, N., CIFTCI-YILMAZ, S. U. L. T. A. N., & Mittler, R. O. N. (2010). Reactive oxygen species homeostasis and signalling during drought and salinity stresses. *Plant, Cell and Environment* **33**: 453-467.

Miranda-Vizuete, A. F. E. B. (1994) Two additional glutaredoxins exist in Escherichia coli: glutaredoxin 3 is a hydrogen donor for ribonucleotide reductase in a thioredoxin/glutaredoxin 1 double mutant. *Proc. Natl. Acad. Sci. USA* **91**: 9813-9817.

Mou, Z., Fan, W.H. and Dong, X.N. (2003) Inducers of plant systemic acquired resistance regulate NPR1 function through redox changes. Cell **113**: 935–944.

Mühlenhoff, U., Gerber, J., Richhardt, N., & Lill, R. (2003). Components involved in assembly and dislocation of iron–sulfur clusters on the scaffold protein Isu1p. *EMBO J.* **22**: 4815-4825.

Mühlenhoff, U., Molik, S., Godoy, J. R., Uzarska, M. A., Richter, N., Seubert, A., ... & Lillig, C. H. (2010). Cytosolic monothiol glutaredoxins function in intracellular iron sensing and trafficking via their bound iron-sulfur cluster. *Cell Metabol.* **12**: 373-385.

Murmu, J., Bush, M. J., DeLong, C., Li, S., Xu, M., Khan, M., ... & Hepworth, S. R. (2010). *Arabidopsis* basic leucine-zipper transcription factors TGA9 and TGA10 interact with floral glutaredoxins ROXY1 and ROXY2 and are redundantly required for anther development. *Plant Physiol.* **154**: 1492-1504.

Nagai, S., & Black, S. (1968). A thiol-disulfide transhydrogenase from yeast. *J. Biol. Chem.* ***243***: 1942-1947.

Nakamura, M., Saeki, K., & Takahashi, Y. (1999). Hyperproduction of recombinant ferredoxins in *Escherichia coli* by coexpression of the ORF1-ORF2-iscS-iscU-iscA-hscB-hscA-fdx-ORF3 gene cluster. *J. Biochem.* **126**: 10-18.

Ndamukong, I., Abdallat, A. A., Thurow, C., Fode, B., Zander, M., Weigel, R., & Gatz, C. (2007). SA-inducible *Arabidopsis* glutaredoxin interacts with TGA factors and suppresses JA-responsive PDF1. 2 transcription. *Plant J.* **50**: 128-139.

Nishida, M., Harada, S., Noguchi, S., Satow, Y., Inoue, H., & Takahashi, K. (1998). Three-dimensional structure of *Escherichia coli* glutathione S-transferase complexed with glutathione sulfonate: catalytic roles of Cys10 and His106. *J. Mol. Biol.* **281**: 135-147.

Noctor, G., Mhamdi, A., Chaouch, S., Han, Y. I., Neukermans, J., MARQUEZ-GARCIA, B. E. L. E. N., ... & Foyer, C. H. (2012). Glutathione in plants: an integrated overview. *Plant, Cell & Environment* **35**: 454-484.

Nordstrand, K., Åslund, F., Holmgren, A., Otting, G., & Berndt, K. D. (1999). NMR structure of *Escherichia coli* glutaredoxin 3-glutathione mixed disulfide complex: implications for the enzymatic mechanism. *J. Mol. Biol.* **286**: 541-552.

Oakley, A. (2011). Glutathione transferases: a structural perspective. *Drug Metab. Rev.* ***43***: 138-151.

Ollagnier-de-Choudens, S., Mattioli, T., Takahashi, Y., & Fontecave, M. (2001). Iron-Sulfur Cluster Assembly CHARACTERIZATION OF IscA AND EVIDENCE FOR A SPECIFIC AND FUNCTIONAL COMPLEX WITH FERREDOXIN. *J. Biol. Chem.* ***276***: 22604-22607.

Ollagnier-de Choudens, S., Nachin, L., Sanakis, Y., Loiseau, L., Barras, F., & Fontecave, M. (2003). SufA from Erwinia chrysanthemi CHARACTERIZATION OF A SCAFFOLD PROTEIN REQUIRED FOR IRON-SULFUR CLUSTER ASSEMBLY. *J. Biol. Chem.* **278**: 17993-18001.

Ortenberg, R., Gon, S., Porat, A., & Beckwith, J. (2004). Interactions of glutaredoxins, ribonucleotide reductase, and components of the DNA replication system of *Escherichia coli. Proc. Natl. Acad. Sci. USA* ***101***: 7439-7444.

Outten, F. W., Djaman, O., & Storz, G. (2004). A suf operon requirement for Fe–S cluster assembly during iron starvation in *Escherichia coli*. *Mol. Micro.***52**: 861-872.

Papayannopoulos, I. A., Gan, Z. R., Wells, W. W., & Biemann, K. (1989). A revised sequence of calf thymus glutaredoxin. *Biochem. Biophys.Res. Comm.* **159**: 1448-1454.

Picciocchi, A., Saguez, C., Boussac, A., Cassier-Chauvat, C., & Chauvat, F. (2007). CGFS-type monothiol glutaredoxins from the cyanobacterium Synechocystis PCC6803 and other evolutionary distant model organisms possess a glutathione-ligated [2Fe-2S] cluster. *Biochemistry* **46**: 15018-15026.

Porat, A., Lillig, C. H., Johansson, C., Fernandes, A. P., Nilsson, L., Holmgren, A., & Beckwith, J. (2007). The reducing activity of glutaredoxin 3 toward cytoplasmic substrate proteins is restricted by methionine 43. *Biochemistry* **46**: 3366-3377.

Prinz, W. A., Åslund, F., Holmgren, A., & Beckwith, J. (1997). The Role of the Thioredoxin and Glutaredoxin Pathways in Reducing Protein Disulfide Bonds in the *Escherichia coli* Cytoplasm. *J. Biol. Chem*. **272**: 15661-15667.

Qin, X.F., Holuigue, L., Horvath, D.M. and Chua, N.H. (1994) Immediate early transcription activation by salicylic acid via the cauliflower mosaic virus as-1 element. *Plant Cell* **6**: 863–874.

Racker, E. (1955). Glutathione-homocystine transhydrogenase. *J. Biol. Chem.* **217**: 867-874.

Reeves, S. A., Parsonage, D., Nelson, K. J., & Poole, L. B. (2011). Kinetic and thermodynamic features reveal that *Escherichia coli* BCP is an unusually versatile peroxiredoxin. *Biochemistry* **50**: 8970-8981.

Ren, G., Stephan, D., Xu, Z., Zheng, Y., Tang, D., Harrison, R. S., ... & Martin, J. L. (2009). Properties of the thioredoxin fold superfamily are modulated by a single amino acid residue. *J. Biol. Chem.* **284**: 10150-10159.

Reynolds, C. M., Meyer, J., & Poole, L. B. (2002). An NADH-dependent bacterial thioredoxin reductase-like protein in conjunction with a glutaredoxin homologue form a unique peroxiredoxin (AhpC) reducing system in *Clostridium pasteurianum*. *Biochemistry* **41**: 1990-2001.

Riondet, C., Desouris, J. P., Montoya, J. G., Chartier, Y., Meyer, Y., & REICHHELD, J. P. (2012). A dicotyledon-specific glutaredoxin GRXC1 family with dimer-dependent redox regulation is functionally redundant with GRXC2. *Plant, Cell and Environment* **35**: 360-373.

Ritz, D., Patel, H., Doan, B., Zheng, M., Åslund, F., Storz, G., & Beckwith, J. (2000). Thioredoxin 2 Is Involved in the Oxidative Stress Response in *Escherichia coli*. *J. Biol. Chem.* **275**: 2505-2512.

Rodríguez-Manzaneque, M. T., Ros, J., Cabiscol, E., Sorribas, A., and Herrero, E.(1999)Grx5 glutaredoxin plays a central role in protection against protein oxidative damage in *Saccharomycescere visiae*. Mol. Cell. Biol. **19**: 8180–8190.

Rossjohn, J., Polekhina, G., Feil, S. C., Allocati, N., Masulli, M., Di Ilio, C., & Parker, M. W. (1998). A mixed disulfide bond in bacterial glutathione transferase: functional and evolutionary implications. *Structure* **6**: 721-734.

Rouhier, N. (2010). Plant glutaredoxins: pivotal players in redox biology and iron–sulphur centre assembly. *New Phytologist* **186**: 365-372.

Rouhier, N., Couturier, J., Johnson, M. K., & Jacquot, J. P. (2010). Glutaredoxins: roles in iron homeostasis. *Trends Biochem. Sci.s*, *35*: 43-52.

Rouhier, N., Gelhaye, E., Sautiere, P. E., Brun, A., Laurent, P., Tagu, D., Gerard, J., de Faÿ, E., Meyer, Y., and Jacquot, J. P. (2001) Isolation and characterization of a new peroxiredoxin from poplar sieve tubes that uses either glutaredoxin or thioredoxin as a donor. Plant Physiol. **127**: 1299–1309.

Rouhier, N., Unno, H., Bandyopadhyay, S., Masip, L., Kim, S. K., Hirasawa, M., ... & Georgiou, G. (2007). Functional, structural, and spectroscopic characterization of a glutathione-ligated [2Fe–2S] cluster in poplar glutaredoxin C1. *Proc. Natl. Acad. Sci. USA* **104**: 7379-7384.

Roy, A., Kucukural, A., & Zhang, Y. (2010). I-TASSER: a unified platform for automated protein structure and function prediction. *Nature Protocols* **5**: 725.

Running, M. P., & Meyerowitz, E. M. (1996). Mutations in the PERIANTHIA gene of *Arabidopsis* specifically alter floral organ number and initiation pattern. *Development* **122**: 1261-1269.

Sagemark, J., Elgán, T. H., Bürglin, T. R., Johansson, C., Holmgren, A., & Berndt, K. D. (2007). Redox properties and evolution of human glutaredoxins. *Proteins: Structure, Function, and Bioinformatics* **68**: 879-892.

Scandalios, J.G. (2002). The rise of ROS. *Trends Biochem Sci* **27**:483–486.

Schürmann, P., & Buchanan, B. B. (2008). The ferredoxin/thioredoxin system of oxygenic photosynthesis. *Antioxid. Redox Signaling* **10**: 1235-1274.

Schwartz, C. J., Djaman, O., Imlay, J. A., & Kiley, P. J. (2000). The cysteine desulfurase, IscS, has a major role in *in vivo* Fe-S cluster formation in *Escherichia coli*. *Proc. Natl. Acad. Sci. USA* **97** : 9009-9014.

Silberg, J. J., Hoff, K. G., Tapley, T. L., & Vickery, L. E. (2001). The Fe/S assembly protein IscU behaves as a substrate for the molecular chaperone Hsc66 from *Escherichia coli*. *J. Biol. Chem.* **276** : 1696-1700.

Song, Y., Cui, J., Zhang, H., Wang, G., Zhao, F. J., & Shen, Z. (2013). Proteomic analysis of copper stress responses in the roots of two rice (*Oryza sativa L.*) varieties differing in Cu tolerance. *Plant and Soil* **366**: 647-658.

Spoel, S.H., Koornneef, A., Claessens, S.M.C. (2003). NPR1 modulates cross-talk between salicylate- and jasmonate dependent defense pathways through a novel function in the cytosol. Plant Cell **15**: 760–770.

Sundaram, S., Rathinasabapathi, B. (2010). Transgenic expression of fern *Pteris vittata* glutaredoxin PvGrx5 in *Arabidopsis thaliana* increases plant tolerance to high temperature stress and reduces oxidative damage to proteins. *Planta* **231**:361–369.

Sundaram, S., Wu, S., Ma, L.Q., Rathinasabapathi, B. (2009). Expression of a *Pteris vittata* glutaredoxin PvGRX5 in transgenic *Arabidopsis thaliana* increases plant arsenic tolerance and decreases arsenic accumulation in the leaves. *Plant Cell Environ*. **32**:851–858.

Szalai, G., Kellős, T., Galiba, G., & Kocsy, G. (2009). Glutathione as an antioxidant and regulatory molecule in plants under abiotic stress conditions. *J. Plant Growth Reg.* **28**: 66-80.

Takahashi, Y., & Nakamura, M. (1999). Functional assignment of the ORF2-iscS-iscU-iscA-hscB-hscA-fdx-0RF3 gene cluster involved in the assembly of Fe-S clusters in *Escherichia coli*. *J. Biochem.* **126**: 917-926.

Terpe, K. (2003). Overview of tag protein fusions: from molecular and biochemical fundamentals to commercial systems. *Applied Microbiol. Biotechnol.* **60**: 523-533.

Thurow, C., Schiermeyer, A., Krawczyk, S., Butterbrodt, T., Nickolov, K. and Gatz, C. (2005) Tobacco bZIP transcription factor TGA2.2 and related factor TGA2.1 have distinct roles in plant defense responses and plant development. *Plant J.* **44**: 100–113.

Uhrig, J. F., Huang, L. J., Barghahn, S., Willmer, M., Thurow, C., & Gatz, C. (2017). CC-type glutaredoxins recruit the transcriptional co-repressor TOPLESS to TGA-dependent target promoters in *Arabidopsis thaliana*. *Biochimica et Biophysica Acta (BBA)-Gene Reg. Mechan.* **1860**: 218-226.

Ulmasov, T., Hagen, G. and Guilfoyle, T. (1994) The ocs element in the soybean GH2/4 promoter is activated by both active and inactive auxin and salicylic acid analogues. *Plant Mol. Biol*. **26**: 1055–1064

Vilella, F., Alves, R., Rodríguez-Manzaneque, M. T., Bellí, G., Swaminathan, S., Sunnerhagen, P., & Herrero, E. (2004). Evolution and cellular function of monothiol glutaredoxins: involvement in iron–sulphur cluster assembly. *Compar. Funct. Genom.* **5**: 328-341.

Vlamis-Gardikas, A., Åslund, F., Spyrou, G., Bergman, T., & Holmgren, A. (1997). Cloning, overexpression, and characterization of glutaredoxin 2, an atypical glutaredoxin from *Escherichia coli*. *J. Biol. Chem.* **272**: 11236-11243.

Vranová, E., Inzé, D., & Van Breusegem, F. (2002). Signal transduction during oxidative stress. *J. Experimental Botany* **53**: 1227-1236.

Wang, Z., Xing, S., Birkenbihl, R. P., & Zachgo, S. (2009). Conserved functions of *Arabidopsis* and rice CC-type glutaredoxins in flower development and pathogen response. *Mol. Plant* **2**: 323-335.

Xing, S., Lauri, A., and Zachgo, S. (2006). Redox regulation and flower development: a novel function for glutaredoxins. *Plant Biol*. **8**: 547–555.

Xing, S., Rosso, M.G., and Zachgo, S.(2005). ROXY1, a member of the plant glutaredoxin family, is required for petal development in *Arabidopsis thaliana*. *Development* **132**:1555–1565.

Xing, S., and Zachgo, S. (2008). ROXY1 and ROXY2, two *Arabidopsis* glutaredoxin genes, are required for anther development. *Plant J*. **53**: 790–801.

Yang, F., Bui, H. T., Pautler, M., Llaca, V., Johnston, R., Lee, B. H., ... & Jackson, D. (2015). A maize glutaredoxin gene, Abphyl2, regulates shoot meristem size and phyllotaxy. *Plant Cell **27***: 121-131.

Yang, J., Yan, R., Roy, A., Xu, D., Poisson, J., & Zhang, Y. (2015). The I-TASSER Suite: protein structure and function prediction. *Nature Methods* **12**: 7-8.

Yeh, A. P., Chatelet, C., Soltis, S. M., Kuhn, P., Meyer, J., & Rees, D. C. (2000). Structure of a thioredoxin-like [2Fe-2S] ferredoxin from *Aquifex aeolicus*. *J. Mol. Biol.* **300**: 587-595.

Yeung, N., Gold, B., Liu, N. L., Prathapam, R., Sterling, H. J., Willams, E. R., & Butland, G. (2011). The *E. coli* monothiol glutaredoxin GrxD forms homodimeric and heterodimeric FeS cluster containing complexes. *Biochemistry* **50**: 8957-8969.

Zaffagnini, M., Bedhomme, M., Marchand, C. H., Couturier, J., Gao, X. H., Rouhier, N., ... & Lemaire, S. D. (2012). Glutaredoxin s12: unique properties for redox signaling. *Antioxid. Redox Signaling* **16**:17-32.

Zaffagnini, M., Michelet, L., Massot, V., Trost, P., & Lemaire, S. D. (2008). Biochemical characterization of glutaredoxins from *Chlamydomonas reinhardtii* reveals the unique properties of a chloroplastic CGFS-type glutaredoxin. *J. Biol. Chem.* **283**: 8868-8876.

Zagorchev, L., Seal, C. E., Kranner, I., & Odjakova, M. (2013). A central role for thiols in plant tolerance to abiotic stress. *Int .J. Mol. Sci.* **14**: 7405-7432.

Zhang, Y. (2008). I-TASSER server for protein 3D structure prediction. *BMC Bioinformatics* **9**: 40

Zhang, Y., Fan, W., Kinkema, M., Li, X. and Dong, X. (1999) Interaction of NPR1 with basic leucine zipper protein transcription factors that bind sequences required for salicylic acid induction of the PR-1 gene. *Proc. Natl Acad. Sci. USA* **96**: 6523–6528.

Zhang, Y.L., Tessaro, M.J., Lassner, M. and Li, X. (2003) Knockout analysis of *Arabidopsis* transcription factors TGA2, TGA5, and TGA6 reveals their redundant and essential roles in systemic acquired resistance. Plant Cell **15**: 2647–2653.

Zheng, M., Åslund, F., & Storz, G. (1998). Activation of the OxyR transcription factor by reversible disulfide bond formation. *Science* **279**: 1718-1722.

Zheng, L., Cash, V. L., Flint, D. H., & Dean, D. R. (1998). Assembly of Iron-Sulfur Clusters Identification of an IscSUA-hscBA-fdx gene cluster from *Azotobacter vinelandii*. *J. Biol. Chem.* **273**: 13264-13272

APPENDIX

Supplemental Table 1. The activities and molecular weights (kDa) of *Escherichia coli* glutaredoxins, thioredoxins, and related proteins as provided by the UniProtKB database.

Protein Identity	Monomer Size (kDa) (UniProtKB)	Activity (UniProtKB)
Glutaredoxin 1	10	Reduces glutathione–protein mixed disulfides, specific reduction of ribonucleotide reductase (RR) and 3'-phosphoadenylylsulfate (PAPS) , provides electrons to BCP peroxidase to catalyse hydrogen peroxide , deactivates *OxyR* transcription factor.
Glutaredoxin 2	24	Reduces some disulfide bonds in a coupled system with glutathione reductase.
Glutaredoxin 3	9	Reduces glutathione–protein mixed disulfides, provide electrons to BCP peroxidase to catalyse hydrogen peroxide.
Glutaredoxin 4	13	[2Fe-2s] cluster assembly. Serves as a substrate for thioredoxin reductase and can form FeS-bound homodimeric and heterodimeric complexes. Acts as a scaffold protein for [2Fe-2S] transfer to apo-ferredoxin (Fdx).
Thioredoxin 1	11.8	Provides electrons to methionine sulfoxide reductase (MSR) and acts as a specific reductase for the peroxidase Tpx in ROS scavenging.
Thioredoxin 2	15.6	Provides electrons to BCP peroxidase to catalyse hydrogen peroxide, deactivates *OxyR* transcription factor.
Glutathione transferase	25	GSH-dependent peroxidase activity toward cumene hydroperoxide.
Glutathione reductase	48.8	Maintains high levels of reduced glutathione in the cytosol.
Thioredoxin reductase	34.6	Reduces thioredoxins and NrdH redoxin.

Supplemental Table 2. The activities and molecular weights (kDa) of *Escherichia coli* proteins involved in iron-sulfur [Fe-S] cluster assembly and redox sensing as provided by the UniProtKB database

	Protein Identity	Monomer Size (kDa) (UniProtKB)	Activity (UniProtKB)
***suf* operon proteins**	SufA	13.3	Scaffold protein for assembly of iron-sulfur clusters and delivery to target proteins.
	SufB	54.7	SufBCD complex acts synergistically with SufE to stimulate the cysteine desulfurase activity of SufS. The SufBCD complex contributes to the assembly or repair of oxygen-labile iron-sulfur clusters under oxidative stress. May facilitate iron uptake from extracellular iron chelators under iron limitation.
	SufC	27.6	Cytoplasmic ABC-ATPase that forms a complex with SufB and SufD.
	SufD	46.8	* See "SufB". Required for the stability of the FhuF protein.
	SufE	15.8	Homodimeric protein which forms a complex with SufS to stimulate cysteine desulfurase activity of SufS.
	SufS	44.9	Homodimeric cysteine desulfurase which mobilizes the sulfur atom from cysteine and provides it to the cluster.
***isc* operon proteins**	IscU	13.8	A scaffold on which IscS assembles Fe-S clusters.
	IscA	11.6	Transfers iron-sulfur clusters to apo-ferredoxin. Recruits intracellular free iron so as to provide iron for the assembly of transient iron-sulfur cluster in IscU in the presence of IscS, L-cysteine and the thioredoxin reductase system. Homodimer that may form tetramers and higher multimers. Binds 2 iron ions per dimer. Repressed by IscR.
	IscS	45	Master enzyme that delivers sulfur to a number of partners involved in Fe-S cluster assembly, tRNA modification or cofactor biosynthesis. Catalyzes the removal of elemental sulfur from cysteine to produce alanine. Functions as a sulfur delivery protein for Fe-S cluster synthesis onto IscU, an Fe-S scaffold assembly protein, as well as other S acceptor proteins. Preferentially binds to disordered IscU on which the Fe-S is assembled, IscU converts to the structured state and then dissociates from IscS to transfer the Fe-S to an acceptor protein.
	IscR	17.3	Regulates the transcription of several operons and genes involved in the biogenesis of Fe-S clusters and Fe-S-containing proteins. Transcriptional repressor of the *iscRSUA* operon. In its apoform, under conditions of oxidative stress or iron deprivation, it activates the *suf* operon. Binds 1 [2Fe-2S] cluster.
	IscX	7.7	May function as iron donor in the assembly of iron-sulfur clusters.
	HscA/Hsc66	65.7	Hsp70 (heat shock protein)-type molecular chaperone involved in the maturation of iron-sulfur cluster-containing proteins whose ATPase activity is stimulated by HscB.
	HscB/Hsc20	20.1	J type co-chaperone involved in the maturation of iron-sulfur cluster-containing proteins.
	[2Fe-2S] ferredoxin	12.3	Probable cellular electron transfer protein involved in the in assembly of Fe-S clusters.
Misc. related proteins	IspH	34- 36	4-hydroxy-3-methylbut-2-enyl diphosphate reductase. Binds $[3Fe\text{-}4S]^{+}$ clusters with overexpression of the *isc* operon.
	SoxR	17.1	Contains a 2Fe-2S iron-sulfur cluster that may act as a redox sensor system that recognizes superoxide during oxidative stress. Activates the transcription of the *soxS* gene which controls the superoxide response regulon.
	YtfE/ Repair of Iron Centers (RIC)	24.9	Di-iron-containing protein involved in the biogenesis and repair of iron-sulfur clusters damaged by oxidative and nitrosative stress conditions.